The United Nations
University

GEOTHERMAL TRAINING PROGRAMME
Orkustofnun, Grensásvegur 9,
IS-108 Reykjavík, Iceland

Reports 2005
Number 2

THERMOECONOMIC ANALYSIS OF A NEW GEOTHERMAL UTILIZATION CHP PLANT IN TSETSERLEG, MONGOLIA

MSc thesis
Department of Mechanical and Industrial Engineering
University of Iceland

by

Purevsuren Dorj
Renewable Energy Corporation
P.O. Box 479,
Ulaanbaatar 210136
MONGOLIA

United Nations University
Geothermal Training Programme
Reykjavík, Iceland
Report 2
Published in June 2005

ISBN 9979-68-166-7

This MSc thesis has also been published in April 2005 by the
Department of Mechanical and Industrial Engineering
University of Iceland

INTRODUCTION

The Geothermal Training Programme of the United Nations University (UNU) has operated in Iceland since 1979 with six month annual courses for professionals from developing countries. The aim is to assist developing countries with significant geothermal potential to build up groups of specialists that cover most aspects of geothermal exploration and development. During 1979-2004, 318 scientists and engineers from 39 countries have completed the six month courses. They have come from Asia (44%), Africa (26%), Central America (14%), and Central and Eastern Europe (16%). There is a steady flow of requests from all over the world for the six month training and we can only meet a portion of the requests. Most of the trainees are awarded UNU Fellowships financed by the UNU and the Government of Iceland.

Candidates for the six month specialized training must have at least a BSc degree and a minimum of one year practical experience in geothermal work in their home countries prior to the training. Many of our trainees have already completed their MSc or PhD degrees when they come to Iceland, but several excellent students who have only BSc degrees have made requests to come again to Iceland for a higher academic degree. In 1999, it was decided to start admitting UNU Fellows to continue their studies and study for MSc degrees in geothermal science or engineering in co-operation with the University of Iceland. An agreement to this effect was signed with the University of Iceland. The six month studies at the UNU Geothermal Training Programme form a part of the graduate programme.

It is a pleasure to introduce the eighth UNU Fellow to complete the MSc studies at the University of Iceland under the co-operation agreement.

Mr. Purevsuren Dorj, MSc in Physical Engineering, of the Renewable Energy Corporation of Mongolia, completed the six month specialized training at the UNU Geothermal Training Programme in October 2001. His research report was entitled "Design of small geothermal heating systems and power generators for rural consumers in Mongolia". After two years of geothermal research work and data collection in Mongolia, he came back to Iceland for MSc studies at the Faculty of Engineering of the University of Iceland in September 2003. In April 2005, he defended his MSc thesis presented here, entitled "Thermoeconomic analysis of a new geothermal utilization CHP plant in Tsetserleg, Mongolia". His studies in Iceland were financed by a fellowship from the Government of Iceland through the UNU Geothermal Training Programme. We congratulate him on his achievements and wish him all the best for the future. We thank the Faculty of Engineering of the University of Iceland for the co-operation, and his supervisors for the dedication.

Finally, I would like to mention that the graphs and diagrams in Purevsuren´s MSc thesis had to be printed in black and white. However, a colour version in a pdf format is available for downloading on our website at page *www.os.is/unugtp/yearbook/2005.*

With warmest wishes from Iceland,

Ingvar B. Fridleifsson, director
United Nations University
Geothermal Training Programme

ACKNOWLEDGEMENTS

The financial support from the UNU Geothermal Training Programme (UNU-GTP) and the agreement between the UNU-GTP and the University of Iceland, which allowed me to complete my MSc degree study in Iceland, are gratefully acknowledged. My special gratitude to the director of UNU-GTP, Dr. Ingvar B. Fridleifsson, and the deputy director, Mr. Lúdvík S. Georgsson, and Mrs. Gudrún Bjarnadóttir for their special help and kindness during my studies.

I am sincerely grateful to my supervisor Professor Páll Valdimarsson, for his guidance and support during all stages of this work. I would like to mention especially his excellent lectures in the Exergy analysis course.

I am grateful to Acad. Chadraa B., president of the Mongolian Academy of Science, for his great efforts in promoting renewable energy development in Mongolia. I am also grateful to my colleagues at the Renewable Energy Corporation of Mongolia, for their support in data collection during all stages of this work.

I would also like to thank all the people at the Rafhönnun Engineering Consultants Company for their financial support and co-operation in the pre-feasibility study of the geothermal project in Tsetserleg, Mongolia, especially chief engineer, Mr. Johann Thor Magnusson, for his industrious personality, hospitality and kindness during my stay in Iceland. Also I would like to thank the other participants, Dr. Einar Tjörvi Elíasson from Kreta Geothermal Consulting, also on behalf of ISOR, and Dr. Thorleikur Jóhannesson from Fjarhitun Consulting Engineering.

I also want to thank the staff of Orkustofnun (National Energy Authority of Iceland) and ISOR (Iceland Geosurvey) for their kind help and assistance which gave me the chance to broaden my knowledge in geothermal exploration.

Younes Noorollahi has been my friend during the last year and a half. We have struggled through many late nights at Orkustofnun and have had a lot of interesting discussions.

I owe many thanks to Mr. Lúdvík S. Georgsson and Mrs. Marcia Kjartansson, for going through the manuscripts and making edits of the English in the final days of manuscript preparation.

Finally, I would express my sincere gratitude to my parents and parents-in-law for their encouragement and the care of my lonely son Bat-Erdene during my and my wife's study time in Iceland. Very special thanks to my wife Munkhsaikhan, for her love and every kind of support during this period.

ABSTRACT

A thermal design and thermoeconomic analysis of a combined heat and power (CHP) production plant for Tsetserleg town, Mongolia, has been completed. The energy and exergy analysis of the plant was studied based on the first and second laws of thermodynamics.

The exergy analysis identifies the plant components with the highest thermodynamic inefficiencies and the processes that cause them. Exergy destruction in the plant represents not only thermodynamic inefficiency but also the opportunity to optimize investment costs associated with the plant being analyzed. It is the objective of thermoeconomic optimization to maximize the exergetic efficiencies of the plant components and to minimize the levelized costs of the heat and electricity generated by the CHP plant.

The main advantage of using the structural method of thermoeconomic optimization is that the various components of the plant can be optimized on their own. The effect of the interaction between a given component and the whole plant is taken into account by the local unit costs of exergy fluxes or those exergy destructions.

Geothermal power plant projects are characterized by high initial capital costs including a lifetime supply of fuel. The total capital investment (TCI) of the new CHP plant in Tsetserleg has been evaluated to be 8.66 M US$ with a 5 km long transmission pipeline, or 12.41 M US$ with a 20 km long transmission pipeline.

It is often difficult to allocate the costs of heat and electricity produced by a CHP plant. In this case, exergy can be used as a basis. With the estimated direct cost of the Kalina PP, the levelized unit cost of heat and electricity show that the CHP plant is economically viable for development for a medium-temperature geothermal resource in Tsetserleg, Mongolia.

Economic analysis shows that CO_2 offset can affect the feasibility of the project.

Geothermal energy will benefit all of Tsetserleg. With its introduction, Tsetserleg will be the first clean and environmentally friendly town in Mongolia. It would serve 18,136 people who would live without GHG, breathing clean air, and living and enjoying comfortable working conditions.

TABLE OF CONTENTS

Page

3. ENERGY AND EXERGY ANALYSES

Page

LIST OF FIGURES

Page

LIST OF TABLES

1. INTRODUCTION

Today humanity uses two main sources for heat and power generation, conventional non-renewable resources such as fossil fuel, and renewable energy resources. In Mongolia, virtually all heat and power comes from coal (bituminous and lignite). The consequence is that the country now has one of the highest greenhouse gas (GHG) emissions per capita and GHG emissions per $GDP in the world (Improved Urban Stoves, 2000). The government of Mongolia is actively supporting projects to alleviate the GHG effect through the use of renewable energy sources, natural gas, energy saving/efficiency and forest conservation.

The pre-feasibility study "Geothermal Project in Tsetserleg, Mongolia" concludes that there are significant indications that geothermal energy can be economically developed in Erdenebulgan soum (Tsetserleg province centre), which is in the Khangai geothermal area (site of the main geothermal activity), and several other towns in the area (Eliasson et al., 2004). But the study only treated the heating aspect of geothermal utilization. In the present work, power generation from a local geothermal resource and its coexistence with a heating system is treated.

Geothermal energy is an important energy resource whose exploration has relatively insignificant environmental impact. The main factor determining the potential use of a particular geothermal resource is the reservoir temperature as summarised in the Lindal diagram (Gudmundsson et al., 1985). The Lindal diagram indicates geothermal water temperature of 80°C is convenient for space heating. Power generation mainly takes place in conventional steam turbines that require fluids at temperatures of at least 150 °C. The second law of thermodynamics binds the conversion efficiency of medium temperature (100-150 °C) heat into power. Generating power from this temperature range of geothermal fluids has made considerable progress due to improvements made in binary fluid technology.

Nowadays, engineers prefer a Kalina cycle rather than an Organic Rankine Cycle (ORC), because it is thermodynamically superior or equal to the ORC (Valdimarsson, 2003a). Its working fluid is technically well known and widely used and a novel approach to increasing efficiency. The Kalina Cycle offered up to 29% more net power output than ORC proposals (Mlcak, 2001). Also, the superiority of the “Kalina” technology with regard to effectiveness and cost was demonstrated and proven in the M.Sc. thesis of Mr. Geir Thorolfsson (Thorolfsson, 2002).

The main objective of the present work is an assessment of plant economy and thermodynamic base-case design and thermoeconomic optimum design of a Combined Heat Power (CHP) plant in Tsetserleg, Mongolia, employing “Kalina” technology. The plant should utilise the local geothermal energy to its greatest efficiency, while securing a heat and power supply and remaining within acceptable cost levels.

2. PROCESS DATA

2.1 Proposed project site

The proposed project site, Tsetserleg, is a province centre of Arkhangai, one of 21 provinces, located in the central part of Mongolia and 468 km east of Ulaanbaatar, the capital city (Figure 1). The number of inhabitants is 18,136 (Statistical Booklet, 2000). The total number of households is 4,373; divided into 2,565 living in conventional housing and 1,808 living in gers (primarily traditional felt tents, see Dorj, 2001).

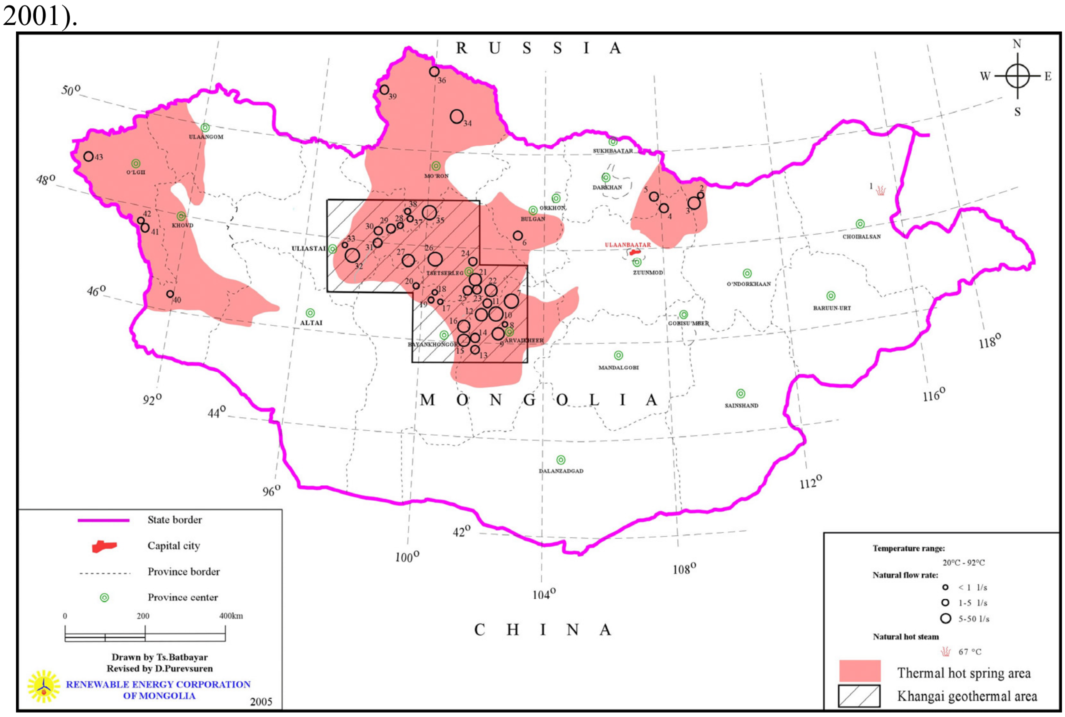

FIGURE 1: Map of Mongolia and location of geothermal resources

Mongolia has rich geothermal resources but geothermal utilization is not widely developed. There are 43 hot springs (Figure 1), mainly distributed in the area of the central provinces, the Khangai geothermal area. Today, the hot springs are used for bathing, health resorts (balneology) and a small amount for greenhouses and building heating. The main incentives for developing geothermal utilization in the rural areas of Mongolia will be to supply geothermal energy for heating, bathing, power generation and industrial purposes. The Khangai geothermal area has such possibilities, along with an important magisterial road between western and central Mongolia and is an area of great tourist attraction (Mongolian Statistics Centre, 2001).

According to geological studies, Arkhangai province has seven hot springs (Figure 2) including (#21) Tsenher, (#22) Tsagaan sum, (#23) Bor tal, (#24) Shivert, (#25) Gyalgar, (#26) Chuluut and (#27) Noyon khangai. The locations and general features of the seven hot springs are summarized below in Table 1.

Currently, no comprehensive investigation has been carried out in Mongolia regarding geothermal resources or of possible energy uses (for heating, power, etc), but scientists have come to some conclusions based on existing tectonic, geochemical, and hydrogeological data (regional geology, rock sphere structure, hot spring study).

Interpretation of geochemical data from geothermal fluids of the five hot springs Noyon khangai, Chuluut, Shivert, Tsenher and Tsagaan sum (Figure 2) was done by Gendenjamts (2003). The subsurface temperatures of the specified five hot springs have been estimated by chemical geothermo-

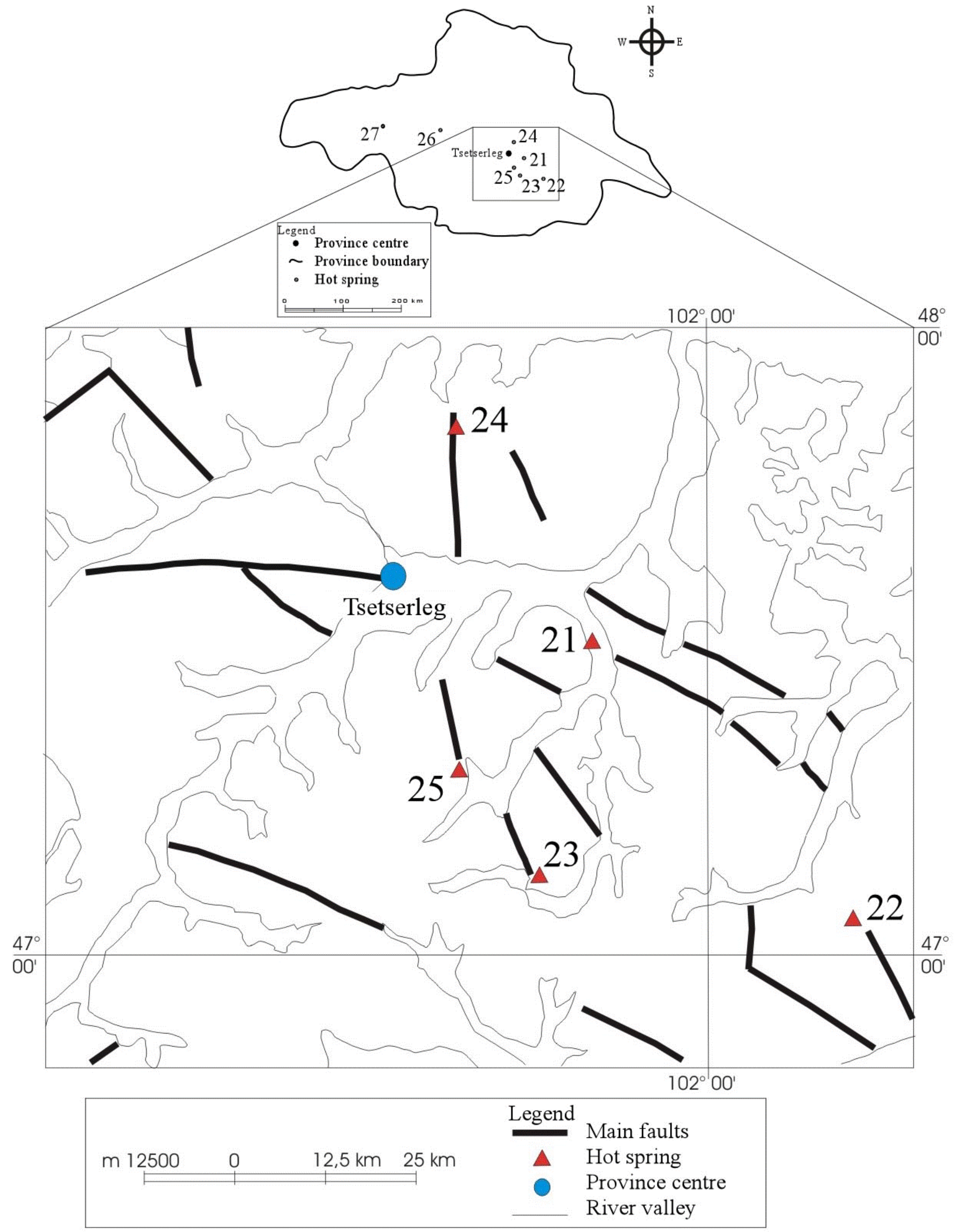

FIGURE 2: Hot springs and main faults in Arkhangai province

TABLE 1: The locations and general features of the seven hot springs

#	Name of hot springs	Latitude	Longitude	Elevation, m	Flowrate, kg/s	Mineral, mg/l	Temperature, ^{0}C
21	Tsenher	47°19’28”N	101°39’00”E	1860	10	239.9	86
22	Tsagaan Sum	47°04’12’’N	102°04’48’’E	1840	8	-	69
23	Bor tal	47°10’19’’N	101°36’58’’E	1880	4.5	258.9	52
24	Shivert	47°39’49”N	101°30’54”E	1710	4	24.8	55
25	Gyalgar	47°11’19”N	101°32’54’’E	1900	1	221.6	52
26	Chuluut	47°50’N	100°15’E	2190	2.5	250.5	44
27	Noyonkhangai	47°45’N	99°25’E	2370	6	-	36

metry. Chalcedony, quartz, Na-K, and Na-K-Ca geothermometer temperatures were calculated. The Na-K geothermometer gave very high and sometimes unrealistic temperatures for all hot springs, whereas results for the Na-K-Ca geothermometer indicate that this empirical geothermometer appears to be applicable for low-temperature waters. The quartz geothermometer temperatures were realistic for hot springs in this area compared to estimated mineral-equilibrium temperatures. But the chalcedony geothermometer provided the most reliable temperatures with predicted subsurface temperature values ranging from 69 to 123°C.

The silica-enthalpy warm spring mixing model handles non-boiled and boiled mixed waters separately with mixing occurring after boiling. The boiling hot spring waters indicate enthalpies from 908 to 1142 kJ/kg for the hot water component or reservoir temperature 212-261°C. This indicates reservoir temperatures may be sufficient for power production.

The calcite saturation indices and the Ryznar stability indices of the specified five hot springs of the Khangai geothermal area show that there is no scaling tendency (Gendenjamts, 2003). The values for hot spring water vary, but fall in the ‘no calcite scaling’ range.

According to the heat flow study of Mongolia, based on 32 stations, the Khangai area has the highest heat flow, 110 mW/m^2, and a geothermal gradient of 45-80°C/km (Ministry of Agriculture and Industry of Mongolia, 1999; Dorofeeva, 1992).

Recently, a proposal for the assessment of the Shivert hot spring area was done by Burentsagaan (2004). The Shivert area is characterized by active tectonic faults. Hot springs are found on the surface, probably in conjunction with the interaction of different fault zones. A preliminary evaluation of temperature data from six exploration wells indicates a clear upflow of 80-100°C water along a high-permeability vertical fracture zone (Burentsagaan, 2004). Finally, he concludes in his analysis that the Shivert area is believed to have considerable potential, but further exploration and consequent assessment is needed before successful utilization can start.

2.2 Brief description on the pre-feasibility study of a geothermal project in Tsetserleg, Mongolia

The study describes firstly a small geothermal pilot project for the Shivert hot spring area utilizing existing geothermal wells. However, the main focus of the report was on the possibilities of constructing a geothermal heating system for Tsetserleg province centre. The Tsetserleg geothermal pilot project would cover the heating demand of the consumers listed in Table 2. It should be noted that these consumers are only a part of all Tsetserleg heat consumers. A summary of the consumers’ heat consumption through the whole year is listed in Table 2 (assuming seven months’ operation).

According to Table 2 the geothermal heating system would provide heat energy of 94,505 GJ per year. The geothermal heating system would be composed of two different types of heating equipment, radiators and floor coil heating. The radiator heating system would provide heat for the existing DH systems and the IBC consumers. Other consumers would be supplied by floor coil heating systems. In the floor coil heating system, the low-temperature hot water is circulated through piping embedded in the concrete floor of the buildings. Its advantages are utility of low-temperature water, silent operation, no air movement, and no effect on humidity.

It can be seen from Table 2 that a total reduction of 23,615 tons/year CO_2 emission or 14,870 tons/year of coal would be achieved for selected consumers. For a period of 20 years the reduction in CO_2 emission due to the utilization of geothermal energy would be 472,297 tons CO_2 emission (or 297,400 tons coal). A rough estimate of 400,000 GJ/year heat consumption is needed for extension of the geothermal DH system to the rest of the Tsetserleg households (1708 gers and 2465 conventional housings). Total CO_2 emission in Tsetserleg due to coal burning for heating, based on the pre-feasibility study estimation, is 51,621 tons per year. Annual coal consumption and CO_2 emission for all heating consumers in Tsetserleg is listed in Table 3.

TABLE 2: Tsetserleg geothermal pilot project; heat consumption, reduced coal and CO_2 emissions for selected consumers per year

Heat consumers	Area, m^2	Volume, m^3	Heat consumption, GJ/year	Reduced coal consumption, tons/year	CO_2 emission reduction, tons/year
Existing DH system consumers (20% increase)	?	135,600	62,117	9,120	14,483
Individual boiler consumers (IBC)	?	45,200	20,706	3,040	4,828
Experimental connection of 100 gers and 100 individual houses	7,630	14,700	4,758	1,000	1,588
Additional 171 private households (plots in new housing development)	10,260	25,650	6,924	1,710	2,716
Total		221,150	94,505	14,870	23,615

TABLE 3: Present annual coal consumption and CO_2 emission in Tsetserleg

Heating system	Number	Coal consumption, tons	Cost, US$	CO_2 emission, tons
DH company	8	7,600	304,000	12,069
Individual boilers	-	3,040	121,600	4,828
Gers	1,808	9,040	361,600	14,356
Houses	2,565	12,825	513,000	20,367
Total		32,505	1,300,200	51,621

In the study, different financial scenarios were developed and the feasibility of the project was demonstrated. The summary of the result of the scenarios indicate the following:

- If wells far from Tsetserleg (20 km) are to be utilized, then the wells must be inexpensive and the DH system size must be large, at least considerably larger (maybe 4 times) than 94,505 GJ per year.
- If the wells are close to Tsetserleg (5 km) then average cost of the wells would suffice if the DH system is large. If the DH system is small then the wells must be of low cost.
- Re-injection could easily destroy the feasibility of the project. The cost assumed for re-injection wells may, however, be too high in the assumptions. It should be noted that geothermal water characteristics, with respect to pollution, is a deciding factor here.

2.3 Proposed new CHP plant

The CHP plant under consideration consists of a heat and power generation Kalina power plant (Kalina PP) and a heat distribution District Heating (DH) system. A block diagram of the CHP plant is shown in Figure 3 and a dashed line distinguishes the Kalina PP and the DH system.

The Kalina PP uses an ammonia-water mixture as a working fluid. The mixture circulates in a closed Kalina cycle. The composition of the mixture is not constant at all states of the cycle. The Kalina cycle is basically a Rankine cycle with additional distillation and absorption units. It is heated by geothermal water and cooled by cooling water. The main components of the power plant consist of a conventional steam turbine, separator, vaporizer, HT recuperator and LT recuperator, condenser heat exchangers and a feed pump, as shown in Figure 3.

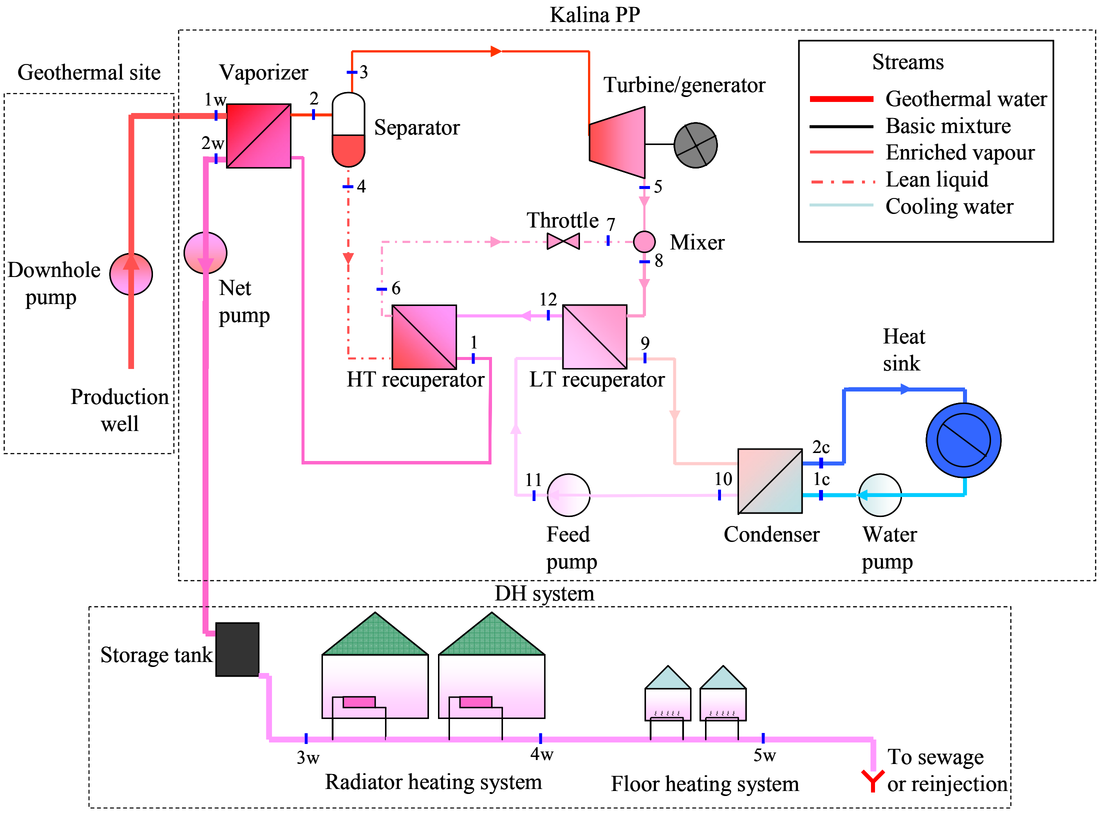

FIGURE 3: A block diagram of the CHP plant in Tsetserleg

Among the degrees of freedom in the design of the CHP plant in Figure 3 are: (a) ammonia-water fraction, (b) DH supply geothermal water temperature, (c) pressure on the high-pressure side, and (d) pressure on the low-pressure side. The design of such a CHP plant is complicated further by the size of the heat exchangers in the Kalina PP and by heat supply to the DH system when peak load occurs during the coldest periods of the year. The boundary conditions for the plant are the geothermal water and the cooling water flowrates. They can be changed by using additional wells.

Both direct and indirect geothermal heating systems are applicable for the design. The selection of the geothermal heating system is more dependent on geothermal fluid corrosion and scaling problems. It means that if the chemical composition of the geothermal fluid permits, direct use in the heating system is preferred. In Figure 3 the DH system is illustrated as a direct geothermal heating system. But both heating system types should be considered.

The main feature of the Kalina cycle is to utilize excess heat for power production when geothermal water temperature is over 80°C. According to Icelandic experience, 80°C hot water is ideal for a geothermal DH system. The Kalina PP on the block diagram shown in Figure 3 is based on the Kalina Cycle System 34 (KCS34) license, which is applicable for low-temperature geothermal plants. This is the same flow scheme as in the Husavik Power Plant in Northern Iceland. Its commercial operation started in the year 2000. If further information is required, readers should consult Mklac (2001) and Maack and Valdimarsson (2002).

An assumption used for the Kalina PP location is that it should be located close to Tsetserleg (not an area close to the explored geothermal resources). The main advantage is to minimise the cost of power transmission lines. The geothermal water transmission pipeline would benefit both the DH system and the Kalina PP. The transmission pipeline cost will be accounted for in the DH system expenses.

2.4 Resources and software used for analysis

Calculations involving the thermodynamic properties of fluids (geothermal water, ammonia-water mixture, and cooling water) and the thermodynamic design of the CHP plant equipment were performed as described in Sections 2 and 5 of the Cengel textbook (Cengel, 1994), and Section 10 of the Holman textbook (Holman, 2002).

The CHP plant thermoeconomic analysis and evaluation and thermoeconomic optimization involving an exergy method were performed as described in Section 7 of the Cengel textbook, Sections 2 and 6 of the Kotas textbook (Kotas, 1985) and Sections 7-9 of the Bejan textbook (Bejan et al., 1996).

The Engineering Equation Solver (EES) software (F-Chart Software, 2004) was used to perform the fluids' thermodynamic property calculations and to run the models for each operating condition; the code for the program is available in Appendix A.

The EES software thermodynamic property functions implemented the steam tables such that any thermodynamic property could be obtained from a built-in function call in terms of any two other properties. Read further details on the EES software in Appendix D.

2.5 Streams in the CHP plant

In a Kalina PP three different types of streams are presented. Figure 3 illustrates those streams and the flow direction in the system components.

A hot water stream (a bold fine line on the left side of Figure 3) in the CHP plant will be supplied from geothermal production wells. According to the pre-feasibility study, a total capacity of the production wells was assumed 80 kg/s.

The basic ammonia-water stream (a fine line in Figure 3 is vaporized in the vaporizer and then separated into a saturated (or enriched) vapour ammonia-water mixture stream (a fine line after the separator in Figure 3) and a saturated (or lean) liquid ammonia-water mixture stream (a short-dashed line in Figure 3) in the separator. The basic stream reappears when the saturated liquid stream is cooled in the HT recuperator and throttled in the throttle valve, and then mixed with the saturated vapour stream passed through the turbine. After that the basic stream is cooled in the LT recuperator and condensed in the condenser. The condensed basic stream is pressurized before re-entering the LT and HT recuperators. Here the basic stream returns to its initial state and the processes are repeated.

A cold water stream (a bold line on right side of Figure 3) cools the basic stream in the condenser and is circulated by a special pump.

A geothermal water stream is the only utility throughout the DH system. The geothermal water is transmitted from the geothermal site through a transmission pipeline, and flows into a storage tank. Then it is distributed by distribution pipelines to the heat consumers where it flows through the consumers' heat radiators and floor coils, and cools down to a temperature of 30°C.

The plant design requires exact data for the thermodynamic properties of the ammonia-water mixture at the inlet and outlet state of the components. To define a thermodynamic system completely, one must specify temperature, pressure and the concentration of all components in the system. However, if the system is at equilibrium, some of the variables are interrelated, as demonstrated by the Gibbs Phase Rule, and it is only necessary to define the independent variables in order to completely describe the system. According to Weast (1982) the Gibbs phase rule is given by:

$$IV=C-PH+2$$

where PH and C stand for the number of phases and chemical components in the system and IV is the number of independent variables.

In the Kalina cycle the phase equilibrium of ammonia and water components involves two phases (liquid and vapour) in equilibrium. According to the Gibbs phase rule, a two-component (C=2) and two-phase (PH=2) system has two independent variables such as temperature and pressure. For a single-component (C=1) (in our case geothermal and cooling water) and two-phase (PH=2) system, one independent intensive variable needs to be specified (IV=1).

2.6 Thermal design of the CHP plant

The thermodynamic design for the CHP plant has been established in EES software. A code for this software is available in Appendix A.

The following plant operating parameters for the Kalina PP design in EES software are used from Dorj (2001):

x_{mix}	= 0.87	Fraction of ammonia-water mixture - [%]
P_{high}	= 30	Pressure on the high pressure side - [bar]
P_{low}	= 5.0	Pressure on the low pressure side - [bar]
T_{high}	= 120 + 273.1	Geothermal water inflow temperature - [K]
T_{low}	= 80 + 273.1	Geothermal water outflow temperature - [K]
$\dot{m}_w$	= 80	Geothermal water flowrate - [kg/s]
η	= 75	Turbine isentropic efficiency - [%]
η_p	= 50	Pump isentropic efficiency - [%]

The following operating parameters are used for the DH system design:

T_{supply}	$= T_{low}$	DH supply geothermal water temperature – [K]
$T_{5,w}$	= 30+273.1	Exiting geothermal water temperature from DH – [K]
$\dot{m}_w$		Geothermal water flowrate, same as Kalina PP

The following simplifying assumptions have been made:

1. All pressure losses are neglected
2. All heat transfer losses are neglected

The calculation software involves the following procedures.

1. Give input parameters of the geothermal water and the ammonia-water mixture (operating parameters)
2. Solve the mass balance equations at the inlet and outlet states of the plant components
3. Solve the energy balance equations for the plant components
4. Call the statement "CALL NH3H2O(Code,In1,In2,In3:T,P,x,h,s,u,v,q)" to define eight output values at the outlet state of plant components
5. Define a specific exergy of each stream
6. Define a time rate of exergy associated with each stream

7. Estimate the size of components using their related methods
8. Estimate component cost using their related sizes, heat and power capacities

The data listed in Table 4 was created by the thermodynamic design model when running it in EES software and it will be used for the CHP plant analysis in the following sections. The state numbers are related to the block diagram in Figure 3.

TABLE 4: Mass flowrate, temperature, and pressure data for the CHP plant

State	Substance	Phase	Mass flowrate, kg/s	Pressure, bars	Temperature, K
1	Ammonia-water mixture	liquid	12.35	30	327.1
2	Ammonia-water mixture	two phase	12.35	30	390.1
3	Ammonia-water mixture	sat. vapour	9.87	30	390.1
4	Ammonia-water mixture	sat. liquid	2.48	30	390.1
5	Ammonia-water mixture	vapour	9.87	5	316.1
6	Ammonia-water mixture	liquid	2.48	30	315.8
7	Ammonia-water mixture	liquid	12.35	5	315.5
8	Ammonia-water mixture	two phase	12.35	5	315.8
9	Ammonia-water mixture	two phase	12.35	5	300.8
10	Ammonia-water mixture	liquid	12.35	5	280.7
11	Ammonia-water mixture	liquid	12.35	30	281.9
12	Ammonia-water mixture	liquid	12.35	30	312.8
1c	Cooling water	liquid	218	-	278.1
2c	Cooling water	liquid	218	-	290.8
1w	Geothermal water	liquid	80	-	393.1
2w	Geothermal water	liquid	80	-	353.1

The result of the CHP plant thermal design has been presented in a flow diagram in Figure 4 and by the solutions in Appendix B. Ascending ordered numbers illustrated on the diagram are the inlet and outlet states of each component. The diagram includes more numerical values, such as the fraction of the ammonia-water mixture, the saturated vapour ammonia-water mixture and the saturated liquid ammonia-water mixture, respectively. Furthermore, values of the energy and exergy associated with the streams have been evaluated at the above specified points. In the following section, more details on the energy and exergy analyses of the CHP plant are given.

Figures 5-8 show T-h, T-$\dot{Q}$, T-e and T-$\dot{Ex}$ diagrams for the ammonia-water mixture of the Kalina cycle and also for geothermal and cooling water, built up from the temperature data in Table 4, and enthalpy (h), heat rate ($\dot{Q}$), specific exergy (e) and exergy rate ($\dot{Ex}$) data in Table 5. In the diagrams a downward arrow notes that a stream is undergoing a cooling process. On the other hand an upward arrow notes that a stream is undergoing a heating process. There is no enthalpy difference between states 6 and 7, so these states have been shown by a point in the diagrams.

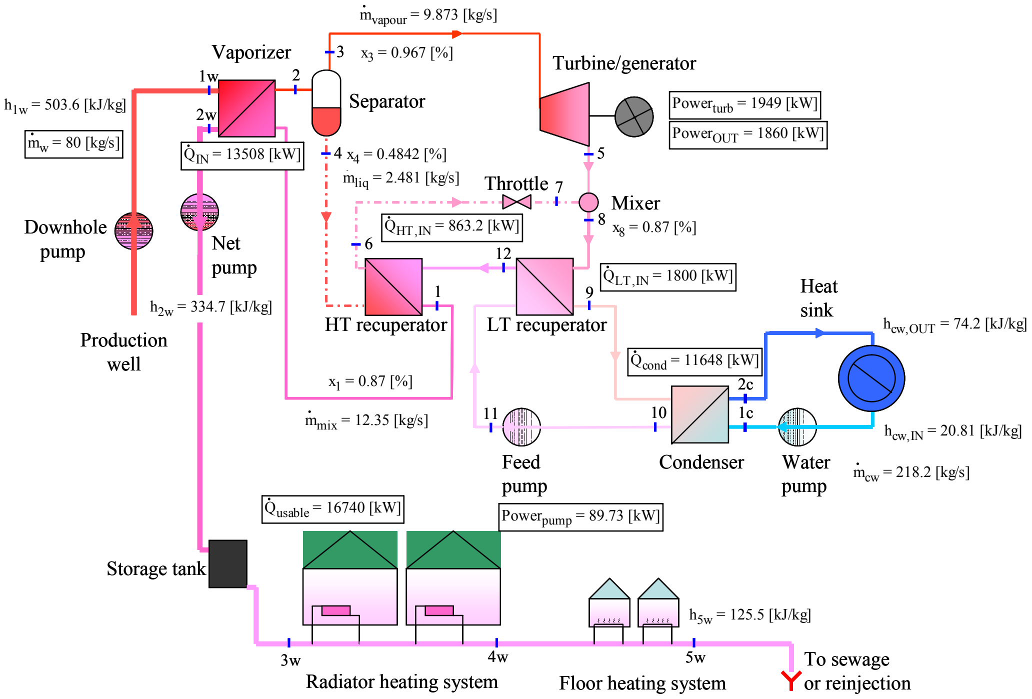

FIGURE 4: Thermodynamic design of the CHP plant

TABLE 5: h, $\dot{Q}$, e and $\dot{E}x$ associated with the streams in the Kalina PP

State	Enthalpy, kJ/kg	Heat rate, kW	Specific exergy, kJ/kg	Exergy rate, kW
1	164	2025	22	275
2	1257	15533	264	3265
3	1498	14786	281	2770
4	301	747	87	216
5	1300	12837	24	239
6	-47	-116	14	34
7	-47	-116	11	28
8	1030	12721	44	545
9	884	10921	29	364
10	-59	-728	0	1
11	-52	-638	4	47
12	94	1162	13	162
1w	504	40285	79	6322
2w	335	26777	36	2882
1c	21	4541	0	0
2c	74	16189	1	259

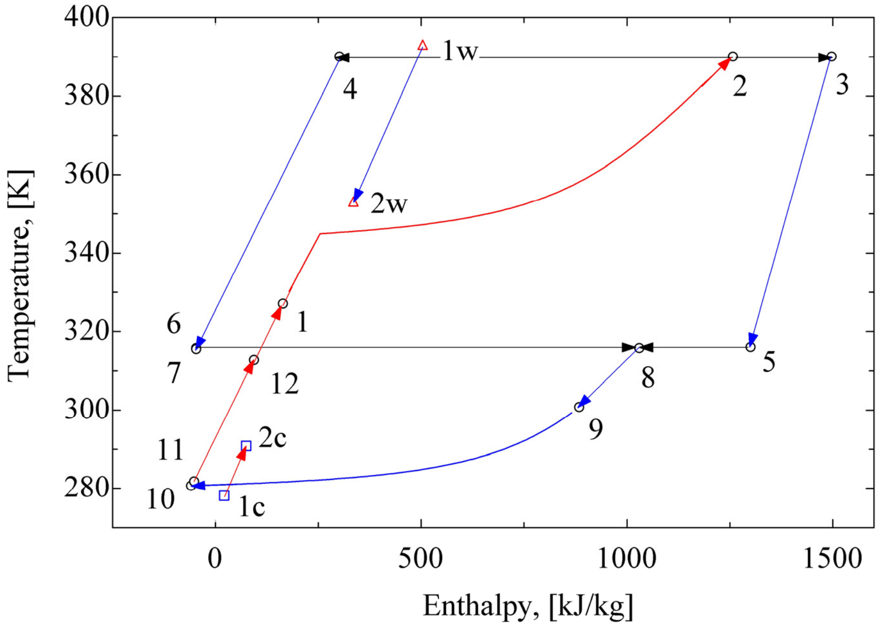

FIGURE 5: T-h diagram of the Kalina cycle

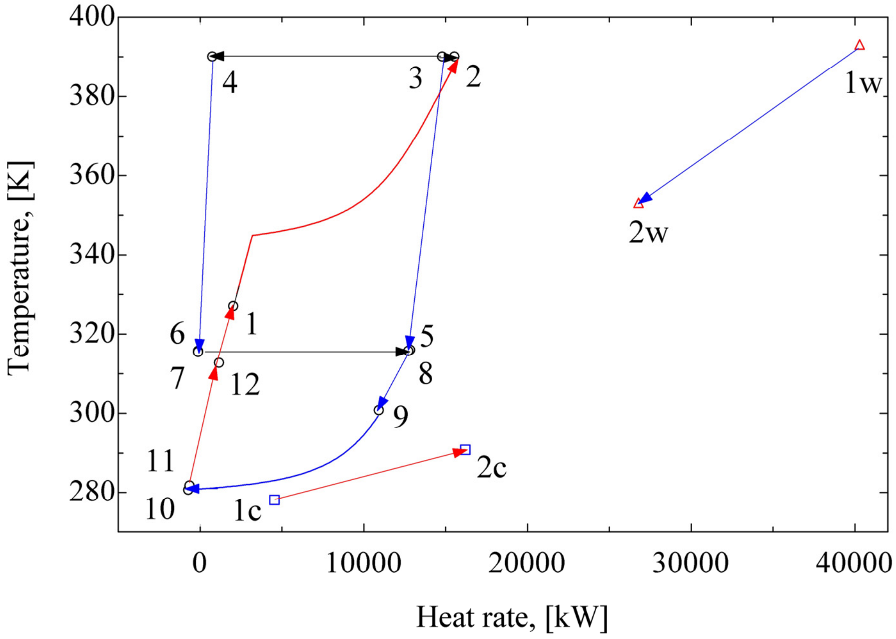

FIGURE 6: T-$\dot{Q}$ diagram of the Kalina cycle

The plots in Figures 7 and 8 show that the specific exergy and exergy rate associated with ammonia-water mixture in state 8 have increased during the mixing process. This is a consequence of the same environmental conditions applied to the exergy calculation of the different streams (basic, saturated vapour and liquid ammonia-water mixture). Possible different environment conditions may be selected for the saturated vapour and liquid streams than for the basic mixture stream.

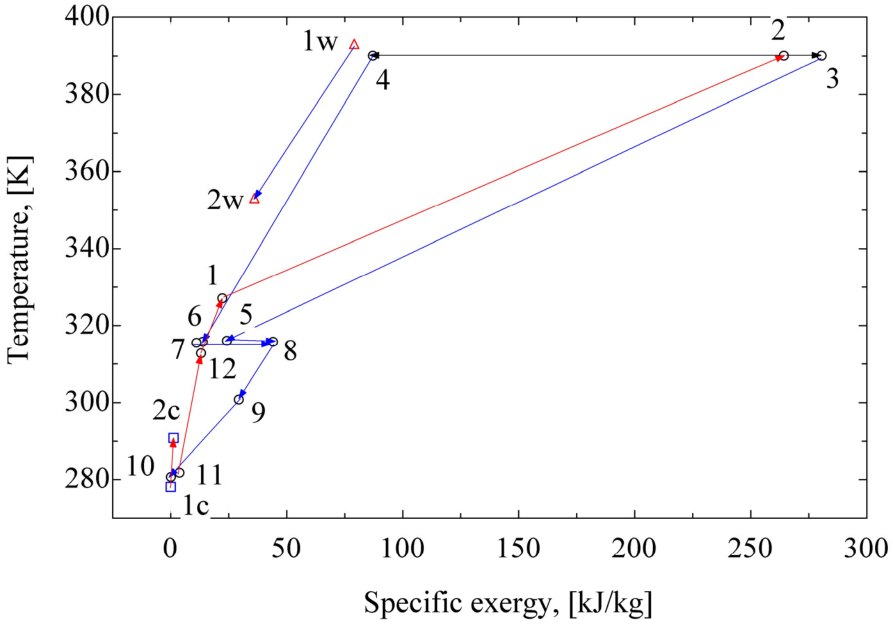

FIGURE 7: T-e diagram of the Kalina cycle

Figures 9-12 show the temperature profiles of the boiling, condensing and heat addition processes inside the heat exchangers, respectively. The ammonia-water mixture boiling curve shown in Figure 9 closely matches the variable temperature drop of the geothermal water. Here about 79.9 percent of the ammonia-water mixture is vaporized in the vaporizer. This partial vaporization also helps to decrease the area between the two curves, thereby increasing plant efficiency. The temperature profile in Figure 10 shows the ammonia-water mixture condenses over a variable temperature range. Its exit temperature from the condenser is below the cooling water exit temperature. It allows a lower turbine back pressure without excessive coolant flow. In the Kalina cycle, the recuperators preheat the feed ammonia-water mixture prior to vaporizer, making possible both higher power conversion efficiency and a higher geothermal water temperature leaving the power plant for use in DH.

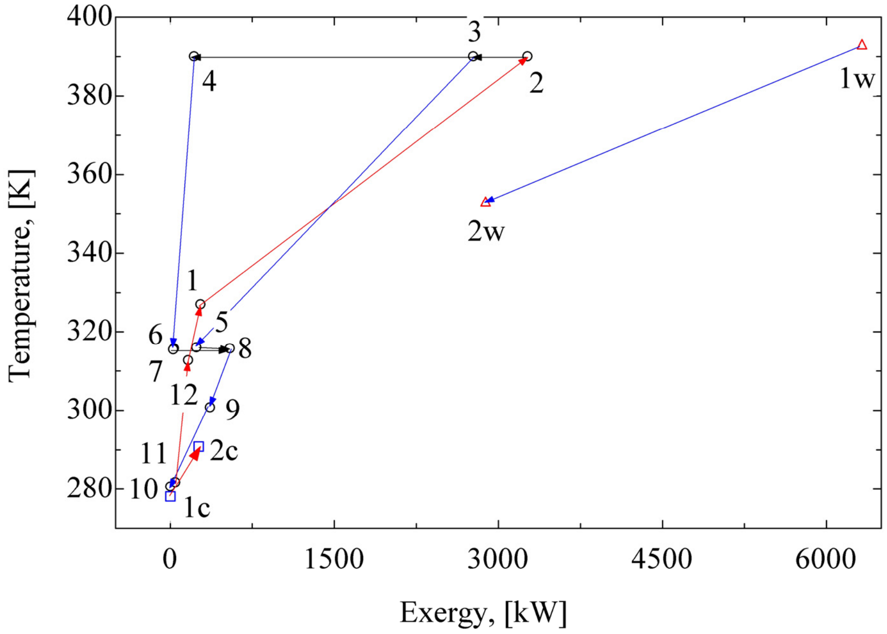

FIGURE 8: T- $\dot{E}x$ diagram of the Kalina cycle

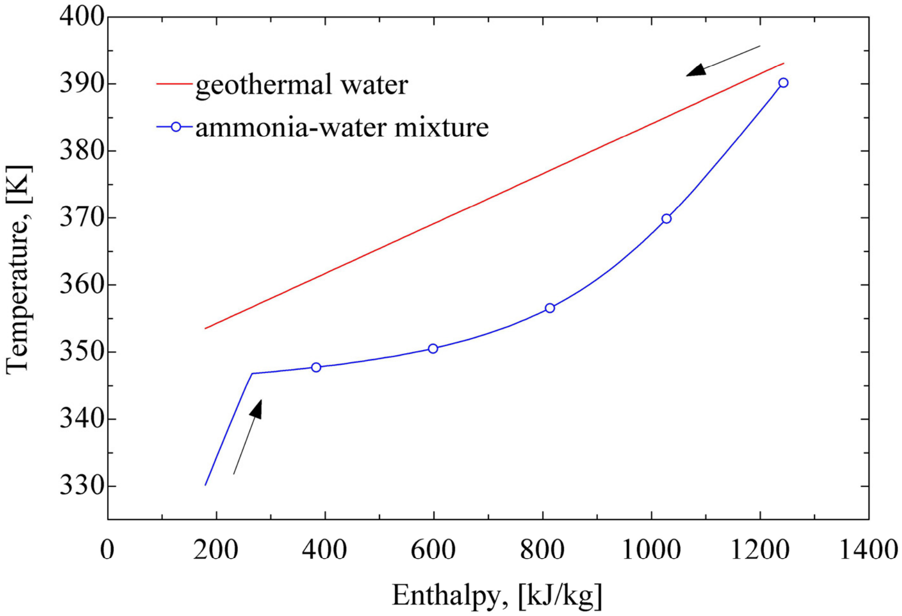

FIGURE 9: dT vs. dh diagram for the vaporizer

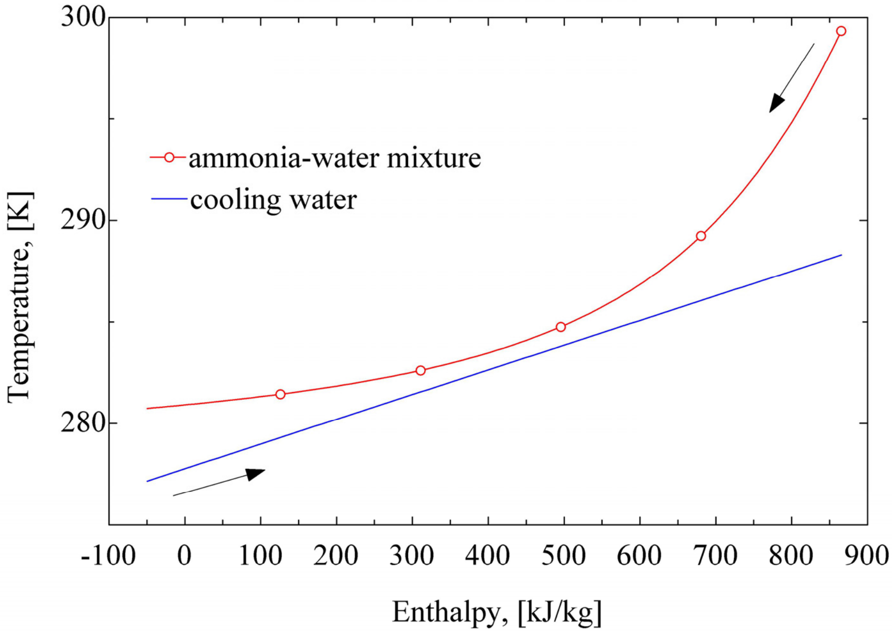

FIGURE 10: dT vs. dh diagram for the condenser

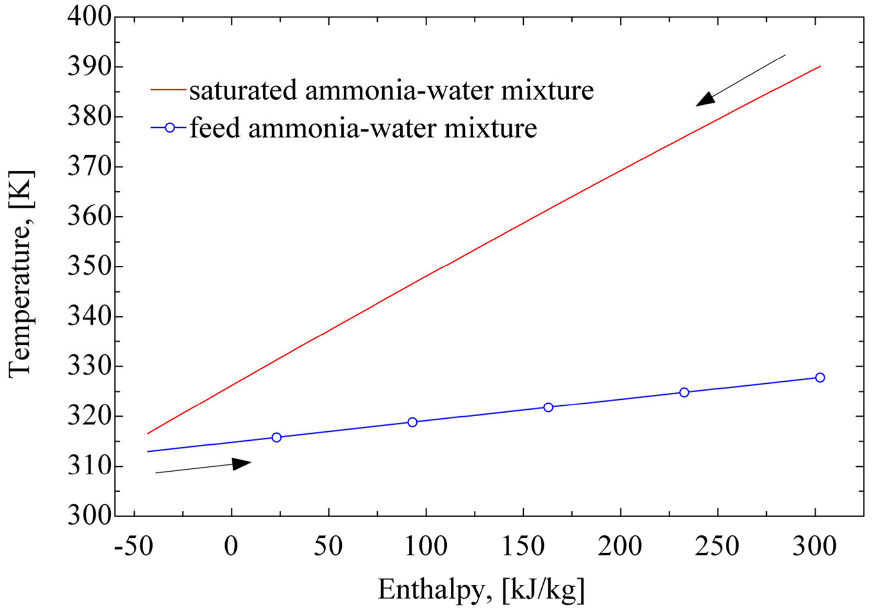

FIGURE 11: dT vs. dh diagram for the HT recuperator

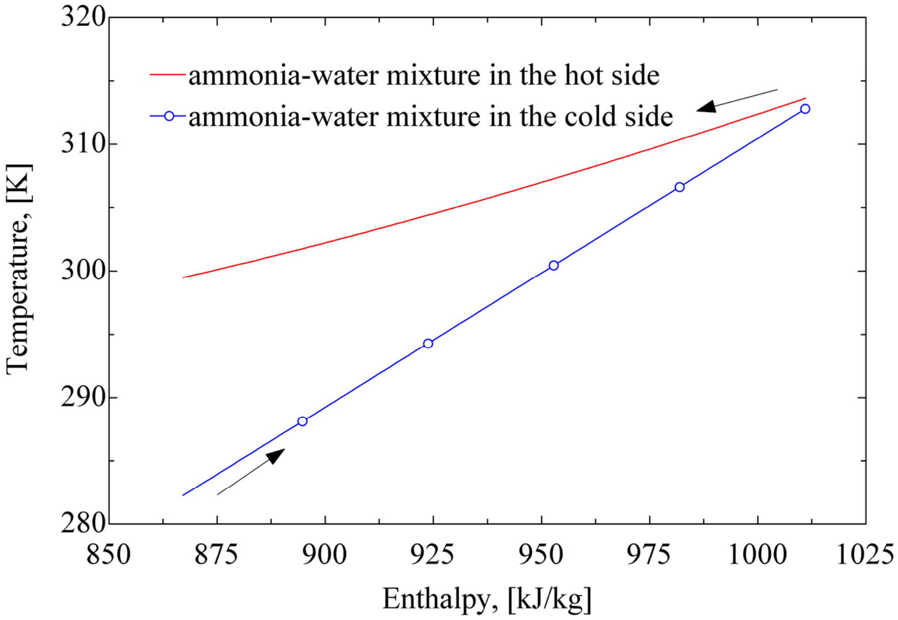

FIGURE 12: dT vs. dh diagram for the LT recuperator

3. ENERGY AND EXERGY ANALYSES

3.1 Streams

The Kalina PP uses an ammonia-water mixture as a working fluid. The fraction and flowrate of the ammonia-water mixture can be the design variables. These can be defined by mass and heat balance of the mixture as follows (also see Equations in line 67-68 in Appendix A):

$$\dot{m}_{mix} x_{mix} = \dot{m}_{vapour} x_3 + \dot{m}_{liq} x_4 \qquad 1$$

$$\dot{m}_{mix} h_2 = \dot{m}_{vapour} h_3 + \dot{m}_{liq} h_4 \qquad 2$$

Here the subscripts *vapour* and *liq* denote saturated vapour ammonia-water mixture in state 3 and saturated liquid ammonia-water mixture in state 4 (Figure 3). Mass flowrate of the mixture, $\dot{m}_{mix}$ can be calculated from the heat balance of the vaporizer (see Equation in line 52 in Appendix A). The left-hand side of this equation represents the hot side stream in the vaporizer, i.e. the geothermal water, and its flowrate is fixed. The geothermal water's thermodynamic properties at input and output states of the vaporizer are defined easily from the two known properties of temperature and quality (see Functions in lines 37-40 in Appendix A).

See more details on nomenclature at the end of the thesis.

3.2 Energy analysis

Here the energy utility of the CHP plant is described. The energy analysis is based on the conservation principle of the first law of thermodynamics. Finally, a Sankey diagram representation of the energy flows in the CHP plant is drawn.

From the thermodynamic design shown in Figure 4, the energy balance for the Kalina PP (when stray heat transfers to the environment $\dot{Q}_0$ is not accounted for) is:

$$\dot{Q}_{IN} = Power_{turb} - Power_{pump} + \dot{Q}_{cond} = Power_{out} + \dot{Q}_{cond} \qquad 3$$

The heat delivered into the Kalina PP is used for net power generation ($Power_{out}$) and the rest is rejected in the condenser. The heat amount delivered from the geothermal water is determined by:

$$\dot{Q}_{IN} = \dot{m}_w (h_{1w} - h_{2w}) \qquad 4$$

Also, for the condenser, $\dot{Q}_{cond}$ the heat rejected by cooling water is:

$$\dot{Q}_{cond} = \dot{m}_{mix} (h_8 - h_9) \qquad 5$$

The turbine power production rate or the actual turbine work (Cengel, 1994) is:

$$Power_{turb} = Power_{isentropic} \eta_{turb} \qquad 6a$$

$$\eta_{turb} = \frac{h_3 - h_5}{h_3 - h_{5s}} \qquad 6b$$

where h_5 and h_{s5} are the enthalpy values at the exit state for actual and isentropic processes, respectively.

Similarly, pump power is defined as:

$$Power_{pump} = Power_{pump,isentropic} \cdot \eta_{pump} \tag{7a}$$

$$Power_{pump,isentropic} = v_{10} \cdot (P_{high} - P_{low}) \tag{7b}$$

where v_{10} is the volume of the ammonia-water mixture at the inlet state of the pump in state 10.

The energy conversion efficiency for a heat engine operating cyclically between two thermal energy reservoirs is (Kotas, 1985):

$$\eta = \frac{W_{NET}}{Q_{IN}} \tag{8}$$

where W_{NET} is the power delivered to the network and Q_{IN} is the corresponding heat transfer to the engine per cycle.

The efficiency of the CHP plant under consideration also known as the first law of thermal efficiency, is:

$$\eta_{I,law} = \frac{Power_{out}}{Q_{IN}} = 13.8\%$$

The highest conversion efficiency of the Kalina PP, the Carnot efficiency, is given by:

$$\eta_{Carnot} = \frac{T_{high} - T_{low}}{T_{high}} = 29.3\% \tag{9}$$

According to Valdimarsson (2003b), the Carnot efficiency should not be used as a reference for a geothermal utilization CHP plant. The maximum obtainable efficiency of a geothermal application is defined by:

$$\eta_{I,law,\max} = \frac{\dot{Ex}_{IN} - \dot{Ex}_{Lo} - \dot{Ex}_{cond,Lo}}{\dot{Q}_{IN}} = 23.5\% \tag{10}$$

Here $\dot{Ex}_{IN}$ is the time rate of the exergy associated with geothermal water, $\dot{Ex}_{L}$ and $\dot{Ex}_{cond,L}$ are the exergy loss rates from the vaporizer and the condenser. See Section 3.3 for more detailed definition of the energy.

The usable supply of heat into the DH system by the geothermal water is estimated as:

$$\dot{Q}_{usable} = \dot{m}_w c_p (tk(T_{low}) - tk(T_{5,w})) \tag{11}$$

where *tk(T)* is the EES function for the conversion of degree Celsius (°C) to Kelvin (K). c_p is specific heat at constant pressure and is defined as the energy required to raise the temperature of a unit mass of a substance by one degree (Cengel, 1994). The expression for the specific heat at constant pressure c_p can be given as:

$$c_p = \left(\frac{\partial h}{\partial T} \right)_p \tag{12}$$

Energy flow through the CHP plant has been calculated (Appendix A) and the values are listed in Table 6.

A comprehensive graphic representation of the energy flow in the plant is given by a Sankey diagram. In the Sankey diagram the width of all fluxes is exactly fitted to the magnitude of energy in the stream. The Sankey diagram for the CHP plant is shown in Figure 13, which was drawn based on data listed in Tables 5 and 6.

TABLE 6: Energy utility of the CHP plant

Energy Utility	Amount	Unit	%
Kalina PP			
Heat input (usable heat >80°C)*	13.50	MWt	87.0
Total feed back	2.03	MWt	13.0
HT recuperator heat utility	0.86	MWt	6
LT recuperator heat utility	1.80	MWt	11
Heat rejected by Condenser	11.65	MWt	75
Turbine power output	1.95	MWe	13
Pump power	0.09	MWe	1
Net power output	1.86	MWe	12
DH system			
Heat input (usable heat >30°C)**	16.74	MWt	100.00

* - estimation based on 120°C geothermal water cooled down to 80°C
** - estimation based on 80°C geothermal water cooled down to 30°C

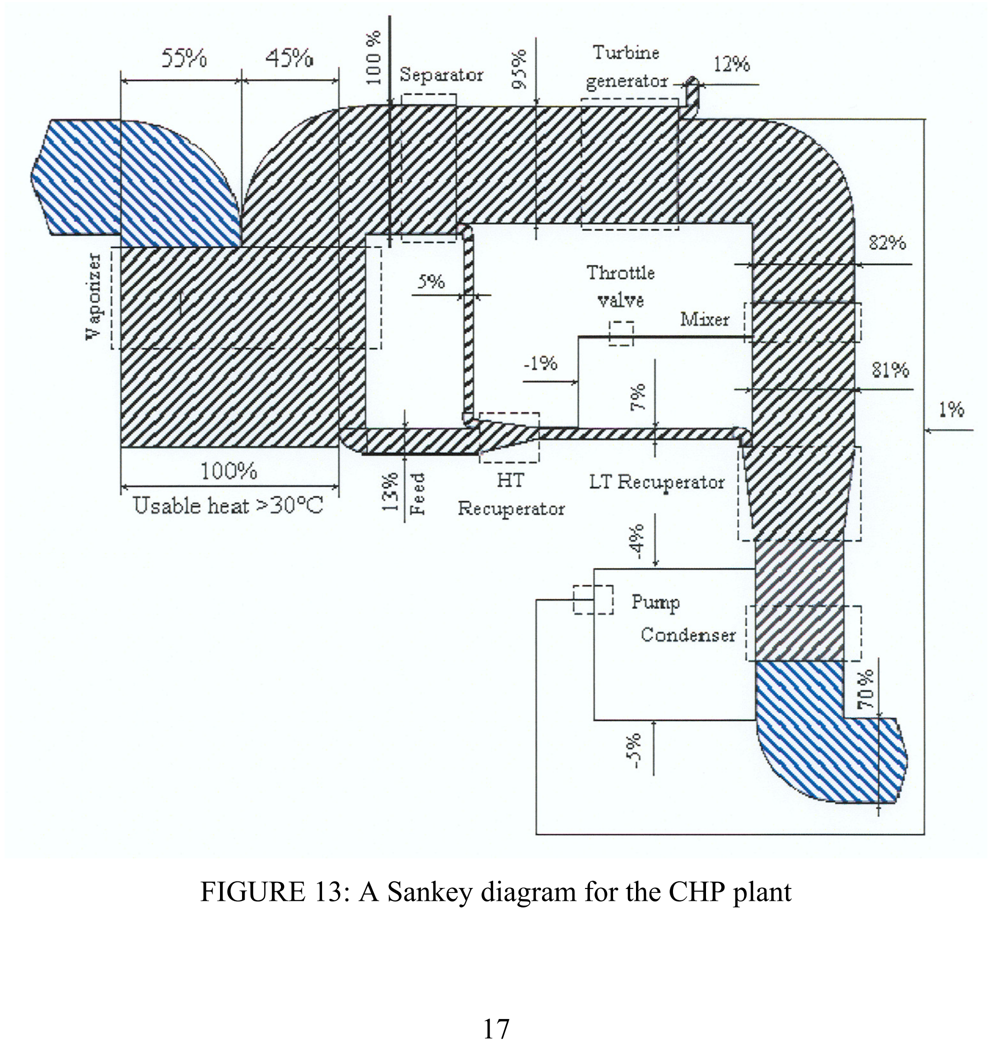

FIGURE 13: A Sankey diagram for the CHP plant

3.3 Exergy analysis

An exergy analysis of the CHP plant is presented here, starting with the basic concepts of exergy and continued with the essential underlying concept of the state of environment. Furthermore, exergy destruction and loss in the components of the plant is discussed. Finally, a Grassman diagram for the CHP plant is made, representing the exergy flows and the exergy destruction and loss rates in the components. The importance of exergy analysis is to understand the nature of exergy destruction and how to minimize it in a design process.

A definition of "exergy" is the useful work potential (or the maximum possible work) of a system when it undergoes a reversible process from a specified initial state to a state of its environment (Bejan et al., 1996). Due to the irreversibility (exergy destruction) of thermal processes, the work obtained is always less than the maximum work. Hence, by analyzing work loss within a plant, imperfections can be pinpointed and quantified, and possible improvements suggested. Also, different sorts of energy can be directly compared in exergetic terms. A Grassmann diagram, on which the width of a flow line is determined by its exergy value, is used to illustrate the exergy flow across a plant.

The environmental state is a restricted equilibrium, where conditions of thermal equilibrium between the system and the environment are satisfied. The state of restricted equilibrium with the environment will be referred to as the environmental state. The Kalina PP will be supplied by cooling water with a temperature of 5°C. Thus, the environmental state of this plant is selected as the 5°C environmental temperature.

The heat delivered by a component of an open system is equal to a specific physical exergy associated with the temperature and pressure of a stream of matter (Bejan et al., 1996). Herein, the open system is a properly selected region in space. Both mass and energy can cross the boundary of a control volume. Thus:

$$e_k = (h_k - h_0) - T_0(s_k - s_0) \qquad 13$$

where e_k is the k-th stream's specific physical exergy. The subscript 0 refers to the environmental state of the process. Thus, the physical exergy of the stream equals the specific physical exergy of the stream multiplied by the stream flowrate as follows:

$$\dot{E}x_k = \dot{m}e_k \qquad 14$$

A component at steady state, an exergy rate balance for the component can be defined as the time rate of exergy transfer at the input and output ($\dot{E}x_{F,k}$) of the plant component, equal to the sum of the desired product, the component's exergy destruction and loss (Bejan et al., 1996):

$$\dot{E}x_{F,k} = \dot{E}x_{D,k} + \dot{E}x_{Lo,k} + \dot{E}x_{P,k} \qquad 15$$

The product represents the desired result produced by the component. The fuel represents the resources used to generate the product.

According to an assumption by Bejan (1996), exergy destruction, $\dot{E}x_{D,k}$ inside a plant occurs through heat transfer and friction. Exergy loss, $\dot{E}x_{Lo,k}$ occurs when stream flows from the plant to the outside and is not of use to any other component. For each component of the Kalina PP, the value of the exergy destruction rate can be obtained from the exergy rate balance, Equation 15. It should be noted that there are two streams flowing from the plant to the outside. These are the geothermal water stream from the vaporizer and the cooling water stream from the condenser. The time rate of exergy associated with the streams, and the exergy destructions and losses in the Kalina PP have been estimated (Appendix A); the values are listed in Table 7.

The first law of efficiency alone is not a realistic measure of the performance of plant, thus the second law of efficiency needs to be defined as the ratio of the exergy recovered (or the desired product) to the exergy supplied to the Kalina PP (Cengel, 1994):

$$\eta_{II,law} = \frac{Power_{OUT}}{\dot{E}x_{IN} - \dot{E}x_{Lo} - \dot{E}x_{cond,Lo}} = 58.5\% \tag{16}$$

A Grassman diagram is a graphical method for describing the exergy flows and their destruction and loss magnitudes in a plant. Figure 14 shows the Grassman diagram for the Kalina PP and was drawn based on the data in Table 7. In Figure 14, a triangle marked by a wide downward diagonal indicates exergy destruction in the components and a rectangle marked by a wide downward diagonal indicates exergy loss from the plant. In the diagram the width of each flux (stream) is exactly fitted to the magnitude of exergy in the stream. Wide arrows in the diagram show the flow directions of the streams. Initially, the Kalina cycle starts with a mixture flux being heated up when it flows as a cold fluid through the vaporizer and into the separator. The geothermal water enters as a hot fluid in the vaporizer and it delivers a certain amount of exergy to the Kalina PP for power generation; the rest is directed to the DH system.

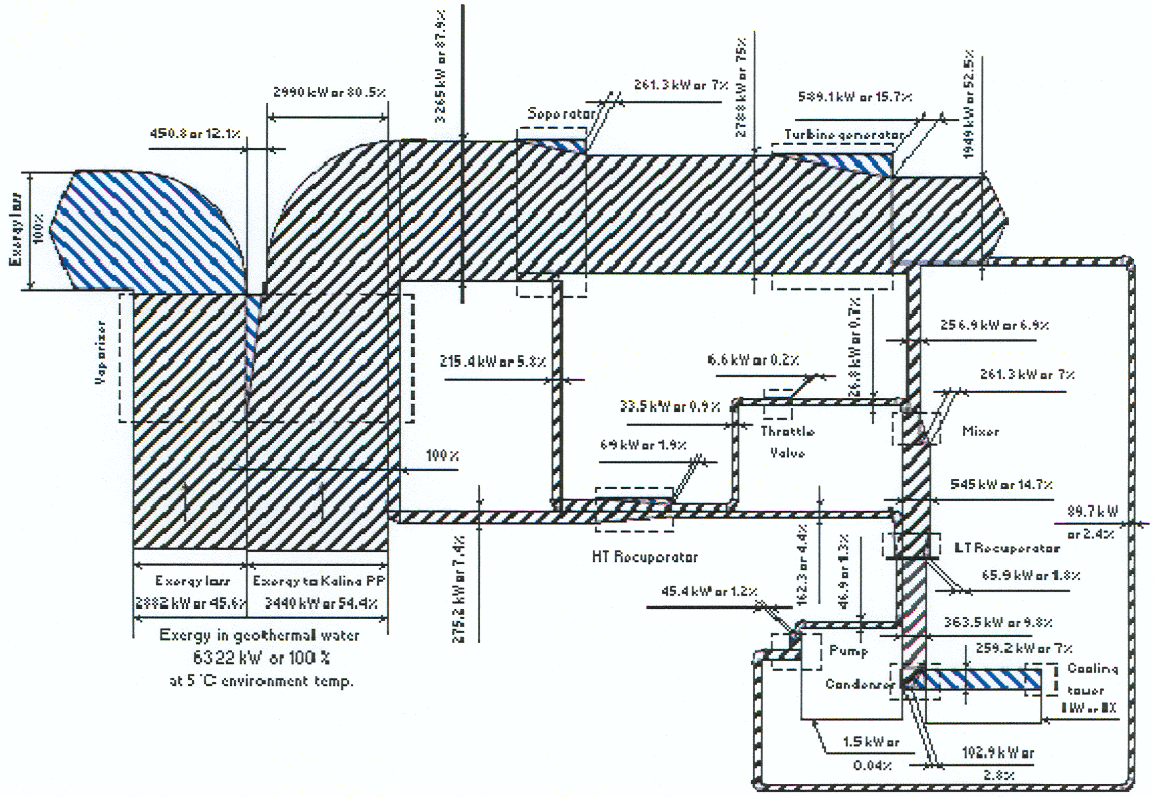

FIGURE 14: A Grassman diagram of exergy rates in the Kalina PP

TABLE 7: Estimated time rate of exergy associated with streams in the Kalina PP and destructions and losses in the components

Time rate of exergy	Notation in EES	Unit, kW	%
In the geothermal water	Ex_{IN}	6322.0	100.0
Loss from the vaporizer	Ex_{Lo}	2882.0	45.6
Added into the vaporizer	Ex_{add}	3440.0	54.4
In the mixture before the vaporizer	$Ex_{vap,IN}$	275.2	7.4
In the mixture after the vaporizer	$Ex_{vap,OUT}$	3265.0	87.9
Rise by the vaporizer	$Ex_{vap,rise}$	2990.0	80.5
Destruction in the vaporizer	$Ex_{vap,D}$	450.8	12.1
In the saturated vapour after separator	Ex_{vapour}	2788.0	75.0
In the saturated liquid after separator	Ex_{liq}	215.4	5.8
Destruction in the separator	$Ex_{sep,D}$	261.3	7.0
Turbine generator	Ex_{turb}	1949.0	52.5
In the saturated vapour after the turbine	$Ex_{turb,out}$	256.9	6.9
Destruction in the turbine	$Ex_{turb,D}$	581.9	15.7
In the saturated liquid after HT recuperator	$Ex_{HT,liq,OUT}$	33.5	0.9
Add by the HT recuperator	$Ex_{HT,liq,add}$	181.9	4.9
In the feed mixture before HT recuperator	$Ex_{HT,IN}$	162.3	4.4
In the feed mixture after HT recuperator	$Ex_{HT,OUT}$	275.2	7.4
Rise by the HT recuperator	$Ex_{HT,rise}$	112.9	3.0
Destruction in the HT recuperator	$Ex_{HT,D}$	69.0	1.9
In the saturated vapour after the throttle	$Ex_{throttle,out}$	26.8	0.7
Destruction in the throttle	$Ex_{throttle,D}$	6.6	0.2
In the mixture after the mixer	Ex_{mixer}	545.0	14.7
Add by the mixer	$Ex_{mixer,add}$	261.3	7.0
Add by the LT recuperator	$Ex_{LT,add}$	181.4	4.9
Rise in the feed mixture by the LT recuperator	$Ex_{LT,rise}$	115.5	3.1
In the mixture after LT recuperator	$Ex_{LT,OUT}$	363.5	9.8
Destruction in the LT recuperator	$Ex_{LT,D}$	65.9	1.8
In the mixture after the condenser	$Ex_{cond,OUT}$	1.5	0.0
Destruction in the condenser	$Ex_{cond,D}$	102.9	2.8
Loss from the condenser	$Ex_{cond,Lo}$	259.2	7.0
Add by the condenser	$Ex_{cond,add}$	362.1	9.7
In the cooling water before the condenser	$Ex_{cw,IN}$	0.0	0.0
In the cooling water after the condenser	$Ex_{cw,OUT}$	259.2	7.0
Rise in the cooling water	$Ex_{cw,rise}$	259.2	7.0
In the feed mixture after the pump	$Ex_{pump,OUT}$	46.9	1.3
Add in the feed mixture by the pump	$Ex_{pump,add}$	45.4	1.2
Destruction in the pump	$Ex_{pump,D}$	44.4	1.2
Pump power	$Power_{pump}$	89.73	2.4
Total exergy destruction	$Ex_{D,total}$	1582.8	
Total exergy loss	$Ex_{Lo, total}$	3141.0	

4. COMPONENT SIZING AND COST ESTIMATION

4.1 Heat exchanger sizing

The size of principal components (heat exchangers, turbine and pump) can be estimated based on the base-case design of the Kalina PP. Basically, the heat exchanger size can be calculated using two different methods, the Log Mean Temperature Difference (LMTD) and the Effectiveness Number of Transfer Unit (NTU) methods (Holman, 2002).

4.1.1 The log mean temperature difference method

For a heat exchanger, the total heat transfer rate per unit time q can be expressed in the following form (Holman, 2002):

$$q = UA\Delta T_m = UA \cdot \left[\frac{(T_{h2} - T_{c2}) - (T_{h1} - T_{c1})}{\ln\left[(T_{h2} - T_{c2})/(T_{h1} - T_{c1})\right]} \right] \qquad 17$$

where U is the overall heat transfer coefficient, A is the surface area for heat transfer consistent with the definition of U, and ΔT_m is the suitable mean temperature difference across the heat exchanger. The two parameters T_{h1} and T_{h2} are the outlet and inlet temperatures of the hot side fluid of the heat exchanger, respectively. The other parameters, T_{c1} and T_{c2} are the inlet and outlet temperatures of the cold side fluid of the heat exchanger.

The grouping of terms in the main square brackets in Equation 17 is called the *log mean temperature difference* (LMTD) or, in other words, the suitable mean temperature difference across the heat exchanger. The size of the heat exchanger can be defined from the relationship in Equation 17.

The HT and LT recuperator sizes can also be estimated by the LMTD method (see Equations in lines 100-101 and Equations in lines 118-119 in Appendix A).

4.1.2 Effectiveness of the NTU method

The other method for estimating principal component sizes is heat transfer analysis by Effectiveness NTU (Holman, 2002). In general, the number of transfer units (NTU) notes the grouping of terms $UA / C_{\min}$, where $C_{\min}$, the heat capacity of the heating fluid, equals the fluid mass flowrate multiplied by the specific heat capacity or $\dot{m}_c c_c$.

When the inlet and outlet temperatures for a given heat exchanger are to be calculated, the analysis frequently involves an iterative procedure because of the logarithmic function in MTD. According to Holman (2002) the definition of heat exchanger effectiveness is given as:

$$Effectiveness = \varepsilon = \frac{actual\_heat\_transfer}{\max imum\_possible\_heat\_transfer} \qquad 18$$

In the case of the vaporizer, the actual heat transfer is computed for the counter-flow heat exchanger, or:

$$\dot{Q}_{IN} = \dot{m}_w (h_{1w} - h_{2w}) = \dot{m}_{mix} (h_2 - h_1)$$

and the maximum possible heat transfer for the vaporizer is calculated as:

$$\dot{Q}_{\max} = \dot{m}_{mix} c_{mix} (tk(T_{high}) - T_1)$$

where c_{mix} is the specific heat of the mixture.

Similar equations are used for the actual and maximum possible heat transfer estimates of the condenser.

The NTU relationships for counter-flow heat exchangers presented in Table 10-4 in Holman (2002), are valid for our case:

$$NTU = \frac{1}{(C-1)} \ln(\frac{\varepsilon - 1}{C\varepsilon - 1}) \tag{19}$$

where C represents $C_{\min} / C_{\max}$, $C_{\max}$ is the heat capacity of the cooling fluid which equals the fluid mass flowrate multiplied by the specific heat capacity $\dot{m}_h c_h$, and $C_{\min}$ is the heat capacity of the heating fluid which equals $\dot{m}_c c_c$.

This approach was applied for the vaporizer and condenser size estimates (see Equations in line 55-64 and Equations in line 129-137 in Appendix A).

The Overall Heat Transfer Coefficient-U

The determination of *U* is often tedious and needs data not yet available in the preliminary stages of the design. Therefore, typical values of *U* are useful for quickly estimating the required surface area. Thus, the overall heat transfer coefficient is used as a typical value for U=1 kW/m^2 K to estimate the sizes of the HT and LT recuperators. Values 0.9 and 1.1 kW/m^2 K were used for size estimation of the vaporizer and the condenser. The value for the vaporizer is the lowest one, for a steam outside and liquid inside the tubes heat exchanger, when it runs under forced circulation. The value for the condenser is based on ammonia outside and cooling water inside the tubes.

Estimated heat transfer surface area of the heat exchangers in the Kalina PP are listed in Table 8.

TABLE 8: Estimated sizes of four heat exchangers

Components	Size, m^2
Condenser	1,923
HT recuperator	44
LT recuperator	208
Vaporizer	1,410
Total	3,585

4.2 Estimation of total capital investment

4.2.1 Estimates of purchased equipment

Estimating the cost of purchased equipment (including spare parts and components) is the first step in any detailed cost estimation. Two good approaches can be used for cost estimation. The best cost estimates for purchased equipment can be obtained directly through vendors' quotations. The second approach is using cost values from past purchase orders, and quotations from experienced professional cost estimators. Here, the second approach was used for cost estimation of the Kalina PP components.

Four heat exchangers are used. In estimation of the purchased equipment cost of the heat exchangers, the base cost C_O=588 US$ per square metre of heat transfer surface area was used. Thus:

$$C_{equipment} = C_O \cdot (size\_of\_equipment)^n \qquad 20$$

where the exponent n is a constant decimal number, in our case 0.8; and *size of equipment* stands for the heat transfer surface area of the heat exchanger. The heat exchangers' heat transfer surface areas are available in Table 8. Using these data the costs of the heat exchangers have been estimated by the relationship in Equation 20 and are presented in Table 9.

TABLE 9: Estimated costs of heat exchangers

Components	Cost, US$
Vaporizer	194,385
HT recuperator	12,095
LT recuperator	42,021
Condenser	249,167

Similarly, the cost for other principal component (the turbine and pump) purchased equipment has been estimated. In this case, the power capacity of each component was applied instead of the heat transfer area, or:

$$C_{equipment} = C_O \cdot (power\_capacity)^n \qquad 21$$

where the base cost, C_O, for the pump is 1120 US$/kW, and for the turbine 4405 US$/kW. The exponents 0.8 and 0.7 were used for size estimation of the pump and turbine. Estimated values of purchased equipment cost of the turbine and the pump are listed in Table 10.

TABLE 10: Capacity and cost of the turbine and pump

Components	Capacity	Unit	Cost, US$
Turbine	1,949.0	kW	856,144
Pump	89.7	kW	462,127

So, the total purchased equipment costs for the Kalina PP is 1,815,939 US$ including the heat exchangers.

4.2.2 Total capital investment

The total capital investment (TCI) of the Kalina PP and the DH system (transmission piping cost and renovation expenses), respectively, has been estimated. The assumptions and method used for the TCI were adopted from Bejan (1996). The total capital investment of the Kalina PP estimated by those assumptions and methods is summarized in Table 11.

In Section 4.2.1, the purchased equipment costs were estimated. The direct costs of the remaining components and indirect costs are estimated using the factors shown in parentheses.

An assumption used for the allowance of funds used during construction (AFUDC) is:

$$LRD + AFUDC = 0.15 \cdot FCI$$

where LRD is the cost of licensing, research and development and is obtained by:

$$LRD = 150 \cdot Power_{turb}$$

According to Bejan (1996) the plant-facilities investment is the difference between fixed-capital investment and land costs. This gives 2,098,318 US$ (rate start 2005 Dollars).

The total non-depreciable and depreciable capital investments and the total net capital investment for the Kalina PP were calculated and are listed in Table 12.

TABLE 11: Estimate of total capital investment for the CHP plant
(all costs are expressed in US dollars at the rate start in 2005)

I Fixed capital investment	
A. Direct costs (DC)	
1 Onsite costs	
Purchased equipment costs	
- Vaporizer	194,385
- HT Recuperator	12,095
- LT Recuperator	42,021
- Condenser	249,167
- Ordinary steam turbine	856,144
- Pump	462,127
Total purchased-equipment cost (PEC)	**1,815,939**
Piping (10% of PEC)	181,594
Total onsite costs	**1,997,533**
2 Offsite costs	
Land	18,159
Total offsite costs	**18,159**
Total direct costs	**2,015,692**
B. Indirect costs	
Contingency (5% of the above sum)	100,785
Total indirect costs	**100,785**
Fixed capital investment (FCI)	**2,116,477**
II Other outlays	
A. Startup costs (Section 4.2.3)	54,181
B. Working capital (Section 4.2.3)	47,288
C. Cost of licensing, research and development (assumption)	292,406
D. Allowance for funds used during construction (assumption)	25,066
Total other outlays	**418,941**
Total capital investment	**2,535,418**

TABLE 12: Expenditures of the Kalina PP, in US$

Cost of land (01/01/2007)	19,826
Escalated PFI (6/30/2007)	2,357,670
Startup costs (6/30/2008)	64,530
Working capital (12/31/2008)	57,986
Cost of licensing, research and development (01/01/2007)	319,113
Total net outlay	**2,819,126**
Total AFUDC	**29,853**
Total capital investment (TCI)	**2,848,979**
Total nondepreciable capital investment (TNDCI)	**77,813**
Total depreciable capital invetment	**2,771,166**
Total net capital investment	**2,848,979**

Hence, the direct capital cost of the Kalina PP as calculated TCI in Table 12 per power production rate, is 1,462 US$/kW.

4.2.3 Fuel, operating and maintenance (O&M) costs

Fuel costs and variable operating costs can easily be calculated from the flow diagrams. When the flow of a stream or of a utility is known, simply multiply the flow by its unit cost and its average total time of operation per year. Thus, the contribution of the flow to total annual costs can be obtained.

Operating and maintenance (O&M) costs can be divided into fixed and variable costs. The fixed O&M costs are composed of costs for operating labour, maintenance labour, maintenance materials, overhead, administration and support, distribution and marketing, research and development, and so forth. The variable operating costs consist of the costs for operating supplies other than fuel cost.

Geothermal water cost
In the CHP plant the geothermal water is assumed as a fuel. The direct cost of the geothermal exploration work, $C_{geothermal}$ =2,066,000 US$, can be estimated based on the direct cost, 1000 US$/kW. According to the World Bank Group (2004), the direct cost for typical low-temperature geothermal resource exploration work varies between 400 and 1000 US$/kW. It includes a preliminary geological survey based on aerial photos or a remote sensing scan, detailed geological and/or geochemical surveys, geophysical surveying and/or shallow thermal gradient well drilling, drilling of test well(s) and well testing, and reservoir modelling.

The levelized specific cost of the geothermal water, $c_{F,sp}$ [US$/kg], is determined as:

$$c_{F,sp,L} = \frac{C_{geothermal} \cdot CRF}{\dot{m}_w t_{op}} \qquad 22$$

where *CRF* is the capital recovery factor (see Section 5.1) and t_{op} is the operating time in a year ($t_{op} = 8040 \cdot 3600$ seconds per year).

Thus, the numerical value of $c_{F,sp,L}$ has been calculated as 0.0001048 US$/kg or 10.48 US ¢/ton. The annual levelized cost of the geothermal water is then 242,666 US$ (entry 8 of Table 13).

O&M cost
The annual fixed and variable O&M costs are estimated here and summarised in Table 13. The following assumptions were used for the annual fixed and variable O&M cost estimation. The average capacity factor for the CHP plant is estimated as 87.5%, which means that the system will operate at full load for 8,040 h (entry 1 of Table 13) out of the total available 8760 h per year. There are assumed 5 labour positions (entry 2 of Table 13) required for operation and maintenance at an average labour rate of 5 US$/h (entry 3 of Table 13). The average number of working hours per labour position is 2,080 h per year (entry 4 of Table 13). Thus, the annual direct labour cost is 52,000 US$. Based on these numbers, the annual fixed O&M costs are estimated to be 104,000 US$. The annual variable O&M costs at full capacity are estimated to be 9,360 US$ (entries 6 and 7 of Table 13).

TABLE 13: Summary of the annual fixed and variable O&M cost

	Item	Cost	Unit
1	Operating time	8,040	h
2	Labour positions	5	
3	Average labour rate	5	US$/h
4	Working hours	2,080	h
5	Direct labour cost	52,000	US$/year
6	Annual fixed O&M cost	104,000	US$/year
7	Annual variable O&M cost	9,360	US$/year
8	Fuel Cost	242,666	US$/year

The levelized annual O&M cost is calculated from Equation 23:

$$C_{L,O\&M} = C_{O\&M} \cdot CELF = C_{O\&M} \cdot \frac{k(1-k^{N_y})}{1-k} \cdot CRF \qquad 23$$

where $k = \dfrac{1+r_n}{1+i_{eff}}$ and r_n is the constant rate of change, the annual nominal escalation rate of 6%. The i_{eff} is the effective rate of return, $i_{eff} = \left(1+\dfrac{i}{p}\right)^p - 1$, with i the interest rate, 10 % (expressed in the Equation, as a fraction, not percentage), and p is the return times per year, in this case once a year.

Thus, the levelized annual O&M cost is calculated to be 208,594 US$.

Finally, the O&M cost of the geothermal field is assumed as a tenth of the annual levelized cost of the geothermal water, or:

$$C_{L,O\&M,geothermal} = C_{geothermal} \cdot CRF \cdot 0.1 = \text{ 24,267 US\$}$$

Start-up and working capital costs

Start-up costs (SUC) for a CHP plant are defined as the sum of the following unescalated costs (Bejan et al., 1996): (a) one month of fixed O&M costs, (b) one month of variable operating costs calculated at full load, (c) one week of full-load geothermal water, and (d) 2% of the plant facilities investment. Thus,

$$SUC = \frac{104{,}000}{12} + \frac{(9{,}360 \cdot 0.875)}{12} + \frac{148{,}985}{52} + 0.02 \cdot 2{,}098{,}318 = \text{ 54,181 US\$}$$

or after escalation to the middle of 2008, *SUC*=64,530 US$ (mid-2008 dollars).

Similarly, working capital (WC) is the sum of the unescalated expenses representing 2 months of geothermal water cost at full load and 3 months of labour costs plus a contingency of 25% of the total of the above two items:

$$WC = \left[\frac{148{,}985}{6} + \frac{52{,}000}{4}\right] \cdot 1.25 = 47{,}288 \qquad \text{US\$}$$

or after escalation to the end of 2008, *WC*=57,986 US$ (end-2008 dollars).

4.2.4 DH system expenses

All expenses of the DH system were estimated in the pre-feasibility study (Eliasson et al., 2004). Thus, it is unnecessary to re-evaluate those expenses. Instead, available data from the pre-feasibility study are used (see section on “Economic analysis included costs’ of DH renovation and transmission pipeline” in Appendix C).

The total capital investment (TCI) of the Kalina PP, the direct cost of geothermal exploration work and DH system expenses have been estimated in preceding subsections. The TCI of the CHP plant is the sum of these expenses. It should be noted that the DH system has two alternatives on the distance between Tsetserleg centre and the geothermal exploration site. So, the TCI of the CHP plant is 8.66 M US$ with a 5 km long transmission pipeline, or 12.41 M US$ with a 20 km long transmission pipeline.

5. THERMOECONOMIC ANALYSIS AND EVALUATION

Thermoeconomics is the discipline which combines the concept of the Exergy method with economic analysis. In the CHP plant thermoeconomics were used for exergy-added cost minimization. In the preceding sections exergy destructions (inefficiencies) of the Kalina PP were evaluated. In practice there is often a need to know how much exergy destructions cost. Knowledge of these costs is useful for improving the cost effectiveness of the plant by reducing the costs of the final product produced by the plant. In addition, it is also applicable for a plant that has more then one product.

5.1 Exergy costing

In the Kalina PP, operating at steady-state, there exist a number of entering and exiting ammonia-water mixture streams as well as both heat and work interactions with the surroundings. Associated with the transfer of these mixture streams are the energy and exergy transfers into and out of the components and exergy destructions caused by irreversibilities within the plant. Since exergy measures the true thermodynamic value of such effects, it is meaningful to use exergy as a basis for assigning costs in the plant.

The costs associated with the time rate of exergy of the geothermal water while entering and exiting the vaporizer, and the time rate of exergy of the power production from the turbine generator can be estimated according to the following equations:

$$\dot{C}_{IN} = c_{E,IN}\dot{E}x_{IN} = c_{E,IN}(\dot{m}_w e_{IN}) \tag{24a}$$

$$\dot{C}_{OUT} = c_{DH,IN}\dot{E}x_{OUT} = c_{DH,INt}(\dot{m}_w e_{DH,IN}) \tag{24b}$$

$$\dot{C}_{turb} = c_{turb}\dot{E}x_{turb} \tag{24c}$$

where $c_{E,IN}$, $c_{DH,IN}$ and c_{turb} denote average costs per unit of exergy in US$/GJ.

The unit costs of exergy associated with geothermal water and power production are evaluated in Section 5.1.3. Exergy costs involve cost balances usually formulated separately for each component. The cost balance applied to the k-th component and the whole system is treated and discussed in the following sections.

5.1.1 Cost balance in the plant

Assume the plant to be a black box, with input and output flows drawn as shown.

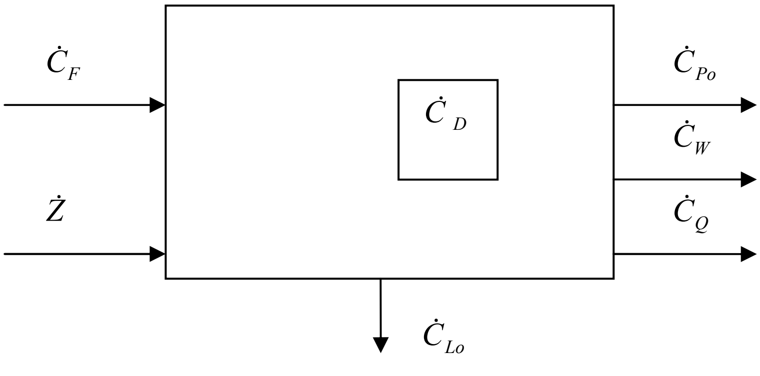

FIGURE 15: Block diagram of a black box equivalent to a power plant

In Figure 15 $\dot{C}_{Po}$, $\dot{C}_W$ and $\dot{C}_Q$ represent power, work and heat (products) cost flows all with unit [\$/s]. $\dot{C}_F$ means fuel cost flow and $\dot{Z}$ stands for capital cost flow in the same unit [\$/s]. The latter is the sum of investment ($\dot{Z}_i$) and O&M ($\dot{Z}_{OM}$) costs.

The *input* cost flow to the plant is the sum of the fuel ($\dot{C}_F$) and capital cost flows ($\dot{Z}$). The *output* cost flow from the plant is the sum of the products ($\dot{C}_P$) cost flow. The plant is not an ideal machine, therefore it should include some inside destruction ($\dot{C}_D$) and outflow of loss ($\dot{C}_{Lo}$) cost flows. So, the cost balance for the overall plant (subscript tot) operating at steady-state is formulated as:

$$\dot{C}_{P,tot} = \dot{C}_{F,tot} - \dot{C}_{L,tot} + \dot{Z} \qquad 25a$$

or in terms of the fuel and product cost rates

$$c_P \dot{E}x_P = c_F \dot{E}x_F - c_{Lo} \dot{E}x_{Lo} + \dot{Z}_{CI} + \dot{Z}_{O\&M} \qquad 25b$$

Here no cost term is directly associated with exergy destruction. The cost associated with exergy destruction in a component is a hidden cost, but a very important one, that can be revealed only through a thermoeconomic analysis (see Section 5.1.3).

The following simplifying assumptions have been made for exergy costing of the heat and power produced from the Kalina PP:

1. All pressure losses are neglected
2. All heat transfer losses are neglected
3. Power input to auxiliary equipment is neglected.

The Kalina PP is designed and its operating parameters evaluated in the previous sections. Using these data and the above assumptions, the following quantities were evaluated (also see Appendices A and C):

Turbine power:

$$Power_{turb} = 1{,}949 \text{ kW}$$

Mass flowrate of the ammonia-water mixture from the mass balance:

$$\dot{m}_{mix} = 12.35 \text{ kg/s}$$

Exergy input rate:

$$\dot{E}x_{IN} = \dot{m}_w \cdot e_{1w} = 80 \cdot 79.03 = 6{,}322 \text{ kW}$$

Steam exergy rate:

$$\dot{E}x_{vapour} = 2{,}770 \text{ kW}$$

Capital-recovery factor (CRF):

$$a_c = \frac{i_{eff}(1+i_{eff})^{N_y}}{(1+i_{eff})^{N_y} - 1} = 0.1175$$

where the period is $N_y = 20 years$.

5.1.2 Cost balance in the component

Similar to Equation 25, the cost balance for each principal component can be written as:

$$\dot{C}_{P,k} = \dot{C}_{F,k} - \dot{C}_{Lo,k} + \dot{Z}_k \tag{26a}$$

or in terms of the fuel and product cost rates

$$c_{P,k}\dot{E}x_{P,k} = c_{F,k}\dot{E}x_{IN,k} - c_{Lo,k}\dot{E}x_{Lo,k} + (\dot{Z}_{CI,k} + \dot{Z}_{O\&M,k}) \tag{26b}$$

where the subscript k denotes the k-th component of the Kalina PP. Before the above equation is solved, it is necessary to calculate the values of the $\dot{Z}_k$ term and the cost associated with exergy loss appearing in the cost balances. The cost associated with exergy loss is calculated in Section 5.1.3. According to Kotas (1985), the capital investment rate, $\dot{Z}_{CI,k}$, of k-th component is calculated as:

$$\dot{Z}_{CI,k} = \frac{CRF \cdot C_{L,k}}{t_{op}} \tag{27}$$

The purchased equipment cost C_k for the components is given in Tables 9-10. Thus, the values $\dot{Z}_{CI,k}$ for each component can be calculated (see Equations in line 8-13 in Appendix C) and escalation to the middle of 2007 is presented in Table 14:

TABLE 14: Capital investment rate of the principal components

Component	$Z_{CI,k}$, $\cdot 10^{-3}$, US$/s
Vaporizer	0.9
Condenser	1.1
HT recuperator	0.1
LT recuperator	0.2
Turbine	3.9
Pump	2.1

Similarly, the O&M cost rate, $\dot{Z}_{O\&M,k}$, of k-th component can be calculated from the following equation:

$$\dot{Z}_{O\&M,k} = \frac{CRF \cdot C_{L,O\&M}}{t_{op}} \cdot \frac{C_k}{PEC} \tag{28}$$

The results of the calculations of the escalated $\dot{Z}_{O\&M,k}$ (see Equations in line 25-30 in Appendix C) are presented in Table 15 for each principal component.

TABLE 15: O&M cost rate of the principal components

Component	$Z_{O\&M,k,}$ $\cdot 10^{-3}$, US$/s
Vaporizer	0.09
Condenser	0.12
HT recuperator	0.01
LT recuperator	0.02
Turbine	0.40
Pump	0.22

5.1.3 Cost of exergy destruction and loss

In the cost balance formulated for a plant (Equation 25b) and a component (Equation 26b), there are no cost terms associated with exergy destruction. The effect of exergy destruction can be demonstrated by combining Equations 15 and 26b (when $\dot{E}x_{F,k}$ is eliminated):

$$c_{P,k}\dot{E}x_{P,k} = c_{F,k}\dot{E}x_{P,k} + (c_F\dot{E}x_{Lo,k} - \dot{C}_{Lo,k}) + (\dot{Z}_{CI,k} + \dot{Z}_{O\&M,k}) + c_F\dot{E}x_{D,k} \qquad 29a$$

or (when $\dot{E}x_{P,k}$ is eliminated)

$$c_{P,k}\dot{E}x_{F,k} = c_{F,k}\dot{E}x_{F,k} + (c_p\dot{E}x_{Lo,k} - \dot{C}_{Lo,k}) + (\dot{Z}_{CI,k} + \dot{Z}_{O\&M,k}) + c_p\dot{E}x_{D,k} \qquad 29b$$

Hence, in costing exergy destruction it is assumed the cost associated with exergy destruction in the k-th component equals the exergy destruction rate on the k-th component multiplied by the unit cost of the product (in this case electricity) or fuel (in this case, geothermal water) as follows:

$$\dot{C}_{D,k} = c_{F,k}\dot{E}x_{D,k} \text{ (when } \dot{E}x_{P,k} \text{ fixed) or } \dot{C}_{D,k} = c_{P,k}\dot{E}x_{D,k} \text{ (when } \dot{E}x_{F,k} \text{ fixed)} \qquad 30$$

For the Kalina PP plant, the right hand side equation is preferred, because the geothermal water resource is restricted. Hence, the cost of the exergy destruction rates in the components can be calculated (see Equations in line 53-60 in Appendix C). The values are listed in Table 16.

TABLE 16: Cost of exergy destruction in the principal components of the Kalina PP

Component	$C_{D,k}$, $\cdot 10^{-3}$, US\$/s
Turbine	5.1
LT recuperator	2.6
HT Recuperator	2.3
Vaporizer	2.3
Condenser	0.5
Pump	0.2

There are two loss streams flowing from the vaporizer and the condenser. The exergy loss stream of the condenser is finally charged to the natural environment. The simplest approach to costing this exergy loss associated with the condenser is to set

$$\dot{C}_{Lo,cond} = 0$$

Another exergy loss stream of the vaporizer is used for heating. Thus, the cost of this stream is estimated differently than the above approach as follows:

$$\dot{C}_{Lo} = c_{E,DH,IN} \cdot \dot{E}_{Lo}$$

where $c_{E,DH,IN}$ is the levelized unit cost of exergy associated with the loss stream of the vaporizer; its numerical value has been evaluated in Section 5.1.3.

5.1.4 Unitary cost of exergy

The levelized unit cost of exergy associated with geothermal water in the Kalina PP or the vaporizer has been estimated (see Equation in line 44 in Appendix C) and its numerical value is:

$$c_{E,IN} = \frac{c_{F,sp,L}}{e_{1w}} = 1.326x10^{-6} \text{ US\$/kJ} = 0.5 \text{ US ¢/kWh}$$

Similarly, the levelized unit cost of exergy associated with geothermal water in the DH system (or with the exergy loss stream from the vaporizer) is:

$$c_{E,DH,IN} = \frac{c_{F,sp,L}}{e_{2w}} = 2.909x10^{-6} \text{ US\$/kJ} = 1 \text{ US ¢/kWh}$$

The levelized unit cost of exergy transfer associated with power production of the turbine generator has also been calculated as:

$$c_{E,turb} = 8.185x10^{-6} \text{ US\$/kJ} = 2.4 \text{ US ¢/kWh}$$

Finally, the cost rates and the levelized unit costs associated with each stream in the Kalina PP have been calculated (see Equations 69-85 in Appendix C) and the results are given in Table 17.

TABLE 17: The levelized cost rate and unit cost of exergy in the Kalina PP

Stream No.	Exergy rate, Ex, kW	Levelized cost rate, C, $\cdot10^{-3}$, US$/s	Levelized cost per exergy unit, c, US$/GJ
1	275.1	9.3	33.8
2	3265.0	16.5	5.1
3	2770.0	14	5.1
4	216.3	1.1	5.1
5	239.1	1.2	5.1
6	34.4	0.2	5.1
7	27.8	0.1	5.1
8	544.9	2.8	5.1
9	363.5	1.8	5.1
10	1.4	0.0	5.1
11	46.8	3.0	63.3
12	162.3	6.3	39.0
1c	0.0	0.0	0.0
2c	0.0	0.0	0.0
1w	6322	8.4	1.3
2w	2882	8.4	2.9
Power prod.	1949.0	17.1	8.8

5.2 Thermoeconomic evaluation

A detailed thermoeconomic evaluation of the base-case design of the Kalina PP should be based on the following variables, calculated for each system component:

- Exergetic efficiency, ε_K
- Exergy destruction and loss ratio, $y_{D,K}$, $y_{Lo,K}$
- Relative cost difference, r_K
- Exergoeconomic factor, f_K

5.2.1 Exergetic efficiency

Exergetic efficiency is a parameter for evaluating the thermodynamic performance of a system. Exergetic efficiency provides a true measure of performance of an energy system from a thermodynamic viewpoint.

Exergetic efficiency ε of the overall plant is the ratio between product and fuel (Bejan et al., 1996):

$$\varepsilon = \frac{\dot{E}x_P}{\dot{E}x_F} = 1 - \frac{\dot{E}x_D + \dot{E}x_{Lo}}{\dot{E}x_F} \tag{31}$$

Exergetic efficiency of the plant components can be estimated in a similar way. Its values have been estimated in lines 86-95 in Appendix C and are listed in order of descending value in Table 18. Exergetic efficiency for the Kalina PP can be calculated as the percentage of the time rate of exergy associated with the geothermal water supplied to the plant that is recovered in the power product of the plant, identifying the product of Kalina PP as the net power generated.

TABLE 18: Exergetic efficiencies of components and overall plant

Component	Exergetic efficiency, ε, %
Separator	92.00
Vaporizer	86.90
Throttle	80.19
Turbine	77.01
Condenser	71.58
LT recuperator	63.65
HT recuperator	62.05
Pump	50.54
Plant	28.25

5.2.2 Exergy destruction and loss ratio

The values of the time rates of exergy destruction $\dot{E}x_D$ (Table 7) provide thermodynamic measures of a plant's inefficiencies. Related to these measures the exergy destruction ratio $y_{D,K}$ can be calculated. The time rate of exergy destruction in plant components can be compared to the time rate of exergy associated with geothermal water provided to the overall plant, $\dot{E}x_{IN}$, giving the exergy destruction ratio:

$$y_{D,K} = \frac{\dot{E}x_{D,k}}{\dot{E}x_{IN}} \tag{32}$$

The exergy loss ratio is defined similarly, by comparing exergy loss to exergy of fuel provided to the overall plant:

$$y_{Lo,K} = \frac{\dot{E}x_{Lo,k}}{\dot{E}x_{IN}} \tag{33}$$

The exergy destruction and loss ratio of the Kalina PP components were estimated by Equations 32-33 (see Equations in lines 96-107 in Appendix C) and their values are listed in Table 19. As illustrated by the data in Table 19, the reduction in overall efficiency caused by exergy destruction and loss can be expressed as: $\varepsilon_{plant} = 1 - \sum y_D - \sum y_{Lo} = 1 - 0.2404 - 0.4771 = 0.2825$.

TABLE 19: Exergy destruction and loss ratio of the components

Component	Exergy destruction ratio, y_D, %
Vaporizer	6.85
Seperator	3.97
Turbine	8.84
HT recuperator	1.05
Throttle	0.10
LT recuperator	1.00
Condenser	1.56
Pump	0.67
Total destruction	24.04
	Exergy loss ratio, y_{Lo}, %
Vaporizer	43.78
Condenser	3.94
Total loss	47.71

5.2.3 Relative cost difference and exergoeconomic factor

The relative cost difference represents the relative increase in the average cost per exergy unit between fuel and product of the component. The relative cost difference r_K for the k-th component is defined by:

$$r_k = \frac{c_{F,k}(\dot{E}x_{D,k} + \dot{E}x_{Lo,k}) + (\dot{Z}_{CI,k} + \dot{Z}_{O\&M,k})}{c_{F,k}\dot{E}x_{P,k}} \qquad 34$$

As Equation 34 indicates, the cost sources in a component may be grouped in two categories. The first consists of exergy destruction and exergy loss, while the second category consists of non-exergy-related costs (capital investment and O&M expenses).

In evaluating the performance of a component, it is important to know the relative significance of each category. This is provided by the exergoeconomic factor f_K defined for component k by:

$$f_k = \frac{(\dot{Z}_{CI,k} + \dot{Z}_{O\&M,k})}{(\dot{Z}_{CI,k} + \dot{Z}_{O\&M,k}) + c_{F,k}(\dot{E}x_{D,k} + \dot{E}x_{Lo,k})} \qquad 35$$

All the parameters in the above two equations were defined in the preceding sections. Thus, the relative cost difference and the exergoeconomic factor for the principal components can also be defined. Those values have been calculated by the equations in lines 109-120 in Appendix C. The results are listed in descending numerical order in Tables 20-21.

TABLE 20: Relative cost difference of the principal components

Component	Relative cost difference, r_k
Condenser	406.7
Pump	6.6
Vaporizer	1.2
Turbine	0.7
HT Recuperator	0.3
LT recuperator	0.2

TABLE 21: Exergoeconomic factor of the principal components

Component	Exergoeconomic factor, $f_{k,}$ %
Pump	85.6
Turbine	59.4
Condenser	40.6
LT recuperator	38.7
Vaporizer	18.1
HT Recuperator	14.8

5.2.4 Improvement procedures

To improve the cost effectiveness of the Kalina PP the following procedures can be used:

1. Rank the principal components in descending order according to $\dot{Z}_K + \dot{C}_{D,k}$. The following list shows the values:

Component	$Z_k+C_{D,k}$, $\cdot 10^{-3}$, US$/s
Turbine	9.4
Vaporizer	3.2
LT recuperator	2.8
Pump	2.5
HT recuperator	2.4
Condenser	1.8

   Improvement should start with design changes on the turbine, vaporizer and LT recuperator, because the estimated values of $\dot{Z}_K + \dot{C}_{D,k}$ for these components are high.

2. From Table 21, it can be seen that the value of the exergoeconomic factor of the pump and turbine are within reasonable limits, with typical values for pumps above 70% and between 35 and 75% for turbines, respectively. This indicates that the designs for the pump and turbine are good. Values are typically lower than 55% for the heat exchangers. The low value of the exergoeconomic factor calculated for the HT recuperator and vaporizer suggest that cost savings in the entire plant must be achieved by improving the efficiency of these heat exchangers (reducing the exergy destruction) even if the capital investment cost for these components may increase.

6. THERMOECONOMIC OPTIMIZATION

The main purpose of thermoeconomic optimization is to achieve, within a given system structure, a balance between the expenditure on capital costs and the exergy costs which will lead to a minimum cost of the plant product.

The different components in the Kalina PP can be categorised as:

1. "Ready made" components selected from a manufacturer's catalogue, such as pumps, turbines, etc.
2. Components specially designed, or "tailor-made" for the plant, e.g. heat exchangers, etc.

The geometric parameters of the "ready made" components may be assumed to have been optimised by the manufacturer. At the thermoeconomic stage of optimization, the plant designer needs only to select a component which fits the technical specifications and whose capital cost is justified by its thermodynamic efficiency. The second type of component is convenient for thermoeconomic optimization, to optimize the particular component size to fit a range of components at different prices.

The advantage of using the exergy method of thermoeconomic optimization is that the various elements of the plant can be optimized on their own, the effect of the interaction between the given element and the whole plant being taken into account by local unit costs of exergy fluxes or those of exergy losses.

The structural method of thermoeconomic optimization

The purpose of the structural method of thermoeconomic optimization is to determine for a selected component the capital cost corresponding to the minimum annual operating cost of the plant and to the minimum unit cost of the product.

The concept of coefficient of structural bond (CSB) is useful in investigating the structure of a system, and in thermoeconomic optimization of components of a plant (Kotas, 1985). CSB is defined as:

$$\sigma_{k,i} = \left(\frac{\partial \dot{I}_{total}}{\partial \dot{I}_k} \right)_{x_i = \mathrm{var}} \qquad 36$$

where $\dot{I}_{total}$ is the time rate of irreversibility (a sum of exergy destruction and loss) of the plant, $\dot{I}_k$ the time rate of irreversibility of the k-th component of the plant, and x_i the parameter of the system which produces the changes.

Estimation of CSB for the heat exchangers in the CHP plant

The most direct method for estimation of CSB is to calculate and plot values of $\dot{I}_{total}$ and $\dot{I}_k$ for a number of values of x_i, and determine the CSB from the slope of the plotted curve. The parameter which produces changes for the plant is the pressure on the high-pressure side P_{high}. The magnitude of P_{high} varies between 22.7 and 31.7 bars with a 1 bar interval. Figure 16 shows a plot of $\dot{I}_{total}$ against $\dot{I}_k$ (time rate of irreversibility of the vaporizer, HT and LT recuperators and condenser) for varying P_{high}.

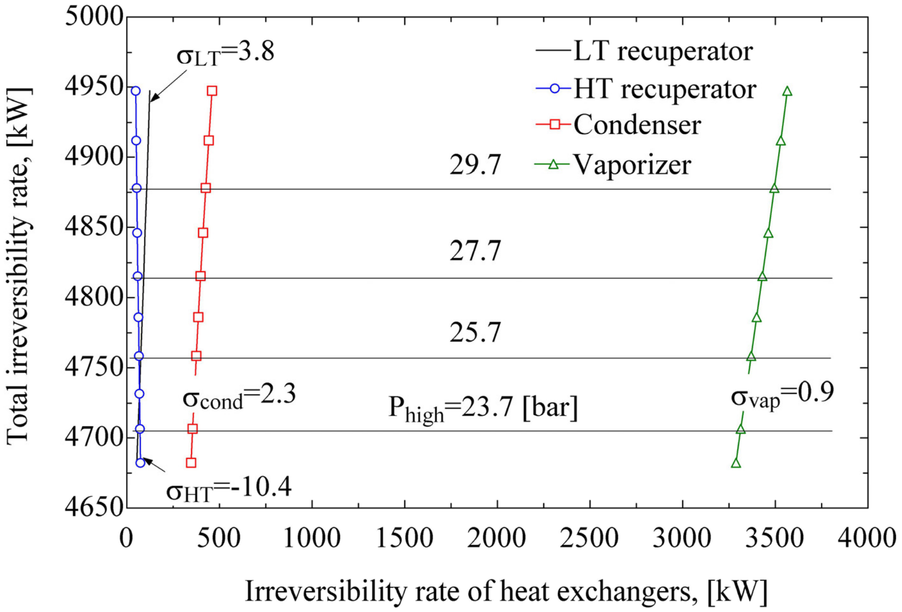

FIGURE 16: Determination of CSB for the vaporizer, HT and LT recuperators and condenser, with P_{high} variable

From the slope of the line the determined value of CSB for the vaporizer is σ_{vap}, 0.9. It is in the range of $\sigma_{vap} < 1$, which means that reduction in input to the system is less than reduction in the irreversibility (or exergy destruction and loss) of the vaporizer. Clearly, here the reduction in the irreversibility rate is accompanied by an increase in the irreversibility rates in other components of the plant. The determined value of CSB for the HT recuperator σ_{recup}, -10.4 is in the range of $\sigma_{recup} < 0$. This indicates that when the irreversibility rate in the recuperator decreases, it increases in other plant elements by a greater amount. This for both the vaporizer and the HT recuperator, is inefficient optimization.

The determined values of CSB for the LT recuperator is σ_{LT} =3.8 and for the condenser, σ_{cond} =2.3, respectively. Clearly, any reduction in the irreversibility rate of the LT recuperator and the condenser gives 3.8 and 2.3 times greater reduction in the irreversibility rate of the plant. The change in P_{high} improves not only the LT recuperator and the condenser but, owing to the bonds between them, other elements. Therefore, it is particularly advantageous to optimize both the LT recuperator and the condenser because of the potentially favourable impact on overall plant efficiency.

LT recuperator size optimisation

The pressure on the high pressure side (P_{high}) is the correct design parameter for variation, because it is related both to exergy destruction and capital cost, and the structural method of thermodynamic optimization is applicable. The optimization aims at determining the capital cost of the LT recuperator corresponding to the minimum annual operating cost of the plant for a given plant output (Kotas, 1985). Optimum conditions can be expressed as:

$$\left(\frac{\partial Ex_{LT,D}}{\partial P_{high}}\right)_{OPT} = -\frac{CRF}{t_{op}c_{LT,luc}} \cdot \frac{\partial C_{LT}}{\partial P_{high}} \qquad 37$$

where $c_{LT,luc}$ is the local unit cost of exergy destruction of the LT recuperator, which gives an indication of the thermoeconomic non-equivalence of exergy destruction in different system components, and is defined as:

$$c_{LT,luc} = c_{E,IN}\sigma_{LT} + \frac{CRF}{t_{op}}\zeta_{LT} \qquad 38$$

All parameters in Equation 38 are known except for the capital cost coefficient ζ_{LT}. The coefficient ζ_{LT} gives a measure of the changes in the capital costs of the components (other than the LT recuperator). The capital cost coefficient of the LT recuperator is:

$$\zeta_{LT} = \frac{\partial C_{vap}}{\partial Ex_{LT}} + \frac{\partial C_{HT}}{\partial Ex_{LT}} + \frac{\partial C_{turb}}{\partial Ex_{LT}} + \frac{\partial C_{cond}}{\partial Ex_{LT}} + \frac{\partial C_{pump}}{\partial Ex_{LT}} \qquad 39$$

A graphic determination of optimum P_{high} for the LT recuperator is used (Figure 17). Plots of the derivatives on both sides of Equation 37 against the variable parameter P_{high} give an intersection (Figure 17). The x-axis value at the intersection defines the optimum $P_{high,OPT} = 31.3$ bars.

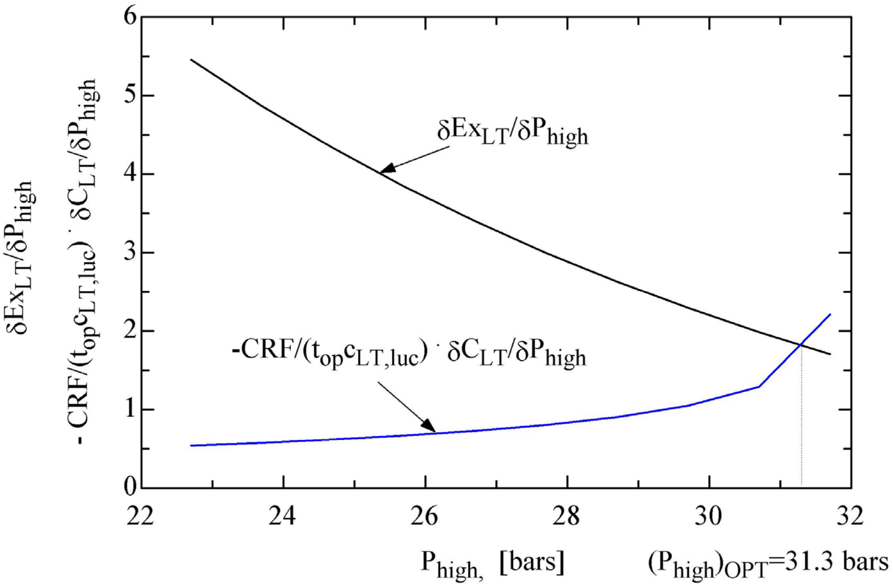

FIGURE 17: Graphic determination of the optimum P_{high} of the Kalina PP

Hence, the optimum size of the LT recuperator is 338 m^2 and the optimum capital cost is:

$$C_{LT,OPT} = 588 \cdot 338^{0.8} = 62{,}044 \text{ US\$}$$

Other component optimum sizes and their related costs can be determined, when the obtained value of the optimum high pressure $P_{high,OPT} = 31.3$ bars is used as the operating parameter to run the thermodynamic design in EES software. The diagram in Figure 18 shows the result of the thermoeconomic optimum design of the Kalina PP.

The installed capacity of a new CHP plant in Tsetserleg has been estimated as 1.98 MWe power and 16.7 MWt heat, assuming a geothermal water flowrate of 80 kg/s with temperature 120°C. Its annual power production would be 54,728 GJ/year and heat production 484,533 GJ/year.

A base-case design and thermal optimum design of the Kalina PP have been completed. A comparison of their TCI, efficiencies and other main parameters is listed in Table 22.

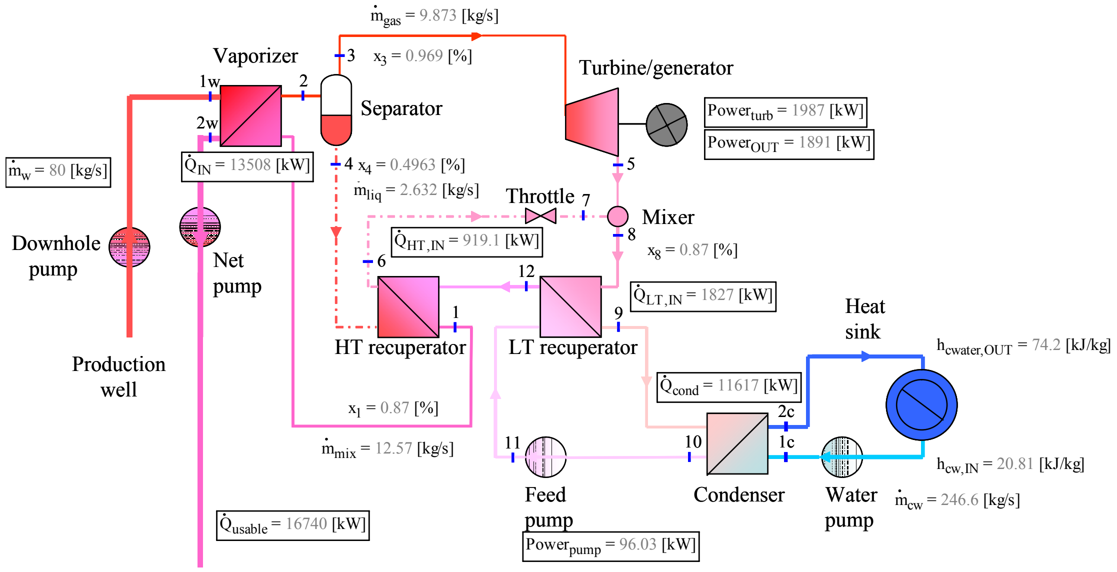

FIGURE 18: A diagram showing the thermoeconomic optimum design of the Kalina PP

From the comparison it can be seen that in the thermal optimum design the unit costs of heat have increased by 0.01 US ¢ per kWh. But the unit cost of electricity has decreased more than the above costs by 0.2 US ¢ per kWh. The cost of geothermal exploration work and the TCI have increased slightly, because the total purchased-equipment cost increased due to the increase of the size of the heat exchangers.

All the exergoeconomic factors of the principal components have a higher value in the optimum design than in the base-case design. The exergoeconomic factor of the LH recuperator, for example, shows the greatest improvement, or 14.8%. The total exergy destruction and loss rates of the plant decreased by 32 kW after optimization. A major advantage of thermoeconomic optimization is that the net power output increased by 31 kW with geothermal water inlet and outlet conditions fixed as the same as in the base-case design.

One of the benefits of thermoeconomic optimization of the Kalina PP can be revealed by the monetary values. Consumers at Tsetserleg could save 30,407 US$ per year in decreased electricity cost. It is expected that savings will increase by 608,145 US$ over the next 20 years.

TABLE 22: A comparison of the base-case and optimum designs

Item	Base-case design	Thermoeconomic optimum design
Unit cost of the geothermal water, US ¢/kWh	0.5	0.5
Unit cost of the heat, US ¢/kWh	1.0	1.0
Unit cost of the power, US ¢/kWh	3.2	3.0
Cost of the geothermal exploration work, US$	2,066,000	2,106,000
Total purchased equipment cost US$	1,816,000	1,855,000
Total capital investment, US$	2,849,000	2,910,000
Exergetic efficiency of the vaporizer, %	87	88
Exergetic efficiency of the HT recuperator, %	62	62.5
Exergetic efficiency of the LT recuperator, %	64	67
Exergetic efficiency of the turbine, %	77	77
Exergetic efficiency of the condenser, %	72	65
Exergetic efficiency of the pump, %	50	50
Exergetic efficiency of the Kalina PP, %	28	29
The first law of efficiency, %	13.8	14.0
The second law of efficiency, %	58.5	58.9
Exergy destruction rate of HT recuperator, kW	69.0	72.7
Exergy destruction rate of LT recuperator, kW	66.0	56.9
Total exergy destruction and loss rate, kW	4724	4692
Exergoeconomic factor of the pump, %	85.6	85.5
Exergoeconomic factor of the turbine, %	59.4	60.4
Exergoeconomic factor of the vaporizer, %	18.1	18.1
Exergoeconomic factor of the condenser, %	40.6	42.8
Exergoeconomic factor of the HT recuperator, %	14.8	15.7
Exergoeconomic factor of the LT recuperator, %	38.7	53.5
Net power output, kW	1860	1891

7. SENSITIVITY ANALYSIS

The geothermal water reservoir temperature and flowrate can affect the component size and the direct investment cost of the Kalina PP. They can also influence the heat and power production yields and the specific costs.

Exploration of the geothermal water reservoir temperature will show either low or high temperatures. The turbine power output yield increases constantly with respect to an increase in reservoir temperature (with the flowrate fixed at design condition) and similarly the flowrate (when the temperature is fixed at design condition) as shown in the plots in Figures 19 and 20. If the desired turbine power output is 3.3 MWe, the necessary conditions are either a reservoir temperature of 150°C or a flowrate of 140 kg/s.

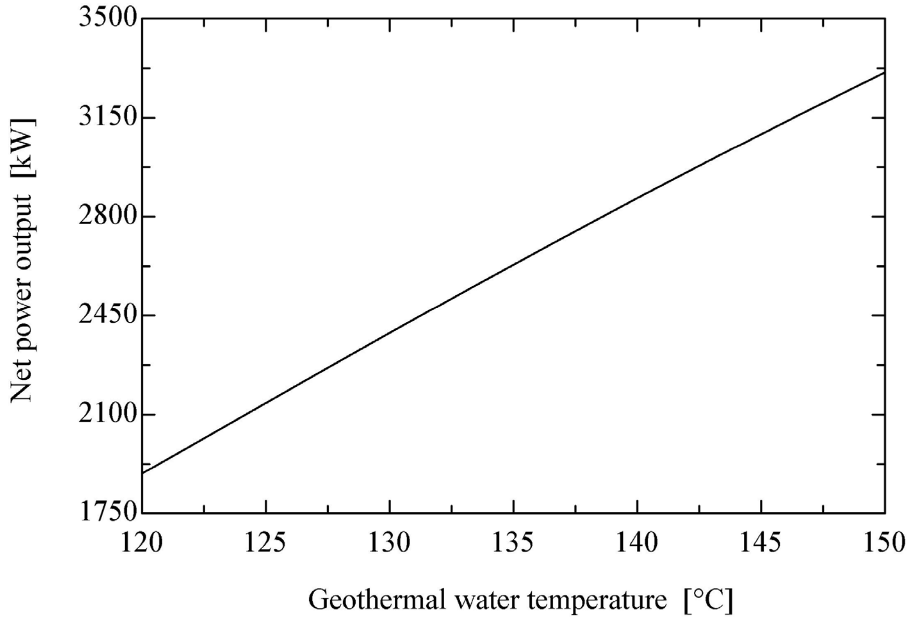

FIGURE 19: Power output vs. geothermal water temperature with geothermal water flowrate of 80 kg/s

The direct cost of geothermal exploration work can affect the unit cost of heat and power production of the CHP plant. This cost can vary from a few hundred dollars to a few thousand dollars per kW depending on the quality of the geothermal resource. As mentioned in Section 4.2.3 the direct cost for typical low-temperature geothermal resource exploration work can vary between 400 and 1000 US$/kW. In the case of the CHP plant in Tsetserleg, the unit cost of products has been evaluated based on the direct cost ranging from half the typical low value of 400 US$/kW to a double high value of 2000 US$/kW. The graph in Figure 21 shows the direct cost of geothermal exploration work versus the levelized unit cost of CHP plant products and the specific cost of geothermal water. The levelized unit costs of electricity generated from the CHP plant has highest value 10.7 US$/GJ (or 3.8 US ¢/kWh) when direct cost reaches the highest value of 2000 US$/kW, still within acceptable electricity cost limits for Tsetserleg consumers. At present Tsetserleg receives power from the Central Energy System and its tariff is the same for residential consumers and industries and entities, 58.64 MNT/kWh (or 4.8 US ¢/kWh).

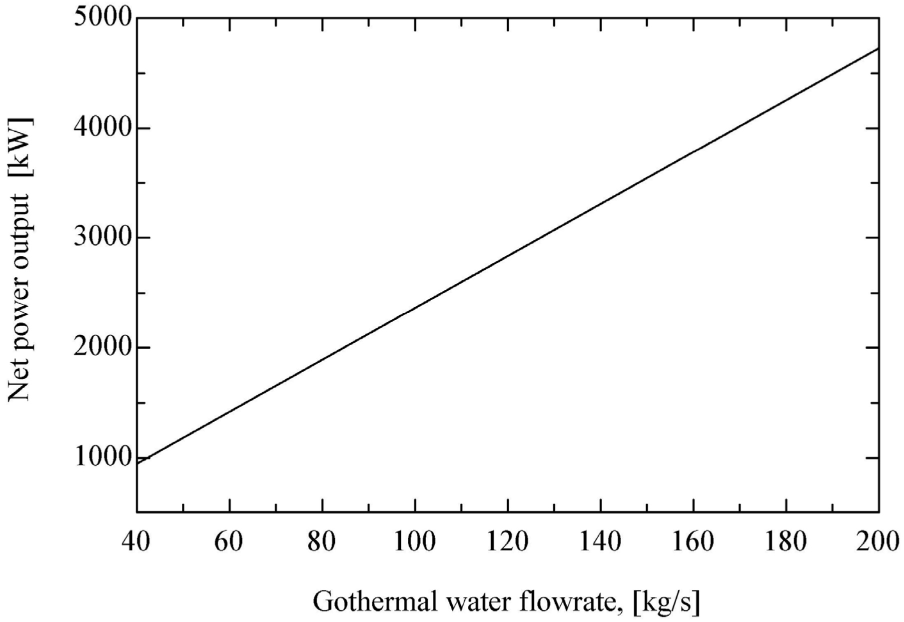

FIGURE 20: Power output vs. geothermal water flowrate with geothermal water temperature 120 °C at Kalina PP inlet state

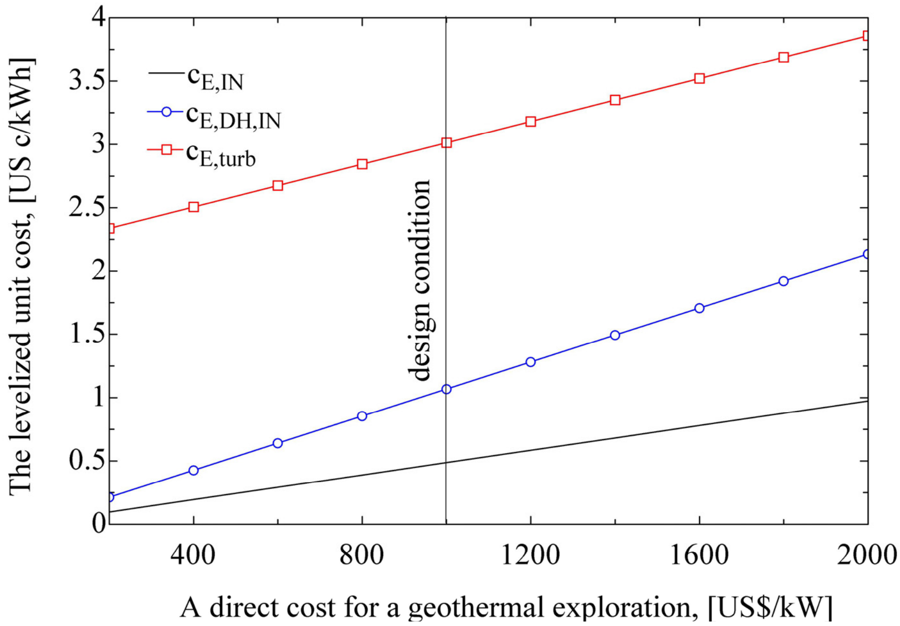

FIGURE 21: The effect of direct cost of geothermal exploration work on the unit costs of geothermal water, heat and power production

The graph shown in Figure 22 demonstrates the unit cost of heat has no relationship with geothermal water flowrate, whereas the unit cost of electricity decreases when geothermal water flowrate increases.

Figure 23 shows the levelized unit cost dependence on geothermal water temperature. The plots show a linear relationship between temperature and the unit costs of geothermal water and heat. Both costs increase together with geothermal water temperature increase. The unit cost of electricity has a quadratic relationship with the geothermal water temperature and is lower at higher temperature.

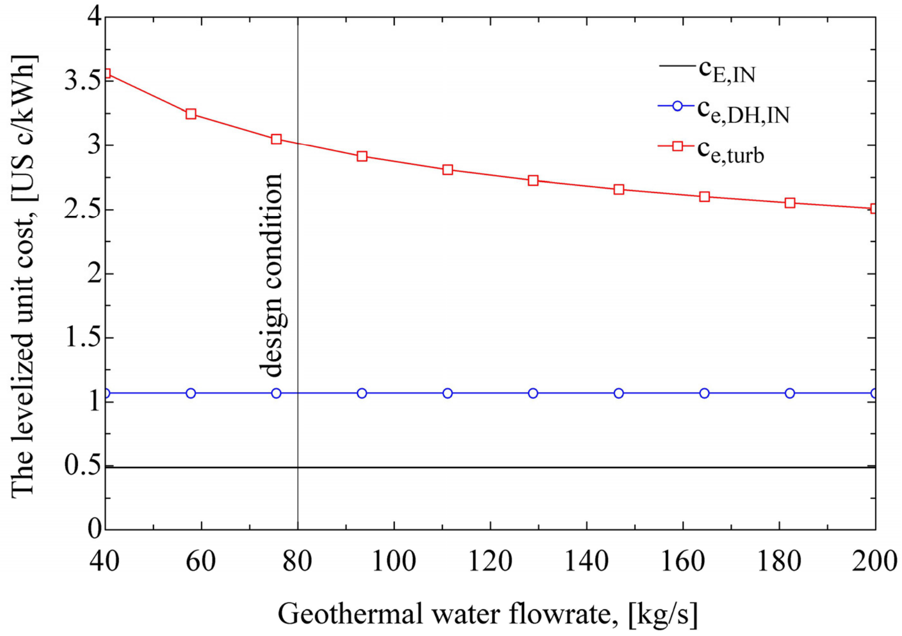

FIGURE 22: Geothermal water flowrate affect on the unit costs of geothermal water, heat and power productions

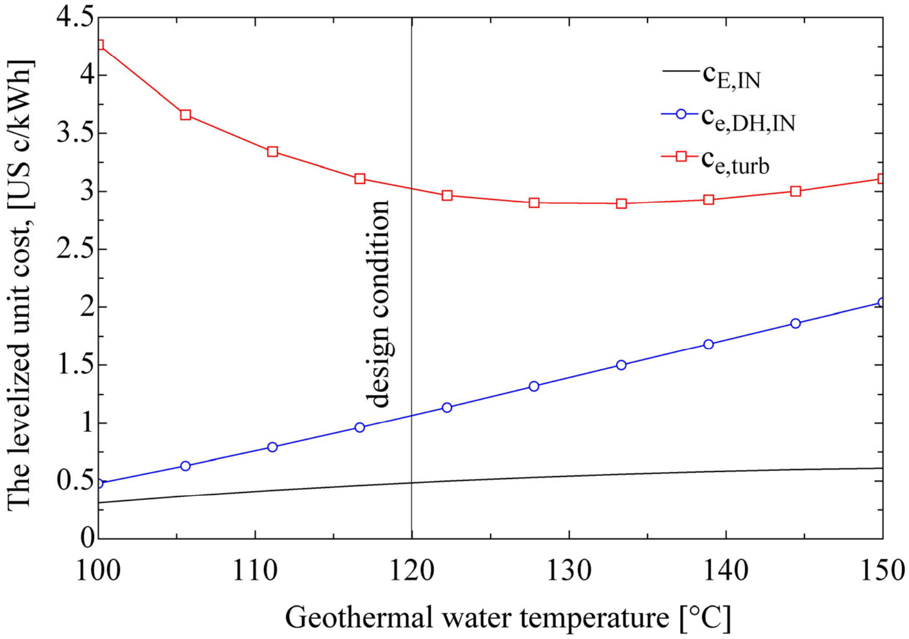

FIGURE 23: Geothermal water temperature affect on the unit costs of geothermal water, heat and power productions

Efficiencies of the first and second laws of thermodynamics for the CHP process can be determined as the electrical power generation efficiency (Valdimarsson, 2003b). All the heat contained in geothermal water is considered a by-product, and does not enter the efficiency calculation. For the CHP process under consideration, these efficiencies have been estimated in lines 168 and 170 in Appendix A and their values are 14.0% and 58.9%. Here it should be noted that geothermal water temperature of 120°C and plant operate at optimum high side pressure P_{high}=31.3 bars are assumed in the calculations.

The geothermal water temperature's influence on the efficiencies of the CHP process can be seen from the plot in Figure 24. The first law of efficiency varies between 12 and 15% during temperature increase, whereas the second law of efficiency increases from 54% to 65%. The first law maximum, Carnot and the plant exergetic efficiencies are also shown in Figure 24. Exergetic efficiency of the plant increases more than the others.

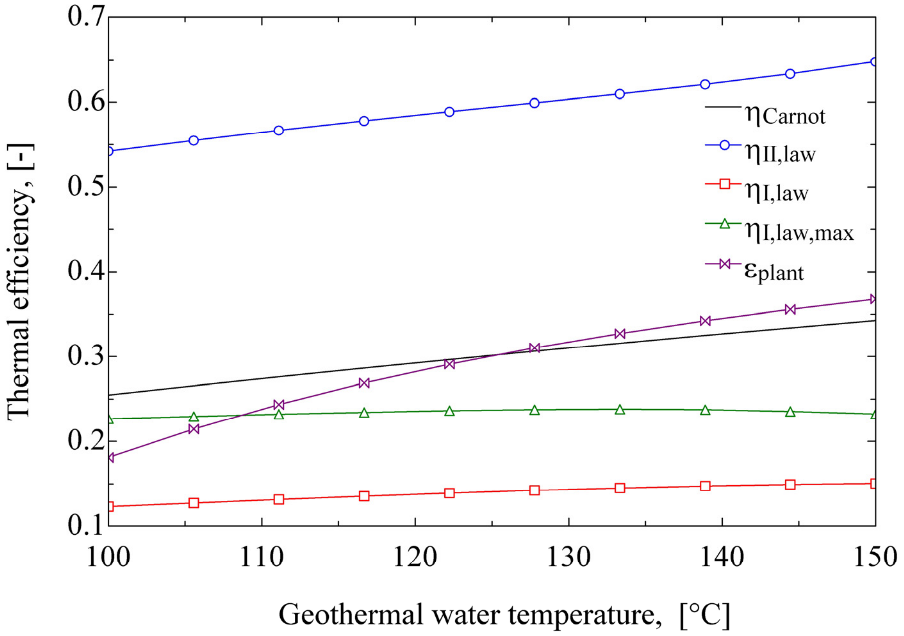

FIGURE 24: Different types of efficiency of the CHP plant vs. geothermal water resource temperature

8. ECONOMIC FEASIBILITY

Several possible scenarios have been investigated in order to make a preliminary estimation of the feasibility of the CHP plant. Two main factors were taken into account, the distance between Tsetserleg and the geothermal exploration site and the TAX value.

Alternatives for distance (same as previously discussed in Section 4.2.4):

1. Not accounted (meaning that the geothermal water would be looked for within the Tsetserleg area);
2. 5 km from Tsetserleg;
3. 20 km from Tsetserleg.

Alternatives for TAX:

1. TAX not included;
2. TAX included.

Two financial analysis methods are used, the Net Present Value (NPV) and the Internal Rate of Return (IRR) for appraisal of the investment project. The NPV method discounts all expected cash flow to the present. The discount rate used here is 10%. The IRR is the discount rate that makes the NPV of the investment equal to zero. If the IRR equals or exceeds the minimum desired rate of return the project can be accepted, otherwise not. The IRR represents the profitability of the project.

8.1 Carbon dioxide (CO_2) credit

As mentioned in Section 2.2 coal is an important source of heat in Tsetserleg. The combustion of coal, however, adds a significant amount of carbon dioxide (CO_2) to the atmosphere per unit of heat energy. In the CHP plant, carbon dioxide reductions were estimated according to Hong and Slatick (1994) as 0.091 ton of carbon dioxide emitted to the atmosphere per GJ heat energy produced by sub-bituminous. Related to this reduction, yearly CO_2 payback was estimated as 3 US$ per ton of CO_2 reduction (see Equations in lines 185-192 in Appendix C).

NPV and IRR were calculated for all alternatives in lines 173-184 and 193-204 in Appendix C both with the addition of CO_2 payback, and not.

Figure 25 shows the NPV dependence on the geothermal water flowrate. The graphs in this figure show a linear relationship between NPV and flowrate. The different alternatives of NPV are marked in the same way as in Figure 27. The figure demonstrates that the minimum geothermal water flowrate is 115 kg/s for a positive NPV excluding CO_2 payback and, therefore, the Tsetserleg project can only be feasible above this point. The minimum geothermal water flowrate is 70 kg/s for a positive NPV when CO_2 payback is included in the project.

The graphs in Figure 26 show the quadratic relationship between NPV and water temperature. It can be seen from the graphs that the minimum geothermal water temperature is 135 °C for a positive NPV, which means that the Tsetserleg project can only be feasible above this point. The minimum geothermal water temperature is 112 °C for a positive NPV when CO_2 payback is included.

Table 23 shows the results of an analysis on the NPV and IRR, and presents several different scenarios. With CO_2 payback excluded, alternatives 22 and 32 are not feasible with a negative NPV@10%. But with CO_2 payback, all alternatives are feasible. Finally, the table shows that CO_2 credit has a positive effect on all alternatives.

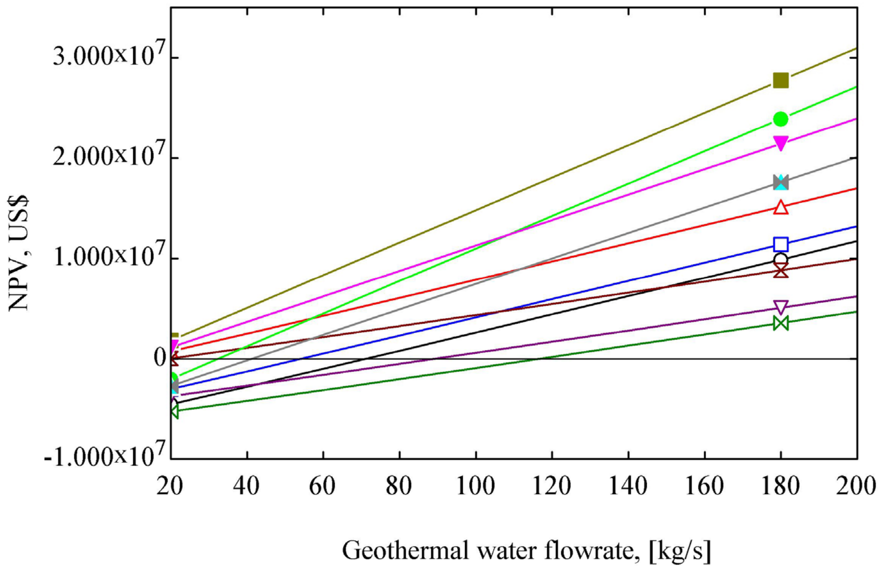

FIGURE 25: The relationship between NPVs and flowrate with geothermal water temperature of 120 °C

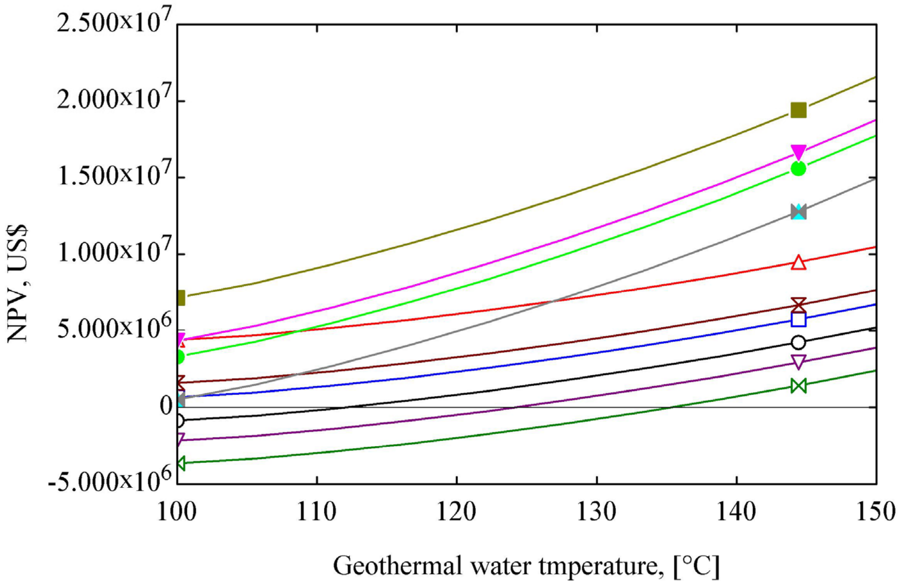

FIGURE 26: The relationship between NPVs and geothermal water temperature with flowrate of 80 kg/s

TABLE 23: NPV and IRR for the different scenarios

Scenario →	11	12	21	22	31	32	
NPV@10%	9.1	3. 5	5.3	-0.25	5.3	-1.7	M US$
IRR	33.4%	19.6%	18.4%	9.5%	15.9%	7.8%	
NPV_{CO2}@10%	11.9	6.3	8.1	2.6	8.1	1	M US$
IRR_{CO2}	40.2%	26.6%	22.5%	14.2%	18.9%	11.2%	

The relationships plotted in Figure 27 demonstrate the optimum value, 0.87, for the fraction of ammonia-water mixture.

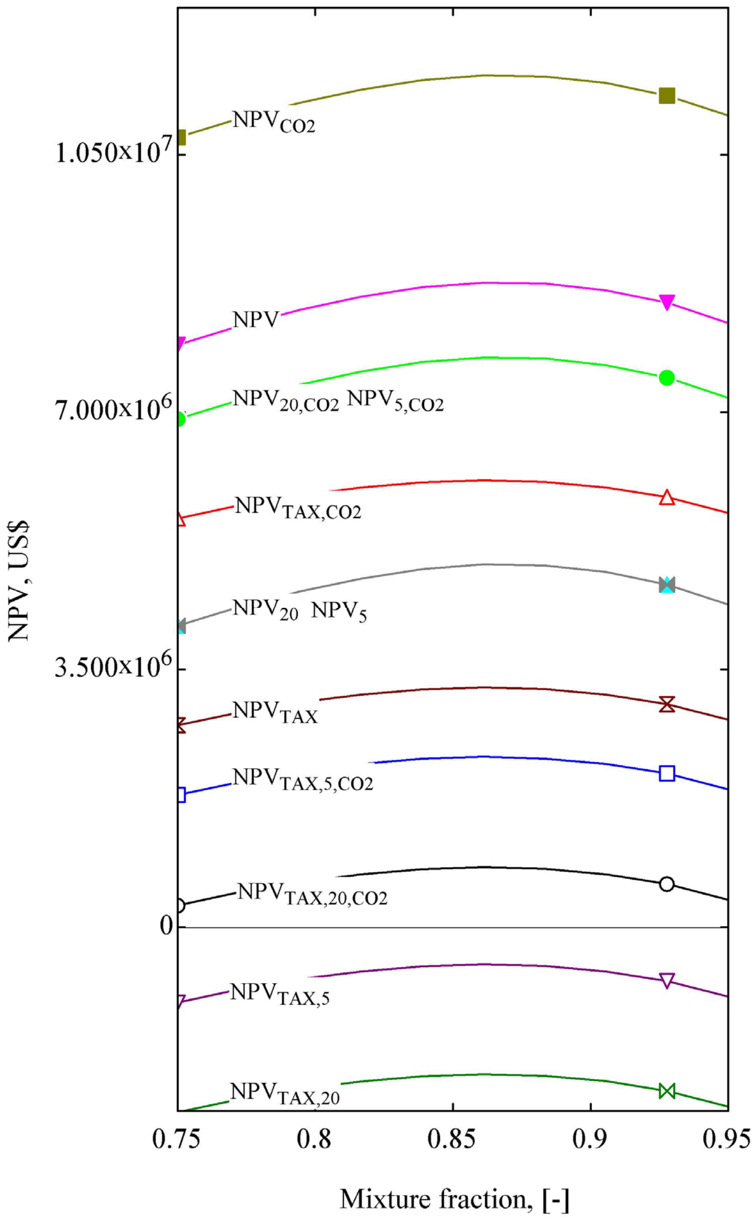

FIGURE 27: The relationship between NPV and the fraction of ammonia-water mixture

9. ENVIRONMENTAL ASPECTS

Geothermal energy provides significant environmental benefits such as a small footprint (Table 24) and low CO_2 emissions (Figure 28). However local impacts must be identified and dealt with (Bronicki, 2004).

TABLE 24: Land area occupied by power plant adopted from Bronicki (2004)

Technology	Land area (m^2 per GWh/year for 30 year)
Geothermal	404
Wind (land with turbines and roads)	1,335
Photovoltaics	3,237
Solar thermal	3,561
Coal (including open pit mining)	3,642

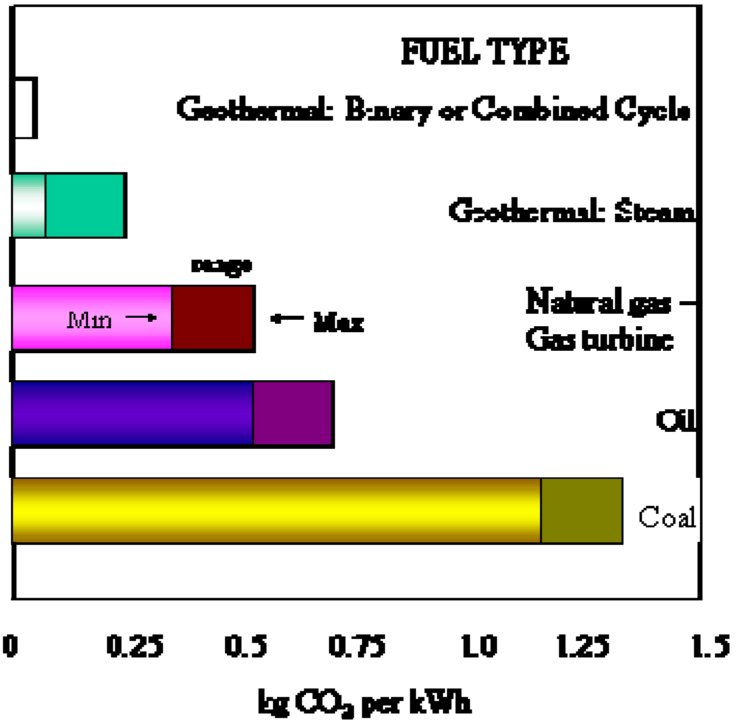

FIGURE 28: CO_2 emissions adopted from Bronicki (2004)

According to the pre-feasibility study, after implementation of the proposed project it is expected that CO_2 emission will have decreased by 472,297 tons and the burning of coal by 297,400 tons for the next 20 years in Tsetserleg. If more geothermal resources were discovered, possible extension of geothermal heating system would become available for the rest of the households, of which 2,465 live in conventional houses and 1,708 live in Gers. It would further decrease CO_2 emission (and coal consumption), by an estimated 662,708 tons (and 417,300 tons coal) for 20 years. The whole Tsetserleg CO_2 reduction potential is then 1,135,005 tons for 20 years.

Geothermal energy will benefit the whole of Tsetserleg. Tsetserleg will be the first clean and environmentally friendly town of Mongolia. It will serve 18,136 people who will live without GHG, breathe clean air, and live and enjoy comfortable working conditions.

Similar geothermal utilization in other neighbouring province centres such as Bayankhongor, Arvaikheer, and Uliastai (Figure 1) within the Khangai area would make a reduction of 170,251 tons

CO_2 emission possible (and consumption of 107,205 tons of coal) per year. CO_2 emission reduction for 20 years for the three centres would then amount to 3,405,015 tons (and 2,144,100 tons of coal).

The power potential of the new geothermal CHP plant could reach 55,000 GJ/year, leading also to decreased CO_2 emissions due to less coal burning in the CHP plant, but that is immaterial to this study. At present power is supplied to Tsetserleg by the Central Energy System, with no CO_2 reduction in Tsetserleg.

Finally, it should be noted that an Environmental Impact Assessment of the new geothermal CHP plant needs to be done before the project starts.

10. CONCLUSIONS AND RECOMMENDATIONS

The installed capacity of a new geothermal utilization CHP plant in Tsetserleg could reach 1.9 MWe power and 16.7 MWt heat production assuming a geothermal water inlet flowrate of 80 kg/s and temperature of 120°C. Its annual production of electricity could be 54,728 GJ/year and of the heat 484,533 GJ/year. According to the pre-feasibility study (Eliasson et al, 2004), heat consumption of all Tsetserleg consumers is estimated to be 400,000 GJ/year. The estimated 484,533 GJ/year of heat production from the new CHP plant would be enough for all Tsetserleg heat consumers. It should be noted that the CHP plant is expected to operate together with a peak load boiler during the coldest period of the year.

The total capital investment (TCI) of the CHP plant has been estimated to be 8.66 M US$ (with a 5 km transmission pipeline), or 12.41 M US$ (with a 20 km transmission pipeline).

The direct capital cost of the Kalina PP in Tsetserleg 1,462 US$/kW is determined in Section 4.2.2 and shows that it is within the international average cost for small geothermal power generation plants (<5 MW), usually in the range of 1200-2800 US$/kW.

The structural method of thermoeconomic optimisation is applicable for a complex such as Kalina PP. The optimum heat transfer area of the LT recuperator is determined to be greater than that of a base-case design. The advantages of thermoeconomic optimization appear in the unit power cost being 0.2 US ¢/kWh lower and all the exergoeconomic factors for the principal components being higher than for the base-case design. The total exergy destruction rate of the plant also decreases 32 kW and the net power output increases by 31 kW for fixed inlet and outlet geothermal water.

The first and second laws of thermal efficiencies for the CHP plant were estimated to be 14.0% and 58.88%, respectively, when the plant operates at an optimum high- pressure P_{high}=31.3 bar. The second law of efficiency of the CHP plant is 65.07 % for a geothermal water supply at a temperature of 150 °C. Similarly, greater power output is 4.5 MW at a geothermal water flowrate of 200 kg/s and a temperature of 120°C.

The direct cost for a typical low-temperature geothermal resource exploration work varies between 400 and 1000 US$/kW (The World Bank Group, 2004). From the sensitivity analysis, it can be seen that the levelized unit cost of electricity generated from the CHP plant has highest value 10.7 US$/GJ (or 3.8 US ¢/kWh) when direct costs reach the highest value of 2000 US$/kW (two times higher than 1000 US$/kW). Still it remain within acceptable heat cost for Tsetserleg consumers. At present Tsetserleg receives power from the Central Energy System and its tariff is 4.8 US ¢/kWh.

The current heat energy cost from the Tsetserleg DH company is 6.31 US$/GJ, based on water heat energy (GJ) at the boiler station wall (Eliasson et al., 2004). The levelized unit cost of heat is estimated to be 3.85 US$/GJ for a 5 km long transmission pipeline, or 4.76 US$/GJ for a 20 km long transmission pipeline, respectively. Both are still lower than present costs.

It can be seen from the plots shown in Figures 25 and 26 that a minimum geothermal water temperature of 135 °C and flowrate 115 kg/s are necessary to reach a positive NPV when CO_2 payback is excluded in the project. But a lower temperature of 112°C and flowrate of 70 kg/s is acceptable for a positive NPV when CO_2 payback is included in the project.

In the economic analysis of the CHP plant two main factors were considered, the distance from the geothermal field to Tsetserleg centre and the tax value. NPV and IRR were used for to appraise the investment of the Tsetserleg project for all alternatives with and without CO_2 payback. In the case of no CO_2 payback, two alternatives are not feasible. But with CO_2 payback, all the calculated alternatives are feasible.

The initial screening of a possible geothermal project in Tsetserleg, Mongolia has now been completed. Based on this study, harnessing of the geothermal resources surrounding of Tsetserleg is recommended. May it facilitate economical, long-term environmental and social benefits.

REFERENCES

Bejan, A., Tsatsaronis, G., and Moran, M., 1996: *Thermal design and optimization*. John Wiley & Sons, Inc. The United States of America, 533 pp.

Bronicki, Y.L., 2004: *Implementing new power plant technologies: Technical and economic aspects*. Web page www.ormat.com/Implementation_wwfooter.pdf

Burentsagaan, B., 2004: Geothermal evaluation of the Geldinganes area in SW-Iceland and proposal for assessment of the Shivert hot spring area in Mongolia. Report 4 in *Geothermal Training in Iceland 2004*, UNU-GTP, Iceland, 25-56.

Cengel, A. Y., 1994: *Thermodynamics: An engineering approach*. McGraw-Hill, Inc, Second Edition, 987 pp.

Dorj, P., 2001: Design of small geothermal heating systems and power generators for rural consumers in Mongolia. Report 3 in *Geothermal Training in Iceland 2001,* UNU-GTP, Iceland, 27-57.

Dorofeeva, R.P., 1992: Geothermal regime of east Siberia and Mongolia. *Papers presented at the International conference on Industrial uses of geothermal energy*, *Reykjavik, Iceland,* 9 pp.

Eliasson, E.T., Magnusson, J.M., Dorj, P., and Johannesson, Th., 2004: *Geothermal project in Tsetserleg, Mongolia. Pre-feasibility study.* Rafhönnun Consulting Engineers, Reykjavik, Iceland.

F-Chart Software 2004: *Engineering Equation Solver* (Student version 7.197). Web page https://www.fchart.com/

Gendenjamts, O., 2003: Interpretation of geochemical data from geothermal fluids at Arskogsstrond, Dalvik, and Hrisey, N-Iceland and in the Khangai Area, Mongolia. Report 10 in *Geothermal Training in Iceland 2003,* UNU-GTP, Iceland, 219-252.

Gudmundsson, J.S., Freeston, D.H., and Lienau, P.J., 1985: *The Lindal diagram. Geoth. Res.* Council, *Transactions*, 9, 15-19.

Holman, J.P., 2002: *Heat transfer*. McGraw-Hill Companies, 665 pp.

Hong, B.D., and Slatick, E. R., 1994: Carbon dioxide emission factors for coal. *Energy Information Administration*, *Quarterly Coal Report*, January-April, 1-8.

Improved Urban Stoves., 2000: *Improved household stoves in Mongolian urban centres*. Project of the Ministry of Nature and Environment of Mongolia.

Kotas, T.J., 1985: *The exergy method of thermal plant analysis*. Anchor Brendon Ltd, Tiptree, Essex, Great Britain, 293 pp.

Maack, R., and Valdimarsson, P., 2002: *Operating experience with Kalina power plant.* Web page http://www.xorka.com

Ministry of Agriculture and Industry of Mongolia., 1999: *Geotherm, sub-programme of the Mineral resource programme,* (in Mongolian). Ministry of Agriculture and Industry, Mongolia.

Mlcak, A.H., 2001: *Design and start-up of the 2 MW Kalina Cycle® Orkuveita Husavikur geothermal power plant in Iceland*. European Geothermal Energy Council, 2nd Business Seminar EGEC 2001, Altheim, Austria.

Mongolian Statistic Centre, 2001: *Statistics of Mongolia, 2000 census*. Mongolian Statistics Centre, Ulaanbaatar. Web page http://statis.gov.mn/index_m.asp.

Statistic Booklet., 2000: *Statistic booklet: Arkhangai, population and housing census*. National Statistical Office, Ulaanbaatar, Mongolia.

Thorolfsson G., 2002: Optimization of low temperature heat utilization for production of electricity, *MSc thesis*, University of Iceland, Dept. of Mechanical Engineering.

Valdimarsson P., 2003a: Factor influencing the economics of the Kalina power cycle and situations of superior performance. *Proceedings of the IGC2003 "Multiple Integrated uses of Geothermal Resources"*, Reykjavik, Iceland, S1 32-40.

Valdimarsson P., 2003b: Production of electricity from geothermal heat-efficiency calculation and ideal cycles. *Proceedings of the IGC2003 "Multiple Integrated uses of Geothermal Resources"*, Reykjavik, Iceland, S1 41-48.

Weast, C. R., 1982: *Handbook of Chemistry and Physics*. CRC Press, Inc. Boca Raton, Florida, F-97.

The World Bank Group., 2004: Geothermal energy an assessment. Web page http://www.worldbank.org/html/fpd/energy/geothermal/assessment.htm

NOMENCLATURE

A	Area, m^2
c_P	Specific heat at constant pressure, kJ/kg K
c_E	Unit cost of exergy, US$/kJ
$c_{E,kWh}$	Unit cost of exergy per kilowatt hour, US ¢/kWh
C_c, C_h	Heat capacity of a cold and hot stream, kW/K
C	Cost, US$
e	Specific exergy, kJ/kg
eff	Effectiveness
Ex	Exergy rate, kW
f	Exergoeconomic factor
h	Enthalpy, kJ/kg
H	Total enthalpy, kW
i_{eff}	Effective rate of return
m	mass
$\dot{m}$	Mass flowrate, kg/s
N_y	Operating year
P	Pressure, bar
q	Vapour mass fraction
Q	Total heat transfer, kJ
$\dot{Q}$	Heat transfer rate, kW
r	Relative cost difference
r_n	Nominal escalation rate
R_c	Heat capacity ratio
s	Entropy, kJ/kg K
t	Tax

t_{op}	Operating time, s
t_{hour}	Working time, h
T	Temperature, K
u	specific internal energy, kJ/kg
U	Overall heat transfer coefficient, kW/m^2 K
v	Specific volume, m^3/kg
x	Ammonia mass fraction
Y	Exergy destruction rate
$\dot{Z}$	Capital investment rate

Greek letters

σ	Coefficient of structural bond
ε	Exergetic efficiency
ζ	Capital cost coefficient
$\eta_{I,law}$	First law of efficiency
$\eta_{II,law}$	Second law of efficiency
$\eta_{\max,I,law}$	Maximum first law of efficiency
η_{Carnot}	Carnot efficiency

Subscripts

act	Actual
add	Added value
c	Cold fluid in heat exchanger or cooling process
cond	Condenser
D	Destruction
eff	Effectiveness
es	Escalated
IN	Inlet conditions
h	Hot fluid in heat exchanger or heating process
high	High-temperature or high-pressure substance
k	k-th component
L	Levelized
Lo	Loss
liq	Liquid
low	Low-temperature or low-pressure substance
max	Maximum
mix	Ammonia-water mixture
OUT	Outlet conditions
p	Constant pressure
rise	Increased value
s	Isentropic
sat	Saturated
sep	Separator
tot	Total
turb	Turbine
vap	Vaporizer
w	Geothermal water
cw	Cooling water
0	Environmental state
1-12	State

Superscripts

˙ (dot)	Quantity per unit time
° (circle)	Standard reference state

Abbreviations used in text

AFUDC	Allowance for funds used during construction
CELF	Capital escalation levelization factor
CGW	Cost of geothermal water
CRF	Capital recovery factor
FCI	Fixed capital investment
HEN	Heat exchanger network
HT	High temperature recuperator
IRR	Internal rate of return
LMTD	Log means temperature difference
LRD	cost of licensing, research and development
LT	Low temperature recuperator
NPV	Net present value
NTU	Number of transfer unit
O&M	Operating and Maintenance
PEC	Purchased equipment cost
PFI	Plant facility investment
SUC	Start-up cost
TAX	Tax payment
TCI	Total capital investment
WC	Working capital

Currency Equivalents
(as of 25 Jan 2005)
Mongolian Currency Unit – togrog (MNT)
US $1.00 = MNT1,207
MNT1.00 = $0.000828
In this thesis, the rate $1.00=MNT1,207 has been used.

Notes

(i) In this report, "US$" refers to US dollars
(ii) In this report, “US ¢” refers to US cents

APPENDIX A: THERMODYNAMIC BASE-CASE DESIGN

Equations

```
function $\mathrm{tk}(T)$   Convertion of °C to K
    $tk := T + 273.1$
end

function $\mathrm{ex}(h,\ s)$   Specific exergy of saturated ammonia-water vapour and liquid (liq)
    $h_0 := \mathrm{h}\,(\mathrm{WATER},\ T = 278.1,\ x = 0)$
    $s_0 := \mathrm{s}\,(\mathrm{WATER},\ T = 278.1,\ x = 0)$
    $T_0 := 278.1$
    $ex := (h - h_0 - T_0 \cdot (s - s_0))$
end

function $e_{mix}\,(x_{mix},\ h,\ s)$   Specific exergy of ammonia-water mixture (mix.)
    $T_0 := 278.1$
    $P_0 := 4.557$
    call $NH3H2O\,(123,\ T_0,\ P_0,\ x_{mix} : T_0,\ P_0,\ x_0,\ h_0,\ s_0,\ u_0,\ v_0,\ q_0)$
    $h_0 := h_0$
    $s_0 := s_0$
    $e_{mix} := h - h_0 - T_0 \cdot (s - s_0)$
end

function $Ex_{mix}\,(m_{mix},\ x_{mix},\ h,\ s)$   Time rate of exergy associated with ammonia-water mix.
    $T_0 := 278.1$
    $P_0 := 4.557$
    call $NH3H2O\,(123,\ T_0,\ P_0,\ x_{mix} : T_0,\ P_0,\ x_0,\ h_0,\ s_0,\ u_0,\ v_0,\ q_0)$
    $h_0 := h_0$
```

$s_0 := s_0$ (23)

$Ex_{mix} := m_{mix} \cdot (h - h_0 - T_0 \cdot (s - s_0))$ (24)

end (25)

Input variables:

$x_{mix} = 0.87$ Fraction of ammonia-water mix., design variable - [%] (26)

$P_{high} = 30$ High-pressure level on the high pressure side, design variable - [bar] (27)

$P_{low} = 5$ Low-pressure level on the low pressure side, design variable -[bar] (28)

$T_{high} = 120$ °C - Geothermal water inflow temperature: constrain - [K] (29)

$T_{low} = 80$ °C - Geothermal water outflow temperature: constrain - [K] (30)

$\dot{m}_w = 80$ Geothermal water flowrate: control parameter - [kg/s] (31)

$\eta_{turb} = 0.75$ Turbine isentropic efficiency - [%] (32)

$\eta_{pump} = 0.5$ Pump isentropic efficiency - [%] (33)

$U = 1.0$ The heat transfer coefficient of the HT and LT recuperators - [kW/m^2 K] (34)

$U_{vap} = 0.9$ The heat transfer coefficient of the vaporizer - [kW/m^2 K] (35)

$U_{ammonia,cond} = 1.1$ The heat transfer coefficient of the ammonia condenser - [kW/m^2 K] (36)

Vaporizer:

$h_{1w} = \text{h}(\text{Water}, T = \text{tk}(T_{high}), x = 0)$ Enthalpy of the geothermal water at state 1w - [kJ/kg] (37)

$s_{1w} = \text{s}(\text{Water}, T = \text{tk}(T_{high}), x = 0)$ Entrophy of the geothermal water at state 1w - [kJ/kg K](38)

$h_{2w} = \text{h}(\text{Water}, T = \text{tk}(T_{low}), x = 0)$ Enthalpy of the geothermal water at state 2w - [kJ/kg] (39)

$s_{2w} = \text{s}(\text{Water}, T = \text{tk}(T_{low}), x = 0)$ Entrophy of the geothermal water at state 2w - [kJ/kg K](40)

$e_{1w} = \text{ex}(h_{1w}, s_{1w})$ Specific exergy of the geothermal water at state 1w - [kJ/kg] (41)

$\dot{Ex}_{IN} = \dot{m}_w \cdot e_{1w}$ Exergy associated with the geothermal water at state 1w - [kW] (42)

$e_{2w} = \text{ex}(h_{2w}, s_{2w})$ Specific exergy of the geothermal water at state 2w- [kJ/kg] (43)

$\dot{Ex}_{Lo} = \dot{m}_w \cdot e_{2w}$ Exergy loss from the vaporizer - [kW] (44)

$\dot{Ex}_{add} = \dot{Ex}_{IN} - \dot{Ex}_{Lo}$ Exergy input to the Kalina PP - [kW] (45)

call $NH3H2O(234, P_{high}, x_{mix}, h_{start} : T_1, P_1, x_1, h_1, s_1, u_1, v_1, q_1)$ Mix. at state 1 (46) call $\mathit{NH3H2O}\,(123,\ \mathrm{tk}(T_{high}-3),\ P_{high},\ x_{mix} : T_2,\ P_2,\ x_2,\ h_2,\ s_2,\ u_2,\ v_2,\ q_2)$ Mix. at state 2(47)

$e_1 = e_{mix}\,(x_{mix},\ h_1,\ s_1)$ Specific exergy of the mix. at state 1 - [kJ/kg] (48)

$e_2 = e_{mix}\,(x_{mix},\ h_2,\ s_2)$ Specific exergy of the mix. at state 2- [kJ/kg] (49)

$\dot{Ex}_{vap,IN} = Ex_{mix}\,(\dot{m}_{mix},\ x_{mix},\ h_1,\ s_1)$ Exergy associated with the mix. at state 1 - [kW] (50)

$\dot{Ex}_{vap,OUT} = Ex_{mix}\,(\dot{m}_{mix},\ x_{mix},\ h_2,\ s_2)$ Exergy associated with the mix. at state 2 - [kW] (51)

$\dot{m}_w \cdot (h_{1w} - h_{2w}) = \dot{m}_{mix} \cdot (h_2 - h_1)$ Heat balance of the vaporizer, $m_{dot,mix}$ calculated (52)

$\dot{Ex}_{vap,rise} = \dot{Ex}_{vap,OUT} - \dot{Ex}_{vap,IN}$ Exergy rise in the feed mix. - [kW] (53)

$\dot{Ex}_{vap,D} = \dot{Ex}_{add} - \dot{Ex}_{vap,rise}$ Exergy destruction in the vaporiser - [kW] (54)

$c_{p,w} = \dfrac{h_{1w} - h_{2w}}{(\mathrm{tk}(T_{high}) - \mathrm{tk}(T_{low}))}$ Specific heat capacity of the geothermal water - [kJ/kg K] (55)

$C_w = \dot{m}_w \cdot c_{p,w}$ Heat capacity of the geothermal water - [kW/K] (56)

$c_{p,mix} = \dfrac{h_2 - h_1}{(T_2 - T_1)}$ Specific heat capacity of the mix. (57)

$C_{mix} = \dot{m}_{mix} \cdot c_{p,mix}$ Heat capacity of the mix. (58)

$\dot{Q}_{IN} = \dot{m}_w \cdot (h_{1w} - h_{2w})$ Heat input to the Kalina PP - [kW] (59)

$\dot{Q}_{max} = C_{mix} \cdot (\mathrm{tk}(T_{high}) - T_1)$ Maximum heat exchange (60)

$\epsilon_{vap,eff} = \dot{Q}_{IN}/\dot{Q}_{max}$ The effectiveness ratio of the vaporizer (61)

$R_{c,vap} = C_{mix}/C_w$ Heat capacity ratio C_{min}/C_{max} (62)

$\mathit{NTU}_{vap} = \dfrac{1}{1 - R_{c,vap}} \cdot \ln\left((1 - \epsilon_{vap,eff} \cdot R_{c,vap})\ /\ (1 - \epsilon_{vap,eff})\right)$ NTU for the vaporizer (63)

$A_{vap} = \mathit{NTU}_{vap} \cdot \dfrac{C_{mix}}{U_{vap}}$ Heat transfer area of the vaporizer (64)

Separator:

call $\mathit{NH3H2O}\,(128,\ \mathrm{tk}(T_{high}-3),\ P_{high},\ 1.0 : T_3,\ P_3,\ x_3,\ h_3,\ s_3,\ u_3,\ v_3,\ q_3)$ (65)

Saturated (sat.) vapour properties at state 3

call $\mathit{NH3H2O}\,(128,\ \mathrm{tk}(T_{high}-3),\ P_{high},\ 0.0 : T_4,\ P_4,\ x_4,\ h_4,\ s_4,\ u_4,\ v_4,\ q_4)$ (66)

Sat. liquid (liq.) at state 4

$\dot{m}_{mix} \cdot x_{mix} = \dot{m}_{vapour} \cdot x_3 + \dot{m}_{liq} \cdot x_4$ Mass balance in the separator (67)

$\dot{m}_{mix} \cdot h_2 = \dot{m}_{vapour} \cdot h_3 + \dot{m}_{liq} \cdot h_4$ Heat balance in the separator (68)

$e_3 = e_{mix}\left(x_3,\ h_3,\ s_3\right)$ Specific exergy of the sat. vapour at state 3 - [kJ/kg] (69)

$e_4 = e_{mix}\left(x_4,\ h_4,\ s_4\right)$ Specific exergy of the sat. liq. at state 4 - [kJ/kg] (70)

$\dot{E}x_{vapour} = Ex_{mix}\left(\dot{m}_{vapour},\ x_3,\ h_3,\ s_3\right)$ Exergy associated with the sat. vapour at state 3 - [kW](71)

$\dot{E}x_{liq} = Ex_{mix}\left(\dot{m}_{liq},\ x_4,\ h_4,\ s_4\right)$ Exergy associated with the sat. liq. at state 4 - [kW] (72)

$\dot{E}x_{sep,D} = \dot{E}x_{vap,OUT} - \dot{E}x_{vapour} - \dot{E}x_{liq}$ Exergy destruction in the separator - [kW] (73)

Turbine:

$Power_{turb} = Power_{turb,s} \cdot \eta_{turb}$ The actual turbine power - [kW] (74)

$Power_{turb,s} = \dot{m}_{vapour} \cdot \left(h_3 - h_{s,5}\right)$ The isentropic turbine power - [kW] (75)

$\eta_{turb} = \dfrac{h_3 - h_{turb,eff}}{\left(h_3 - h_{s,5}\right)}$ The adiabatic efficiency of turbine (76)

call $NH3H2O\left(235,\ P_{low},\ x_3,\ s_3 : T_{s,5},\ P_{s,5},\ x_{s,5},\ h_{s,5},\ s_{s,5},\ u_{s,5},\ v_{s,5},\ q_{s,5}\right)$ (77)

Sat. vapour after isentropic turbine

call $NH3H2O\left(234,\ P_{low},\ x_3,\ h_{turb,eff} : T_5,\ P_5,\ x_5,\ h_5,\ s_5,\ u_5,\ v_5,\ q_5\right)$ (78)

Sat. vapour after actual turbine

$e_5 = e_{mix}\left(x_5,\ h_5,\ s_5\right)$ Specific exergy of the sat. vapour at state 5 - [kJ/kg] (79)

$\dot{E}x_{turb,OUT} = Ex_{mix}\left(\dot{m}_{vapour},\ x_5,\ h_5,\ s_5\right)$ Exergy associated with the sat. vapour at state 5 - [kW](80)

$\dot{E}x_{turb} = Power_{turb}$ Exergy transfer associated with turbine work - [kW] (81)

$\dot{E}x_{turb,D} = \dot{E}x_{vapour} - \dot{E}x_{turb} - \dot{E}x_{turb,OUT}$ Exergy destruction in the turbine - [kW] (82)

HT Recuperator:

$\dot{Q}_{HT,IN} = \dot{m}_{liq} \cdot \left(h_4 - h_6\right)$ Heat transfer rate of the sat. liq. - [kW] (83)

$\dot{Q}_{HT,OUT} = \dot{m}_{mix} \cdot \left(h_{start} - h_{12}\right)$ Heat transfer rate of the feed mix. - [kW] (84)

$\dot{m}_{liq} \cdot \left(h_4 - h_6\right) = \dot{m}_{mix} \cdot \left(h_{start} - h_{12}\right)$ Heat balance in the HT recuperator (85)

$T_{HT} = 312.8$ T$_{HT}$=T[8]-3 Supposed temperature at state 12 - [K] (86)

$T_{liq} = T_{HT} + 3$ Supposed temperature at state 6 - [K] (87)

call $NH3H2O\left(123,\ T_{liq},\ P_{high},\ x_4 : T_6,\ P_6,\ x_6,\ h_6,\ s_6,\ u_6,\ v_6,\ q_6\right)$ Mix. at state 6 (88)

call $NH3H2O\left(123,\ T_{HT},\ P_{high},\ x_{mix} : T_{12},\ P_{12},\ x_{12},\ h_{12},\ s_{12},\ u_{12},\ v_{12},\ q_{12}\right)$ Mix. at state 12(89)

$e_6 = e_{mix}\left(x_4,\ h_6,\ s_6\right)$ Specific exergy of the mix. at state 6 - [kJ/kg] (90)

$\dot{E}x_{HT,liq,OUT} = Ex_{mix}\left(\dot{m}_{liq},\ x_4,\ h_6,\ s_6\right)$ Exergy associated with the mix. at state 6 - [kW] (91)

$e_{12} = e_{mix}\left(x_{12},\ h_{12},\ s_{12}\right)$ Specific exergy of the mix. at state 12 - [kJ/kg] (92)

$\dot{E}x_{HT,IN} = Ex_{mix}\left(\dot{m}_{mix},\ x_{12},\ h_{12},\ s_{12}\right)$ Exergy associated with the mix. at state 12 - [kW] (93)

$\dot{E}x_{HT,OUT} = \dot{E}x_{vap,IN}$ (94)

$\dot{E}x_{HT,liq,add} = \dot{E}x_{liq} - \dot{E}x_{HT,liq,OUT}$ Exergy added by the mix. - [kW] (95)

$\dot{E}x_{HT,rise} = \dot{E}x_{HT,OUT} - \dot{E}x_{HT,IN}$ Exergy rise in the feed mix - [kW] (96)

$\dot{E}x_{HT,D} = \dot{E}x_{HT,liq,add} - \dot{E}x_{HT,rise}$ Exergy destruction in the HT recuperator - [kW] (97)

$c_{p,liq} = \dfrac{h_4 - h_6}{(T_4 - T_6)}$ Specific heat capacity of the mix. - [kJ/kg K] (98)

$c_{p,HT,c} = \dfrac{h_1 - h_{12}}{(T_1 - T_{12})}$ Specific heat capacity of the feed mix. - [kJ/kg K] (99)

$$LMTD_{HT} = \frac{(T_4 - T_1) - (T_6 - T_{12})}{\ln\left((T_4 - T_1)\,/\,(T_6 - T_{12})\right)} \quad (100)$$

$A_{HT} = \dfrac{\dot{Q}_{HT,IN}}{(U \cdot LMTD_{HT})}$ Heat transfer area calculated- [m^2] (101)

Throttle:

call $NH3H2O\left(234,\ P_{low},\ x_4,\ h_6 : T_7,\ P_7,\ x_7,\ h_7,\ s_7,\ u_7,\ v_7,\ q_7\right)$ Mix. at state 7 (102)

$e_7 = e_{mix}\left(x_7,\ h_7,\ s_7\right)$ Specific exergy of the mix. at state 7 - [kJ/kg] (103)

$\dot{E}x_{throttle,OUT} = Ex_{mix}\left(\dot{m}_{liq},\ x_7,\ h_7,\ s_7\right)$ Exergy associated with the mix at state 7 - [kW] (104)

$\dot{E}x_{throttle,D} = \dot{E}x_{HT,liq,OUT} - \dot{E}x_{throttle,OUT}$ Exergy destruction in the throttle - [kW] (105)

Mixer:

$\dot{m}_{mix} \cdot h_{mixer} = \dot{m}_{vapour} \cdot h_5 + \dot{m}_{liq} \cdot h_7$ Heat balance in the mixer (106)

$\dot{m}_{mix} \cdot x_{mixer} = \dot{m}_{vapour} \cdot x_5 + \dot{m}_{liq} \cdot x_7$ Mass balance in the mixer (107)

call $NH3H2O\left(234,\ P_{low},\ x_{mixer},\ h_{mixer} : T_8,\ P_8,\ x_8,\ h_8,\ s_8,\ u_8,\ v_8,\ q_8\right)$ Mix. at state 8 (108)

$e_8 = e_{mix}\left(x_8,\ h_8,\ s_8\right)$ Specific exergy of the mix. at state 8 - [kJ/kg] (109)

$\dot{E}x_{mixer} = Ex_{mix}\left(\dot{m}_{mix},\ x_8,\ h_8,\ s_8\right)$ Exergy associated with the mix. at state 8 - [kW] (110)

$\dot{E}x_{mixer,add} = \dot{E}x_{mixer} - \dot{E}x_{turb,OUT} - \dot{E}x_{throttle,OUT}$ Exergy added by the mixer - [kW] (111)

LT Recuperator:

call $\mathit{NH3H2O}\,(234,\ P_{low},\ x_{mix},\ h_c : T_9,\ P_9,\ x_9,\ h_9,\ s_9,\ u_9,\ v_9,\ q_9)$ Mix. at state 9 (112)

$c_{p,LT,h} = \dfrac{h_8 - h_9}{(T_8 - T_9)}$ Specific heat capacity of the mix. - [kJ/kg K] (113)

$c_{p,LT,c} = \dfrac{h_{12} - h_{11}}{(T_{12} - T_{11})}$ Specific heat capacity of the feed mix. - [kJ/kg K] (114)

$\dot{Q}_{LT,IN} = (h_{mixer} - h_c) \cdot \dot{m}_{mix}$ Heat transfer rate of the mix. - [kW] (115)

$\dot{Q}_{LT,OUT} = (h_{12} - (h_{11})) \cdot \dot{m}_{mix}$ Heat transfer rate of the feed mix. - [kW] (116)

$(h_{12} - h_{11}) \cdot \dot{m}_{mix} = (h_{mixer} - h_c) \cdot \dot{m}_{mix}$ Heat balance of the LT recuperator (117)

$\mathit{LMTD}_{LT} = \dfrac{(T_8 - T_{12}) - (T_9 - T_{11})}{\ln\left((T_8 - T_{12})\,/\,(T_9 - T_{11})\right)}$ (118)

$A_{LT} = \dfrac{\dot{Q}_{LT,IN}}{(U \cdot LMTD_{LT})}$ Heat transfer area calculated - [m^2] (119)

$e_9 = e_{mix}\,(x_9,\ h_9,\ s_9)$ Specific exergy of the mix. at state 9 - [kJ/kg] (120)

$\dot{Ex}_{LT,OUT} = Ex_{mix}\,(\dot{m}_{mix},\ x_9,\ h_9,\ s_9)$ Exergy associated with the mix. at state 9 - [kW] (121)

$\dot{Ex}_{LT,add} = \dot{Ex}_{mixer} - \dot{Ex}_{LT,OUT}$ Exergy added by the mix. - [kW] (122)

$\dot{Ex}_{LT,rise} = \dot{Ex}_{HT,IN} - \dot{Ex}_{pump,OUT}$ Exergy rise in the feed mix. - [kW] (123)

$\dot{Ex}_{LT,D} = \dot{Ex}_{LT,add} - \dot{Ex}_{LT,rise}$ Exergy destruction in the LT recuperator - [kW] (124)

Condenser:

$T_{clow} = \mathrm{tk}(5)$ Cooling water inlet temperature, design variable - [K] (125)

$T_{chigh} = T_9 - 10$ Cooling water outlet temperature, design variable - [K] (126)

$\dot{Q}_{cond} = (h_9 - h_{10}) \cdot \dot{m}_{mix}$ Heat loss through the condenser - [kW] (127)

$\dot{m}_{cw} = \dfrac{\dot{Q}_{cond}}{((T_{chigh} - T_{clow}) \cdot c_{p,cond,c})}$ The cooling water flowrate [kg/s] (128)

$c_{p,cond,c} = \dfrac{h_{cw,OUT} - h_{cw,IN}}{(T_{chigh} - T_{clow})}$ Specific heat capacity of the cooling water (129)

$c_{p,cond,h} = \dfrac{h_9 - h_{10}}{(T_9 - T_{10})}$ Specific heat capacity of mix. [kJ/kg K] (130)

$C_{cond,c} = \dot{m}_{cw} \cdot c_{p,cond,c}$ Heat capacity of the cooling water - [kW/K] (131)

$C_{cond,h} = \dot{m}_{mix} \cdot c_{p,cond,h}$ Heat capacity of the mix. - [kW/K] (132)

$\dot{Q}_{max,cond} = C_{cond,h} \cdot (T_9 - T_{clow})$ **Maximum heat exchange in the condenser** (133)

$\epsilon_{cond,eff} = \dot{Q}_{cond} / \dot{Q}_{max,cond}$ **Condenser effectiveness** (134)

$R_{c,cond} = C_{cond,h} / C_{cond,c}$ **Heat capacity ratio C_{min}/C_{max}** (135)

$NTU_{cond} = \frac{1}{1 - R_{c,cond}} \cdot \ln\left((1 - \epsilon_{cond,eff} \cdot R_{c,cond}) \,/\, (1 - \epsilon_{cond,eff})\right)$ (136)

$A_{cond} = NTU_{cond} \cdot C_{cond,h} / U_{ammonia,cond}$ **Heat transfer area - [m^2]** (137)

call $NH3H2O\,(238,\ P_{low},\ x_{mix},\ 0.0 : T_{10},\ P_{10},\ x_{10},\ h_{10},\ s_{10},\ u_{10},\ v_{10},\ q_{10})$ **Mix. at state 10**(138)

$e_{10} = e_{mix}\,(x_{10},\ h_{10},\ s_{10})$ **Specific exergy of the mix. at state 10 - [kJ/kg]** (139)

$\dot{Ex}_{cond,OUT} = Ex_{mix}\,(\dot{m}_{mix},\ x_{10},\ h_{10},\ s_{10})$ **Exergy associated with the mix. at state 10 - [kW]**(140)

$\dot{Ex}_{cond,add} = \dot{Ex}_{LT,OUT} - \dot{Ex}_{cond,OUT}$ (141)

$\dot{Ex}_{cond,D} = \dot{Ex}_{cond,add} - \dot{Ex}_{cw,rise}$ **Exergy destruction in the condenser - [kW]** (142)

$\dot{Ex}_{cond,Lo} = \dot{Ex}_{cw,rise}$ **Exergy loss from the condenser - [kW]** (143)

$h_{cw,IN} = \mathrm{h}\,(\mathrm{Water},\ T = T_{clow},\ x = 0)$ **Enthalpy of the cooling water at state 1c- [kJ/kg]** (144)

$s_{cw,IN} = \mathrm{s}\,(\mathrm{Water},\ T = T_{clow},\ x = 0)$ **Entropy of the cooling water at state 1c- [kJ/kg K]** (145)

$h_{cw,OUT} = \mathrm{h}\,(\mathrm{Water},\ T = T_{chigh},\ x = 0)$ **Enthalpy of the cooling water at state 2c- [kJ/kg]** (146)

$s_{cw,OUT} = \mathrm{s}\,(\mathrm{Water},\ T = T_{chigh},\ x = 0)$ **Entropy of the cooling water at state 2c- [kJ/kg K]** (147)

$e_{cw,IN} = \mathrm{ex}(h_{cw,IN},\ s_{cw,IN})$ **Specific exergy of the cooling water at state 1c - [kJ/kg K]** (148)

$e_{cw,OUT} = \mathrm{ex}(h_{cw,OUT},\ s_{cw,OUT})$ **Specific exergy of the cooling water at state 2c - [kJ/kg K]** (149)

$\dot{Ex}_{cw,IN} = \dot{m}_{cw} \cdot e_{cw,IN}$ **Exergy associated with the cooling water at state 1c - [kW]** (150)

$\dot{Ex}_{cw,OUT} = \dot{m}_{cw} \cdot e_{cw,OUT}$ **Exergy associated with the cooling water at state 2c - [kW]** (151)

$\dot{Ex}_{cw,rise} = \dot{Ex}_{cw,OUT} - \dot{Ex}_{cw,IN}$ **Exergy rise in the cooling water - [kW]** (152)

Pump:

$Power_{pump} = Power_{pump,s} / \eta_{pump}$ **The actual pump power - [kW]** (153)

$Power_{pump,s} = W_{pump,s} \cdot \dot{m}_{mix}$ (154)

$W_{pump,s} = v_{10} \cdot (P_{high} - P_{low}) \cdot 100$ **The specific isentropic pump power** (155)

$W_{pump} = W_{pump,s} / \eta_{pump}$ **The specific actual pump power** (156)

$h_{pump} = h_{10} + W_{pump}$ **The enthalpy value at the exit state for actual process** (157) call $NH3H2O(234,\ P_{high},\ x_{mix},\ h_{pump} : T_{11},\ P_{11},\ x_{11},\ h_{11},\ s_{11},\ u_{11},\ v_{11},\ q_{11})$ Mix. at state 11(158)

$e_{11} = e_{mix}(x_{11},\ h_{11},\ s_{11})$ Specific exergy of the mix. at state 11 - [kJ/kg] (159)

$\dot{Ex}_{pump,OUT} = Ex_{mix}(\dot{m}_{mix},\ x_{11},\ h_{11},\ s_{11})$ Exergy associated with the mix. at state 11 - [kW](160)

$\dot{Ex}_{pump,add} = \dot{Ex}_{pump,OUT} - \dot{Ex}_{cond,OUT}$ Exergy added by the pump - [kW] (161)

$\dot{Ex}_{pump,D} = Power_{pump} - \dot{Ex}_{pump,add}$ Exergy destruction in the pump - [kW] (162)

Total exergy destruction rate in the Kalina PP:

$\dot{Ex}_{D,total} = \dot{Ex}_{vap,D} + \dot{Ex}_{sep,D} + \dot{Ex}_{turb,D} + \dot{Ex}_{HT,D} + \dot{Ex}_{LT,D} + \dot{Ex}_{throttle,D} + \dot{Ex}_{pump,D} + \dot{Ex}_{cond,D}$(163)

Total exergy loss rate from in the Kalina PP:

$\dot{Ex}_{Lo,total} = \dot{Ex}_{Lo} + \dot{Ex}_{cond,Lo}$ (164)

Exergy balance of the Kalina PP:

$\dot{Ex}_{IN} + \dot{Ex}_{mixer,add} = \text{Power}_{OUT} + \dot{Ex}_{D,total} + \dot{Ex}_{Lo,total}$

Energy balance of the Kalina PP:

$\dot{Q}_{IN} = \text{Power}_{OUT} + \dot{Q}_{cond}$

Net power production rate:

$Power_{OUT} = Power_{turb} - Power_{pump}$ (165)

Total heat transfer area of the heat exchangers:

$A_{tot} = A_{vap} + A_{HT} + A_{LT} + A_{cond}$ (166)

Efficiencies:

$\eta_{Carnot} = \dfrac{\text{tk}(T_{high}) - \text{tk}(5)}{\text{tk}(T_{high})}$ Carnot efficiency with temperature 5°C cooling water (167)

$\eta_{I,law} = Power_{OUT}/\dot{Q}_{IN}$ The first law of thermal efficiency (168)

$\eta_{I,law,max} = \dfrac{\dot{Ex}_{IN} - \dot{Ex}_{Lo} - \dot{Ex}_{cond,Lo}}{\dot{Q}_{IN}}$ The first law of maximum thermal efficiency (169)

$\eta_{II,law} = \dfrac{Power_{OUT}}{\left(\dot{Ex}_{IN} - \dot{Ex}_{Lo} - \dot{Ex}_{cond,Lo}\right)}$ The second law of thermal efficiency (170)

Usable heat into the DH system:

$T_{5w} = \text{tk}(30)$ The geothermal water temperature at state 5w [K] (171)

$h_{5w} = \text{h}(\text{Water},\ T = T_{5w},\ x = 0)$ The enthalpy of the geothermal water at state 5w [kJ/kg K](172)

$T_{supply} = \text{tk}(T_{low})$ Supply water temperature to the DH (173)

$c_{p,usable} = \dfrac{h_{2w} - h_{5w}}{(T_{supply} - T_{5w})}$ Specific heat capacity of the geothermal water at state 5 - [kJ/kg K](174)

$\dot{Q}_{usable} = \dot{m}_w \cdot c_{p,usable} \cdot (T_{supply} - T_{5w})$ Usable heat above 30 °C - [kW] (175)

APPENDIX B: SOLUTION OF THE BASE-CASE DESIGN

$A_{cond} = 1923$ [m^2]
$A_{tot} = 3584$ [m^2]
$C_{cond,h} = 578.7$ [kW/K]
$c_{p,cond,h} = 46.84$ [kJ/kg-K]
$c_{p,LT,c} = 4.711$ [kJ/kg-K]
$c_{p,usable} = 4.185$ [kJ/kg-K]
$\epsilon_{cond,eff} = 0.8849$
$\eta_{II,law} = 0.5846$
$\eta_{pump} = 0.5$
$\dot{Ex}_{cond,add} = 362.1$ [kW]
$\dot{Ex}_{cond,OUT} = 1.498$ [kW]
$\dot{Ex}_{cw,rise} = 259.2$ [kW]
$\dot{Ex}_{HT,IN} = 162.3$ [kW]
$\dot{Ex}_{HT,OUT} = 275.2$ [kW]
$\dot{Ex}_{liq} = 215.4$ [kW]
$\dot{Ex}_{LT,add} = 181.4$ [kW]
$\dot{Ex}_{LT,rise} = 115.5$ [kW]
$\dot{Ex}_{pump,add} = 45.35$ [kW]
$\dot{Ex}_{sep,D} = 261.3$ [kW]
$\dot{Ex}_{turb} = 1949$ [kW]
$\dot{Ex}_{vapour} = 2788$ [kW]
$\dot{Ex}_{vap,OUT} = 3265$ [kW]
$e_{2w} = 36.03$ [kJ/kg]
$h_{1w} = 503.6$ [kJ/kg]
$h_c = 884$ [kJ/kg]
$h_{mixer} = 1030$ [kJ/kg]
$h_{turb,eff} = 1300$
$\dot{m}_{cw} = 218.2$ [kg/s]
$\dot{m}_{vapour} = 9.873$ [kg/s]
$NTU_{vap} = 5.916$
$Power_{pump,s} = 44.86$ [kW]
$P_{high} = 30$ [bar]
$\dot{Q}_{HT,IN} = 863.2$ [kW]
$\dot{Q}_{LT,IN} = 1800$ [kW]
$\dot{Q}_{max,cond} = 13163$ [kW]
$R_{c,vap} = 0.635$
$s_{cw,IN} = 0.0755$
$T_{chigh} = 290.8$ [K]
$T_{HT} = 312.8$ [K]
$T_{supply} = 353.1$ [K]
$U_{vap} = 0.9$ [kW/m^2-K]
$x_{mix} = 0.87$ [%]

$A_{HT} = 43.81$ [m^2]
$A_{vap} = 1410$ [m^2]
$C_{mix} = 214.5$ [kW/K]
$c_{p,HT,c} = 4.882$ [kJ/kg-K]
$c_{p,LT,h} = 9.744$ [kJ/kg-K]
$c_{p,w} = 4.221$ [kJ/kg-K]
$\epsilon_{vap,eff} = 0.9545$
$\eta_{I,law} = 0.1377$
$\eta_{turb} = 0.75$
$\dot{Ex}_{cond,D} = 102.9$ [kW]
$\dot{Ex}_{cw,IN} = 1.920 \times 10^{-7}$ [kW]
$\dot{Ex}_{D,total} = 1583$ [kW]
$\dot{Ex}_{HT,liq,add} = 181.9$ [kW]
$\dot{Ex}_{HT,rise} = 112.9$ [kW]
$\dot{Ex}_{Lo} = 2882$ [kW]
$\dot{Ex}_{LT,D} = 65.95$ [kW]
$\dot{Ex}_{mixer} = 545$ [kW]
$\dot{Ex}_{pump,D} = 44.38$ [kW]
$\dot{Ex}_{throttle,D} = 6.628$ [kW]
$\dot{Ex}_{turb,D} = 581.9$ [kW]
$\dot{Ex}_{vap,D} = 450.8$ [kW]
$\dot{Ex}_{vap,rise} = 2990$ [kW]
$e_{cw,IN} = 8.798 \times 10^{-10}$ [kJ/kg]
$h_{2w} = 334.7$ [kJ/kg]
$h_{cw,IN} = 20.81$ [kJ/kg]
$h_{pump} = -51.64$ [kJ/kg]
$LMTD_{HT} = 19.7$ [K]
$\dot{m}_{liq} = 2.481$ [kg/s]
$\dot{m}_w = 80$ [kg/s]
$Power_{OUT} = 1860$ [kW]
$Power_{turb} = 1949$ [kW]
$P_{low} = 5$ [bar]
$\dot{Q}_{HT,OUT} = 863.2$ [kW]
$\dot{Q}_{LT,OUT} = 1800$ [kW]
$\dot{Q}_{usable} = 16740$ [kW]
$s_{1w} = 1.527$ [kJ/kg-K]
$s_{cw,OUT} = 0.2632$
$T_{clow} = 278.1$ [K]
$T_{liq} = 315.8$ [K]
$U = 1$ [kW/m^2-K]
$W_{pump} = 7.263$
$x_{mixer} = 0.87$ [%]

$A_{LT} = 207.8$ [m^2]
$C_{cond,c} = 913.8$ [kW/K]
$c_{p,cond,c} = 4.188$ [kJ/kg-K]
$c_{p,liq} = 4.682$
$c_{p,mix} = 17.36$ [kJ/kg-K]
$C_w = 337.7$ [kW/K]
$\eta_{Carnot} = 0.2925$
$\eta_{I,law,max} = 0.2355$
$\dot{Ex}_{add} = 3440$ [kW]
$\dot{Ex}_{cond,Lo} = 259.2$ [kW]
$\dot{Ex}_{cw,OUT} = 259.2$ [kW]
$\dot{Ex}_{HT,D} = 69.04$ [kW]
$\dot{Ex}_{HT,liq,OUT} = 33.45$ [kW]
$\dot{Ex}_{IN} = 6322$ [kW]
$\dot{Ex}_{Lo,total} = 3141$ [kW]
$\dot{Ex}_{LT,OUT} = 363.6$ [kW]
$\dot{Ex}_{mixer,add} = 261.3$ [kW]
$\dot{Ex}_{pump,OUT} = 46.85$ [kW]
$\dot{Ex}_{throttle,OUT} = 26.83$ [kW]
$\dot{Ex}_{turb,OUT} = 256.9$ [kW]
$\dot{Ex}_{vap,IN} = 275.2$ [kW]
$e_{1w} = 79.03$ [kJ/kg]
$e_{cw,OUT} = 1.188$ [kJ/kg]
$h_{5w} = 125.5$ [kJ/kg]
$h_{cw,OUT} = 74.2$ [kJ/kg]
$h_{start} = 163.9$ [kJ/kg]
$LMTD_{LT} = 8.664$ [K]
$\dot{m}_{mix} = 12.35$ [kg/s]
$NTU_{cond} = 3.655$
$Power_{pump} = 89.73$ [kW]
$Power_{turb,s} = 2599$ [kW]
$\dot{Q}_{cond} = 11648$ [kW]
$\dot{Q}_{IN} = 13508$ [kW]
$\dot{Q}_{max} = 14151$ [kW]
$R_{c,cond} = 0.6332$
$s_{2w} = 1.075$ [kJ/kg-K]
$T_{5w} = 303.1$ [K]
$T_{high} = 120$ [C]
$T_{low} = 80$ [C]
$U_{ammonia,cond} = 1.1$ [kW/m^2-K]
$W_{pump,s} = 3.631$

APPENDIX C: ECONOMIC MODEL

Equations

Levelised cost of components:

$C_{vap} = (588) \cdot (A_{vap})^{0.8}$ Cost of the vaporizer - [US$] (1)

$C_{HT} = (588) \cdot (A_{HT})^{0.8}$ Cost of the HT recuperator - [US$] (2)

$C_{LT} = (588) \cdot (A_{LT})^{0.8}$ Cost of the LT recuperator - [US$] (3)

$C_{cond} = (588) \cdot (A_{cond})^{0.8}$ Cost of the condenser - [US$] (4)

$C_{pump} = (1120) \cdot (Power_{OUT})^{0.8}$ Cost of the pump - [US$] (5)

$C_{turb} = (4405) \cdot (Power_{OUT})^{0.7}$ Cost of the turbine - [US$] (6)

$PEC_{total} = (C_{vap} + C_{cond} + C_{HT} + C_{LT} + C_{pump} + C_{turb})$ Total purchased equipment cost (7)

Capital investment rate for the major components per second:

$\dot{Z}_{vap} = (CRF/t_{op}) \cdot C_{vap} \cdot (1 + r_n)^2$ Capital investment rate of the vaporizer - [US$/s] (8)

$\dot{Z}_{turb} = (CRF/t_{op}) \cdot C_{turb} \cdot (1 + r_n)^2$ Capital investment rate of the turbine - [US$/s] (9)

$\dot{Z}_{LT} = (CRF/t_{op}) \cdot C_{LT} \cdot (1 + r_n)^2$ Capital investment rate of the LT recuperator - [US$/s] (10)

$\dot{Z}_{HT} = (CRF/t_{op}) \cdot C_{HT} \cdot (1 + r_n)^2$ Capital investment rate of the HT recuperator - [US$/s] (11)

$\dot{Z}_{cond} = (CRF/t_{op}) \cdot C_{cond} \cdot (1 + r_n)^2$ Capital investment rate of the condenser - [US$/s] (12)

$\dot{Z}_{pump} = (CRF/t_{op}) \cdot C_{pump} \cdot (1 + r_n)^2$ Capital investment rate of the condenser - [US$/s] (13)

Operating and Maintenance (O&M) cost of CHP plant:

$C_{L,O\&M,geothermal} = C_{L,geothermal} \cdot 0.1$ O&M cost of th geothermal field (14)

O&M cost rate of the major components of the Kalina PP:

$n_{labour} = 5$ Labour positions 5 persons (15)

$Salary = 5$ Average labor rate - [US$/h] (16)

$t_{work} = 2080$ Working hours per year (17)

$C_{labour} = n_{labour} \cdot Salary \cdot t_{work}$ Direct labour cost (18)

$C_{O\&M,fixed} = C_{labour} \cdot 2$ Fixed O&M cost (19)

$$C_{O\&M,Variable} = C_{O\&M,fixed} \cdot 0.09 \quad \text{Variable O\&M cost} \tag{20}$$

$$CGW = c_{F,sp,L} \cdot t_{op} \cdot \dot{m}_w \quad \text{Geothermal water cost in the whole year - [US\$]} \tag{21}$$

$$C_{O\&M} = C_{O\&M,fixed} + C_{O\&M,Variable} \quad \text{The annual O\&M cost - [US\$]} \tag{22}$$

$$C_{L,O\&M} = C_{O\&M} \cdot (1+0.05)^{2.5} \cdot CELF \quad \text{The levelised annual O\$M cost - [US\$]} \tag{23}$$

$$C_{L,DH,O\&M} = 450000 \quad \text{O\&M cost of the DH, data used from the pre-feasibility study - [US\$]} \tag{24}$$

$$\dot{Z}_{O\&M,vap} = \frac{CRF \cdot C_{L,O\&M} \cdot C_{vap}/PEC_{total}}{t_{op}} \quad \text{O\&M cost rate of the vaporiser - [US\$/s]} \tag{25}$$

$$\dot{Z}_{O\&M,turb} = \frac{CRF \cdot C_{L,O\&M} \cdot C_{turb}/PEC_{total}}{t_{op}} \quad \text{O\&M cost rate of the turbine - [US\$/s]} \tag{26}$$

$$\dot{Z}_{O\&M,HT} = \frac{CRF \cdot C_{L,O\&M} \cdot C_{HT}/PEC_{total}}{t_{op}} \quad \text{O\&M cost rate of the HT recuperator - [US\$/s]} \tag{27}$$

$$\dot{Z}_{O\&M,LT} = \frac{CRF \cdot C_{L,O\&M} \cdot C_{LT}/PEC_{total}}{t_{op}} \quad \text{O\&M cost rate of the LT recuperator - [US\$/s]} \tag{28}$$

$$\dot{Z}_{O\&M,cond} = \frac{CRF \cdot C_{L,O\&M} \cdot C_{cond}/PEC_{total}}{t_{op}} \quad \text{O\&M cost rate of the condenser - [US\$/s]} \tag{29}$$

$$\dot{Z}_{O\&M,pump} = \frac{CRF \cdot C_{L,O\&M} \cdot C_{pump}/PEC_{total}}{t_{op}} \quad \text{O\&M cost rate of the pump - [US\$/s]} \tag{30}$$

Exergy costing:

$$CRF = \frac{i_{eff} \cdot (1+i_{eff})^{N_y}}{\left((1+i_{eff})^{N_y} - 1\right)} \quad \text{Capital recovery factor (CRF)} \tag{31}$$

$$N_y = 20 \quad \text{Perod of repayment [year]} \tag{32}$$

$$i_{eff} = 0.10 \quad \text{Effective rate of return - [\%]} \tag{33}$$

$$t_{op} = 8040 \cdot 3600 \quad \text{Time of operating plant per year - [s]} \tag{34}$$

$$C_{g,base} = 1000 \quad \text{Direct cost for a low-temperature geothermal resource exploration work - [US\$/kW]} \tag{35}$$

$$C_{geothermal} = C_{g,base} \cdot Power_{turb} \cdot (1+r_n)^1 \quad \text{Cost of the geothermal exploration work - [US\$]} \tag{36}$$

$$C_{L,geothermal} = C_{geothermal} \cdot CRF \quad \text{The levelized cost of the geothermal water - [US\$/year]} \tag{37}$$

$$P_{o,geothermal} = C_{L,geothermal}/CELF \quad \text{Payment at the beginning of the first year - [\$]} \tag{38}$$

$$CELF = \frac{CRF \cdot k \cdot \left(1 - k^{N_y}\right)}{(1-k)} \quad \text{Constant-escalation levelization factor} \tag{39}$$

$k = \dfrac{1 + r_n}{(1 + i_{eff})}$ k coefficient (40)

$r_n = 0.06$ Nominal escalation rate (41)

$c_{F,sp,L} = \dfrac{C_{L,geothermal}}{(\dot{m}_w \cdot t_{op})}$ The levelized specific cost of the geothermal water - [US$/kg] (42)

$c_{geothermal,sp} = c_{F,sp,L} \cdot 1000 \cdot 100$ The levelised specific cost of the geothermal water -[US c/tonne](43)

$c_{E,IN} = c_{F,sp,L} / e_{1w}$ The levelised unit cost of exergy to the Kalina PP - [US$/kJ] (44)

$c_{E,DH,IN} = c_{F,sp,L} / e_{2w}$ The levelised unit cost of exergy to the DH system - [US$/kJ] (45)

$c_{E,water,IN} = 0$ The levelised unit cost of exergy of the cooling water at the inlet - [US$/kJ] (46)

$c_{E,water,OUT} = 0$ The levelised unit cost of exergy of the cooling water at the outlet - [US$/kJ] (47)

The cost rate balance of the major components in the Kalina PP

$$c_{E,vap} \cdot \dot{E}x_{vap,OUT} - c_{E,HT} \cdot \dot{E}x_{vap,IN} = c_{E,IN} \cdot \left(\dot{E}x_{vap,OUT} - \dot{E}x_{vap,IN}\right) + \dot{Z}_{vap} + \dot{Z}_{O\&M,vap} + \dot{C}_{D,vap} \quad (48)$$

$$c_{E,turb} = c_{E,vap} + \frac{\dot{Z}_{turb} + \dot{Z}_{O\&M,turb} + c_{E,vap} \cdot \dot{E}x_{turb,D}}{Power_{turb}} \quad (49)$$

$$c_{E,HT} \cdot \dot{E}x_{HT,OUT} - c_{E,LT} \cdot \dot{E}x_{HT,IN} = c_{E,vap} \cdot \left(\dot{E}x_{HT,OUT} - \dot{E}x_{HT,IN}\right) + \dot{Z}_{HT} + \dot{Z}_{O\&M,HT} + \dot{C}_{D,HT} \quad (50)$$

$$c_{E,LT} \cdot \dot{E}x_{HT,IN} - c_{E,pump} \cdot \dot{E}x_{pump,OUT} = c_{E,vap} \cdot \left(\dot{E}x_{HT,IN} - \dot{E}x_{pump,OUT}\right) + \dot{Z}_{LT} + \dot{Z}_{O\&M,LT} + \dot{C}_{D,LT} \quad (51)$$

$$c_{E,pump} \cdot \dot{E}x_{pump,OUT} - c_{E,vap} \cdot \dot{E}x_{cond,OUT} = c_{E,turb} \cdot \dot{E}x_{pump,OUT} + \dot{Z}_{pump} + \dot{Z}_{O\&M,pump} + \dot{C}_{D,pump} \quad (52)$$

The cost rate of components' exergy destruction per hour:

$\dot{C}_{D,vap} = c_{E,vap} \cdot \dot{E}x_{vap,D}$ The cost rate of the vaporiser exergy destruction - [US$/s] (53)

$\dot{C}_{D,sep} = c_{E,vap} \cdot \dot{E}x_{sep,D}$ The cost rate of the seperator exergy destruction - [US$/s] (54)

$\dot{C}_{D,turb} = c_{E,turb} \cdot \dot{E}x_{turb,D}$ The cost rate of the turbine exergy destruction - [US$/s] (55)

$\dot{C}_{D,HT} = c_{E,HT} \cdot \dot{E}x_{HT,D}$ The cost rate of the HT recuperator exergy destruction - [US$/s] (56)

$\dot{C}_{D,LT} = c_{E,LT} \cdot \dot{E}x_{LT,D}$ The cost rate of the LT recuperator exergy destruction - [US$/s] (57)

$\dot{C}_{D,throttle} = c_{E,vap} \cdot \dot{E}x_{throttle,D}$ The cost rate of the throttle exergy destruction - [US$/s] (58)

$\dot{C}_{D,cond} = c_{E,vap} \cdot \dot{E}x_{cond,D}$ The cost rate of the condenser exergy destruction - [US$/s] (59)

$\dot{C}_{D,pump} = c_{E,vap} \cdot \dot{E}x_{pump,D}$ The cost rate of the pump exergy destruction - [US$/s] (60)

Unit cost of exergy rate:

$c_{E,IN,kWh} = c_{E,IN} \cdot 100 \cdot 3600$ associated with the geothermal water to the Kalina PP - [USc/kWh](61)

$c_{E,DH,IN,kWh} = c_{E,DH,IN} \cdot 100 \cdot 3600$ associated with the geothermal water to the DH system - [USc/kWh](62)

$c_{E,vap,kWh} = c_{E,vap} \cdot 100 \cdot 3600$ associated with the mix. from the vaporizer - [USc/kWh] (63)

$c_{E,turb,kWh} = c_{E,turb} \cdot 100 \cdot 3600$ associated with the power output from the turbine - [USc/kWh](64)

$c_{E,HT,kWh} = c_{E,HT} \cdot 100 \cdot 3600$ associated with the mix. from the HT recuperator - [USc/kWh] (65)

$c_{E,LT,kWh} = c_{E,LT} \cdot 100 \cdot 3600$ associated with the mix. from the LT recuperator - [USc/kWh] (66)

$c_{E,water,kWh} = c_{E,water,OUT} \cdot 100 \cdot 3600$ associated with the cooling water from the condenser - [USc/kWh](67)

$c_{E,pump,kWh} = c_{E,pump} \cdot 100 \cdot 3600$ associated with the mix. from the pump - [USc/kWh] (68)

Levelized cost rates - [US$/s]

$\dot{C}_1 = c_{E,HT} \cdot \dot{E}x_{vap,IN}$ (69)

$\dot{C}_2 = c_{E,vap} \cdot \dot{E}x_{vap,OUT}$ (70)

$\dot{C}_3 = c_{E,vap} \cdot \dot{E}x_{vapour}$ (71)

$\dot{C}_4 = c_{E,vap} \cdot \dot{E}x_{liq}$ (72)

$\dot{C}_6 = c_{E,vap} \cdot \dot{E}x_{HT,liq,OUT}$ (73)

$\dot{C}_5 = c_{E,vap} \cdot \dot{E}x_{turb,OUT}$ (74)

$\dot{C}_7 = c_{E,vap} \cdot \dot{E}x_{throttle,OUT}$ (75)

$\dot{C}_8 = c_{E,vap} \cdot \dot{E}x_{mixer}$ (76)

$\dot{C}_9 = c_{E,vap} \cdot \dot{E}x_{LT,OUT}$ (77)

$\dot{C}_{10} = c_{E,vap} \cdot \dot{E}x_{cond,OUT}$ (78)

$\dot{C}_{11} = c_{E,pump} \cdot \dot{E}x_{pump,OUT}$ (79)

$\dot{C}_{12} = c_{E,LT} \cdot \dot{E}x_{HT,IN}$ (80)

$\dot{C}_{1c} = c_{E,water,IN} \cdot \dot{E}x_{cw,IN}$ (81)

$\dot{C}_{2c} = c_{E,water,OUT} \cdot \dot{E}x_{cw,OUT}$ (82)

$\dot{C}_{1w} = c_{E,IN} \cdot \dot{E}x_{IN}$ (83)

$\dot{C}_{2w} = c_{E,DH,IN} \cdot \dot{E}x_{Lo}$ (84)

$\dot{C}_{turb} = c_{E,turb} \cdot Power_{turb}$ (85)

Thermoeconomic evaluation

Exergetic efficiency

$$\epsilon_{vap} = \dot{E}x_{vap,rise}/\dot{E}x_{add} \tag{86}$$

$$\epsilon_{sep} = 1 - \dot{E}x_{sep,D}/\dot{E}x_{vap,OUT} \tag{87}$$

$$\epsilon_{turb} = \frac{Power_{turb}}{\dot{E}x_{vapour} - \dot{E}x_{turb,OUT}} \tag{88}$$

$$\epsilon_{HT} = \dot{E}x_{HT,rise}/\dot{E}x_{HT,liq,add} \tag{89}$$

$$\epsilon_{throttle} = 1 - \dot{E}x_{throttle,D}/\dot{E}x_{HT,liq,OUT} \tag{90}$$

$$\epsilon_{mixer} = \frac{\dot{E}x_{mixer}}{\left(\dot{E}x_{throttle,OUT} + \dot{E}x_{turb,OUT}\right)} \tag{91}$$

$$\epsilon_{LT} = \dot{E}x_{LT,rise}/\dot{E}x_{LT,add} \tag{92}$$

$$\epsilon_{cond} = \frac{\dot{E}x_{cw,OUT}}{\left(\dot{E}x_{LT,OUT} - \dot{E}x_{cond,OUT}\right)} \tag{93}$$

$$\epsilon_{pump} = \frac{\dot{E}x_{pump,OUT} - \dot{E}x_{cond,OUT}}{Power_{pump}} \tag{94}$$

$$\epsilon_{plant} = \frac{Power_{OUT}}{\dot{E}x_{IN} + \dot{E}x_{mixer,add}} \tag{95}$$

Exergy destruction ratio

$$Y_{vap,D} = \frac{\dot{E}x_{vap,D}}{\dot{E}x_{IN} + \dot{E}x_{mixer,add}} \tag{96}$$

$$Y_{sep,D} = \frac{\dot{E}x_{sep,D}}{\dot{E}x_{IN} + \dot{E}x_{mixer,add}} \tag{97}$$

$$Y_{turb,D} = \frac{\dot{E}x_{turb,D}}{\dot{E}x_{IN} + \dot{E}x_{mixer,add}} \tag{98}$$

$$Y_{HT,D} = \frac{\dot{E}x_{HT,D}}{\dot{E}x_{IN} + \dot{E}x_{mixer,add}} \tag{99}$$

$$Y_{LT,D} = \frac{\dot{E}x_{LT,D}}{\dot{E}x_{IN} + \dot{E}x_{mixer,add}} \tag{100}$$

$$Y_{cond,D} = \frac{\dot{E}x_{cond,D}}{\dot{E}x_{IN} + \dot{E}x_{mixer,add}} \tag{101}$$

$$Y_{throttle,D} = \frac{\dot{E}x_{throttle,D}}{\dot{E}x_{IN} + \dot{E}x_{mixer,add}} \tag{102}$$

$$Y_{pump,D} = \frac{\dot{E}x_{pump,D}}{\dot{E}x_{IN} + \dot{E}x_{mixer,add}} \tag{103}$$

$$Y_{D,total} = Y_{vap,D} + Y_{sep,D} + Y_{turb,D} + Y_{HT,D} + Y_{LT,D} + Y_{cond,D} + Y_{throttle,D} + Y_{pump,D} \tag{104}$$

Exergy loss ratio

$$Y_{vap,Lo} = \frac{\dot{E}x_{Lo}}{\dot{E}x_{IN} + \dot{E}x_{mixer,add}} \tag{105}$$

$$Y_{cond,Lo} = \frac{\dot{E}x_{cond,Lo}}{\dot{E}x_{IN} + \dot{E}x_{mixer,add}} \tag{106}$$

$$Y_{Lo,total} = Y_{vap,Lo} + Y_{cond,Lo} \tag{107}$$

$$Y_{rest} = 1 - \epsilon_{plant} - Y_{D,total} - Y_{Lo,total} \tag{108}$$

Relative cost difference

$$r_{vap} = \frac{c_{E,IN} \cdot \left(\dot{E}x_{vap,D} + \dot{E}x_{Lo}\right) + \dot{Z}_{vap} + \dot{Z}_{O\&M,vap}}{c_{E,IN} \cdot \dot{E}x_{vap,OUT}} \tag{109}$$

$$r_{turb} = \frac{c_{E,vap} \cdot \dot{E}x_{turb,D} + \dot{Z}_{turb} + \dot{Z}_{O\&M,turb}}{c_{E,vap} \cdot \left(Power_{turb} + \dot{E}x_{turb,OUT}\right)} \tag{110}$$

$$r_{HT} = \frac{c_{E,vap} \cdot \dot{E}x_{HT,D} + \dot{Z}_{HT} + \dot{Z}_{O\&M,HT}}{c_{E,vap} \cdot \left(\dot{E}x_{HT,OUT} + \dot{E}x_{HT,liq,OUT}\right)} \tag{111}$$

$$r_{LT} = \frac{c_{E,vap} \cdot \dot{E}x_{LT,D} + \dot{Z}_{LT} + \dot{Z}_{O\&M,LT}}{c_{E,vap} \cdot \left(\dot{E}x_{LT,OUT} + \dot{E}x_{HT,IN}\right)} \tag{112}$$

$$r_{cond} = \frac{c_{E,vap} \cdot \left(\dot{E}x_{cond,Lo} + \dot{E}x_{cond,D}\right) + \dot{Z}_{cond} + \dot{Z}_{O\&M,cond}}{c_{E,vap} \cdot \dot{E}x_{cond,OUT}} \tag{113}$$

$$r_{pump} = \frac{c_{E,turb} \cdot \dot{E}x_{pump,D} + \dot{Z}_{pump} + \dot{Z}_{O\&M,pump}}{c_{E,turb} \cdot \dot{E}x_{pump,OUT}} \tag{114}$$

Exergoeconomic factor

$$f_{vap} = \frac{\dot{Z}_{vap} + \dot{Z}_{O\&M,vap}}{\dot{Z}_{vap} + \dot{Z}_{O\&M,vap} + c_{E,IN} \cdot \left(\dot{E}x_{vap,D} + \dot{E}x_{Lo}\right)} \tag{115}$$

$$f_{turb} = \frac{\dot{Z}_{turb} + \dot{Z}_{O\&M,turb}}{\dot{Z}_{turb} + \dot{Z}_{O\&M,turb} + c_{E,vap} \cdot \dot{E}x_{turb,D}} \tag{116}$$

$$f_{HT} = \frac{\dot{Z}_{HT} + \dot{Z}_{O\&M,HT}}{\dot{Z}_{HT} + \dot{Z}_{O\&M,HT} + c_{E,vap} \cdot \dot{E}x_{HT,D}} \tag{117}$$

$$f_{LT} = \frac{\dot{Z}_{LT} + \dot{Z}_{O\&M,LT}}{\dot{Z}_{LT} + \dot{Z}_{O\&M,LT} + c_{E,vap} \cdot \dot{E}x_{LT,D}} \tag{118}$$

$$f_{pump} = \frac{\dot{Z}_{pump} + \dot{Z}_{O\&M,pump}}{\dot{Z}_{pump} + \dot{Z}_{O\&M,pump} + c_{E,turb} \cdot \dot{E}x_{pump,D}} \tag{119}$$

$$f_{cond} = \frac{\dot{Z}_{cond} + \dot{Z}_{O\&M,cond}}{\dot{Z}_{cond} + \dot{Z}_{O\&M,cond} + c_{E,vap} \cdot \left(\dot{E}x_{cond,D} + \dot{E}x_{cond,Lo}\right)} \tag{120}$$

Rank by $Z_{component}+\dot{C}_{D,component}$

$$Z\&C_{vap} = \dot{Z}_{vap} + \dot{Z}_{O\&M,vap} + \dot{C}_{D,vap} \tag{121}$$

$$Z\&C_{turb} = \dot{Z}_{turb} + \dot{Z}_{O\&M,turb} + \dot{C}_{D,turb} \tag{122}$$

$$Z\&C_{HT} = \dot{Z}_{HT} + \dot{Z}_{O\&M,HT} + \dot{C}_{D,HT} \tag{123}$$

$$Z\&C_{LT} = \dot{Z}_{LT} + \dot{Z}_{O\&M,LT} + \dot{C}_{D,LT} \tag{124}$$

$$Z\&C_{cond} = \dot{Z}_{cond} + \dot{Z}_{O\&M,cond} + \dot{C}_{D,cond} \tag{125}$$

$$Z\&C_{pump} = \dot{Z}_{pump} + \dot{Z}_{O\&M,pump} + \dot{C}_{D,pump} \tag{126}$$

Economic analysis:

Fixed capital investment:

$TDC = PEC_{total} + C_{piping} + C_{land}$ Total direct cost of the project - [US$] (127)

$C_{land} = (PEC_{total} \cdot 0.01)$ Assumed cost for the land rent - [US$] (128)

$C_{land,es} = C_{land} \cdot (1 + r_n)^{1.5}$ Its escalated value - [US$] (129)

$C_{piping} = 0.1 \cdot PEC_{total}$ Piping cost - [US$] (130)

$C_{piping,es} = C_{piping} \cdot (1 + r_n)^2$ Escalated piping cost - [US$] (131)

$TIDC = TDC \cdot 0.05$ Total indirect cost of the project 5% of the TDC (132)

$FCI = TIDC + TDC$ Fixed capital investment - [US$] (133)

$C_{PFI} = FCI - C_{land}$ Plant Facility Investment - [US$] (134)

$C_{PFI,es} = C_{PFI} \cdot (1 + r_n)^2$ Escalated PFI - [US$] (135)

Other outlays:

Startup cost (SUC)

$$SUC = C_{O\&M,fixed}/12 + C_{O\&M,Variable}/12 + P_{o,geothermal}/52 + C_{PFI} \cdot 0.02 \ \text{[US\$]} \tag{136}$$

$$SUC_{es} = SUC \cdot (1 + r_n)^3 \quad \text{Escalated SUC - [US\$]} \tag{137}$$

Working capital (WC)

$$WC = (P_{o,geothermal}/6 + C_{labour}/4) \cdot 1.25 \ \text{[US\$]} \tag{138}$$

$$WC_{es} = WC \cdot (1 + r_n)^{3.5} \quad \text{Escalated WC - [US\$]} \tag{139}$$

Cost of lisensing, research and development

$$LRD = (150) \cdot Power_{turb} \ \text{[US\$]} \tag{140}$$

$$LRD_{es} = LRD \cdot (1 + r_n)^{1.5} \quad \text{Escalated LRD - [US\$]} \tag{141}$$

Allowance for funds used during construction

$$AFUDC = FCI \cdot 0.15 - LRD \ \text{[US\$]} \tag{142}$$

$$AFUDC_{es} = AFUDC \cdot (1 + r_n)^3 \quad \text{Escalated AFUDC - [US\$]} \tag{143}$$

Total capital investment

$$TCI = C_{PFI,es} + C_{land,es} + SUC_{es} + WC_{es} + LRD_{es} + AFUDC_{es} \quad \text{TCI cost of Kalina PP - [US\$]} \tag{144}$$

$$C_{plant} = TCI/Power_{turb} \quad \text{Direct capital cost of Kalina PP per installed kW capacity - [US\$/kW]} \tag{145}$$

$$TCI_{non,depreciable} = C_{land,es} + WC_{es} \quad \text{Total nondepreciable capital investment - [US\$]} \tag{146}$$

$$TCI_{depreciable} = TCI - TCI_{non,depreciable} \quad \text{Total depreciable capital investment - [US\$]} \tag{147}$$

Total revenue estimation

$$C_{usable} = \left(c_{E,DH,IN} \cdot \dot{Q}_{usable} \cdot t_{op}\right) \quad \text{Total revenue from the usable heat or by product - [US\$]} \tag{148}$$

$$Q_{sellable} = \dot{Q}_{usable} \cdot \frac{t_{op}}{10^6} \quad \text{Total sellable heat in a whole year - [GJ]} \tag{149}$$

$$C_{en,electricity} = c_{E,turb,kWh} \cdot Power_{OUT} \cdot 8040/100 \quad \text{Total revenue from the electricity - [US\$]} \tag{150}$$

$$Power_{annually} = Power_{OUT} \cdot \frac{t_{op}}{10^6} \quad \text{Annual power production - [GJ]} \tag{151}$$

$$C_{income} = C_{usable} + C_{en,electricity} - C_{L,O\&M} - C_{L,O\&M,geothermal} \quad \text{Yearly income of the CHP plant - [US\$]} \tag{152}$$

Taxation

$t = 0.40$ Mongolian top income tax rate 40 percent (153)

$TAX = C_{income} \cdot t$ Tax payment (154)

Income after tax payment

$C_{income,TAX} = C_{income} - TAX$ Total income after tax paid (155)

Economic analysis including costs' of DH renovation and transmission pipeline:

$C_{trans,pipe,5} = 250000 \cdot 5$ 300 mm diameter transmission pipeline cost 250000 USD/km (156)

$C_{trans,pipe,20} = 250000 \cdot 20$ (157)

$C_{DH,renovation} = 2400000$ An assumption, [US$] (158)

$C_{DH,5} = C_{trans,pipe,5} + C_{DH,renovation}$ 5 km piping and distribution pipiline renovation expenses(159)

$C_{DH,20} = C_{trans,pipe,20} + C_{DH,renovation}$ 20 km piping and distribution pipeline renovation expenses(160)

$TCI_{CHP,5} = TCI + C_{geothermal} + C_{DH,5}$ TCI of the CHP plant with 5 km transmission pipeline(161)

$TCI_{CHP,20} = TCI + C_{geothermal} + C_{DH,20}$ TCI of the CHP plant with 20 km transmission pipeline(162)

$Z_{DH,5} = (CRF/t_{op}) \cdot C_{DH,5}$ Capital investment rate for the DH system - [US$/s] (163)

$Z_{DH,20} = (CRF/t_{op}) \cdot C_{DH,20}$ Capital investment rate for the DH system - [US$/s] (164)

$c_{E,DH,5} = c_{E,DH,IN} + Z_{DH,5}/\dot{Q}_{usable}$ The unit cost of heat with 5 km transmission pipeline (165)

$C_{usable,DH,5} = c_{E,DH,5} \cdot \dot{Q}_{usable} \cdot t_{op}$ Revenue from heat consumers with 5 km transmission pipeline(166)

$c_{E,DH,20} = c_{E,DH,IN} + Z_{DH,20}/\dot{Q}_{usable}$ The unit cost of heat with 20 km transmission pipeline (167)

$C_{usable,DH,20} = c_{E,DH,20} \cdot \dot{Q}_{usable} \cdot t_{op}$ Revenue from heat consumers with 20 km transmission pipeline(168)

$TAX_{DH,5} = C_{income,DH,5} \cdot t$ (169)

$C_{income,DH,5} = C_{usable,DH,5} + C_{en,electricity} - C_{L,O\&M} - C_{L,O\&M,geothermal} - C_{L,DH,O\&M}$ (170)

$TAX_{DH,20} = C_{income,DH,20} \cdot t$ (171)

$C_{income,DH,20} = C_{usable,DH,20} + C_{en,electricity} - C_{L,O\&M} - C_{L,O\&M,geothermal} - C_{L,DH,O\&M}$ (172)

NPV and IRR analysis:

$NPV = -TCI - C_{geothermal} + C_{income}/CRF$ (173)

$$NPV_{TAX} = -TCI - C_{geothermal} + \frac{C_{income} - Tax}{CRF} \quad (174)$$

$$NPV_5 = -TCI_{CHP,5} + C_{income,DH,5}/CRF \tag{175}$$

$$NPV_{20} = -TCI_{CHP,20} + C_{income,DH,20}/CRF \tag{176}$$

$$NPV_{TAX,5} = -TCI_{CHP,5} + \frac{C_{income,DH,5} - TAX_{DH,5}}{CRF} \tag{177}$$

$$NPV_{TAX,20} = -TCI_{CHP,20} + \frac{C_{income,DH,20} - TAX_{DH,20}}{CRF} \tag{178}$$

$$TCI + C_{geothermal} = \frac{C_{income}}{\left(\left(IRR \cdot (1+IRR)^{N_y}\right) / \left((1+IRR)^{N_y} - 1\right)\right)} \tag{179}$$

$$TCI + C_{geothermal} = \frac{C_{income} - TAX}{\left(IRR_{Tax} \cdot (1+IRR_{Tax})^{N_y}\right) / \left((1+IRR_{Tax})^{N_y} - 1\right)} \tag{180}$$

$$TCI_{CHP,5} = \frac{C_{income,DH,5}}{\left(IRR_5 \cdot (1+IRR_5)^{N_y}\right) / \left((1+IRR_5)^{N_y} - 1\right)} \tag{181}$$

$$TCI_{CHP,20} = \frac{C_{income,DH,20}}{\left(IRR_{20} \cdot (1+IRR_{20})^{N_y}\right) / \left((1+IRR_{20})^{N_y} - 1\right)} \tag{182}$$

$$TCI_{CHP,5} = \frac{C_{income,DH,5} - TAX_{DH,5}}{\left(IRR_{5,Tax} \cdot (1+IRR_{5,Tax})^{N_y}\right) / \left((1+IRR_{5,Tax})^{N_y} - 1\right)} \tag{183}$$

$$TCI_{CHP,20} = \frac{C_{income,DH,20} - TAX_{DH,20}}{\left(IRR_{20,Tax} \cdot (1+IRR_{20,Tax})^{N_y}\right) / \left((1+IRR_{20,Tax})^{N_y} - 1\right)} \tag{184}$$

CO_2 credit:

$Q_{subbitiminous} = 18.4$ Energy content of sub-bituminous - [GJ/ton] (185)

$\eta_{boiler} = 0.4$ Boiler efficiency (186)

$m_{subbitiminous} = \dfrac{Q_{sellable}}{(Q_{subbitiminous} \cdot \eta_{boiler})}$ Yearly reduction of sub-bituminous - [ton] (187)

$Q_{yearly,subbitiminous} = m_{subbitiminous} \cdot Q_{subbitiminous}$ Yearly energy content of sub-bituminous (188)

$CO_{2,heat} = 0.091$ Tons of CO_2 per GJ heat energy produced by the sub-bituminous (189)

$CO_{2,reduction} = CO_{2,heat} \cdot Q_{yearly,subbitiminous}$ Yearly reduction of CO_2 (190)

$CO_{2,payback} = 3$ CO_2 fund payback per ton of CO_2 - [US$/ton] (191)

$C_{CO,2,payback} = CO_{2,reduction} \cdot CO_{2,payback}$ Yearly CO_2 payback - [US$] (192)

NPV and IRR with CO_2 payback

$$NPV_{CO,2} = -TCI - C_{geothermal} + \frac{C_{CO,2,payback} + C_{income}}{CRF} \tag{193}$$

$$NPV_{TAX,CO,2} = -TCI - C_{geothermal} + \frac{C_{CO,2,payback} + C_{income} - Tax}{CRF} \tag{194}$$

$$NPV_{5,CO,2} = -TCI - C_{geothermal} - C_{DH,5} + \frac{C_{CO,2,payback} + C_{income,DH,5}}{CRF} \tag{195}$$

$$NPV_{20,CO,2} = -TCI - C_{geothermal} - C_{DH,20} + \frac{C_{CO,2,payback} + C_{income,DH,20}}{CRF} \tag{196}$$

$$NPV_{TAX,5,CO,2} = -TCI - C_{geothermal} - C_{DH,5} + \frac{C_{CO,2,payback} + C_{income,DH,5} - TAX_{DH,5}}{CRF} \tag{197}$$

$$NPV_{TAX,20,CO,2} = -TCI - C_{geothermal} - C_{DH,20} + \frac{C_{CO,2,payback} + C_{income,DH,20} - TAX_{DH,20}}{CRF} \tag{198}$$

$$TCI + C_{geothermal} = \frac{C_{CO,2,payback} + C_{income}}{\left(IRR_{CO,2} \cdot (1 + IRR_{CO,2})^{N_y}\right) / \left((1 + IRR_{CO,2})^{N_y} - 1\right)} \tag{199}$$

$$TCI + C_{geothermal} = \frac{C_{CO,2,payback} + C_{income} - TAX}{\left(IRR_{Tax,CO,2} \cdot (1 + IRR_{Tax,CO,2})^{N_y}\right) / \left((1 + IRR_{Tax,CO,2})^{N_y} - 1\right)} \tag{200}$$

$$TCI + C_{geothermal} + C_{DH,5} = \frac{C_{CO,2,payback} + C_{income,DH,5}}{\left(IRR_{5,CO,2} \cdot (1 + IRR_{5,CO,2})^{N_y}\right) / \left((1 + IRR_{5,CO,2})^{N_y} - 1\right)} \tag{201}$$

$$TCI + C_{geothermal} + C_{DH,20} = \frac{C_{CO,2,payback} + C_{income,DH,20}}{\left(IRR_{20,CO,2} \cdot (1 + IRR_{20,CO,2})^{N_y}\right) / \left((1 + IRR_{20,CO,2})^{N_y} - 1\right)} \tag{202}$$

$$TCI + C_{geothermal} + C_{DH,5} = \frac{C_{CO,2,payback} + C_{income,DH,5} - TAX_{DH,5}}{\left(IRR_{5,Tax,CO,2} \cdot (1 + IRR_{5,Tax,CO,2})^{N_y}\right) / \left((1 + IRR_{5,Tax,CO,2})^{N_y} - 1\right)} \tag{203}$$

$$TCI + C_{geothermal} + C_{DH,20} = \frac{C_{CO,2,payback} + C_{income,DH,20} - TAX_{DH,20}}{\left(IRR_{20,Tax,CO,2} \cdot (1 + IRR_{20,Tax,CO,2})^{N_y}\right) / \left((1 + IRR_{20,Tax,CO,2})^{N_y} - 1\right)} \tag{204}$$

APPENDIX D: INTRODUCTION OF THE EES SOFTWARE

The NH3H2O procedure provides the thermodynamic properties of ammonia-water mixtures in subcooled, saturated and superheated conditions. The procedure is called from EES by the statement:

CALL NH3H2O(Code,In1,In2,In3: T,P,x,h,s,u,v,q)

The 4 parameters to the left of the colon are inputs to the procedure; the eight values to the right are outputs whose values are set by the NH3H2O procedure. The NH3H2O routine operates in SI units with T=[K], P=[bar], x=[ammonia mass fraction], h=[kJ/kg], s=[kJ/kg-K], u=[kJ/kg], v=[m^3/kg], and q=[vapour mass fraction].

Code is a 3 digit integer indicating which of the 8 possible properties are provided as input values. For example, a Code value of 123 indicates that the values of properties 1, 2, and 3 are provided in inputs In1, In2, and In3, respectively. The property numbers correspond to their positions in the outputs. Properties 1, 2, and 3 are thus temperature (T), pressure (P), and ammonia mass fraction (x).